Your file Votre référence
ISBN: 978-0-494-71550-5
Our file Notre référence
ISBN: 978-0-494-71550-5

Mammalian Hibernation – Genes and Free Radicals

Marcus Allan

B. Sc. Carleton University, 2008

A Thesis Submitted to the Faculty of Graduate Studies and Research in partial fulfillment of the requirements for the degree of

Master of Science

Department of Biology

Carleton University

Ottawa, Ontario, Canada

Abstract

When environmental conditions become unfavorable, such as during winter, many small mammals are able to enter into a state of dormancy known as hibernation in order to conserve energy. Energy conservation is accomplished via a drastic decline in metabolic and physiological activity in association with a decrease in body temperature, which is periodically interspersed with brief bouts of arousal back to their euthermic values. These drastic changes in oxygen consumption and concentration, perfusion of tissues and energy consumption results in an elevated susceptibility to oxidative stress which can cause severe tissue damage. Hibernators are able to mitigate this damage using antioxidants and their associated pathways in a coordinated response. In the present study, the role of the redox sensitive transcription factor NF-κB was investigated to gain insight into its regulation during hibernation. NF-κB is an essential transcription factor which is known to regulate many targets including antioxidant, antiapoptotic/pro-survival and pro-inflammatory genes. The extent and duration of the NF-κBs response depends on its interactions with its multiple upstream effectors. During hibernation it was found that NF-κB and its signaling components have different expression patterns which are tissue dependant and change along the torpor–arousal cycle. Overall, NF-κB was found to be maximally activated during entrance into torpor, with its cytoprotective downstream genes being upregulated in time for next subsequent arousal in both liver and skeletal muscle tissue. Therefore, these results suggest that antioxidant defenses are upregulated throughout torpor-arousal and that NF-κB may help mediate such protective responses.

Acknowledgments

I would like to thank my supervisor, Kenneth Storey for his support and encouragement throughout my stay here. He has taught me many valuable life skills and given great insight into the opportunities that science can create and what we as individuals are capable of. Thanks to Jan Storey for editing my work and making this lab such a success.

I would like to thank my parents, Robert and Mary, for the continuous support throughout my life. If it was not for them I would not be as great of a success as I am today.

To all my friends in the lab and at Carleton University thanks for the love and see you tonight! My final thank you is to NSERC, which not only provided funding for this research, but allowed me to buy Prada and travel the world! Remember everyone, its all about the signal transduction!

Table of Contents

List of Abbreviations

3,3', 5, 5'- Tetramethylbenzidine	TMB
Activating Protein	AP
Active In The Cold Room	ACR
Adenosine Triphosphate	ATP
Base Pair	BP
Body Temperature	Tb
Brown Adipose Tissue	BAT
CCAAT/Enhancer Binding Protein	C/EBP
Complementary DNA	cDNA
Diethylpyrocarbonate	DEPC
Dithiothreitol	DTT
Double Distilled Water	ddH_2O
Early-Arousal	EAR
Early-Hibernation	EHIB
Ethylenediaminetetraacteic Acid	EDTA
Electron Transport Chain	ETC
Endoplasmic Reticulum	ER
Entrance Into Torpor	ENT
Enzyme-Linked Immunosorbent Assay	ELISA
Forkhead box O	FOXO
Heat Shock Factor	HSF
IκB kinase	IKK

Immunoglobulin-Like Fold, Plexin, Transcription Factor	IPT
Insulin like Growth Factor	IGF
Ischemia/Reperfusion	I/R
Heme Oxygenase 1	HO-1
Hypoxia-Inducible Factor	HIF
Late-Arousal	LAR
Late-Hibernation	LHIB
Lipopolysaccharides	LPS
Mitogen Activated Protein Kinase	MAPK
Molecular Weight	MW
NF-E20-Related Factor 2	Nrf2
NF-κB-Inducing Kinase	NIK
Nuclear factor-κB	NF-κB
Phosphate Buffered Saline	PBS
Phosphoinositide 3 Kinase	PI(3)K
Polymerase Chain Reaction	PCR
Polyunsaturated Fatty Acid	PUFA
Pyruvate Dehydrogenase	PDH
Pyruvate Dehydrogenase Kinase Isoenzyme 4	PDK4
Reactive Oxygen Species	ROS
Rel Homology Domain	RHD
Reverse Transcription	RT
S-Adenosyl Methionine	SAM

Signal Transducers And Activators Of Transcription	STAT
Sodium Dodecyl Sulfate	SDS
Standard Error Of The Mean	SEM
Superoxide Dismutase	SOD
Transcription Factor	TF
Tricarboxylic Acid Cycle	TCA
Tumor Necrosis factor	TNF
Ultraviolet	UV
White Adipose Tissue	WAT

List of Figures

Chapter 1

General Introduction

Introduction:

Hibernation is a state of seasonal heterothermy that is characterized by long periods of cold torpor and is utilized by a variety of small mammals to endure the low temperatures and food scarcity encountered during the winter months. The patchwork distribution of mammals that can hibernate (including selected placentals, marsupials and monotremes), together with the fact that some birds can hibernate, has lead to the idea that the genes responsible for the phenotype occur in the genomes of all mammals (Srere et al., 1992). To ensure survival over the many months of the hibernating season, a coordinated, controlled suppression of metabolism occurs and normal body temperature (Tb) regulation by the hypothalamus is unhooked so that Tb falls to near ambient (as low as 0-5°C) during each torpor bout (Storey, 1987). Torpor bouts are interspersed with brief periods (generally <1 day) of arousal back to euthermia (Tb ~37°C). The low metabolic rate (typically <5% of the euthermic value) and low Tb during the torpor phase of hibernation result in energy savings of up to ~90% compared with the energy that would otherwise be used to maintain euthermia during the hibernation season (Wang & Lee, 1996).

Therefore, by eliminating the need to maintain euthermia, the hibernating phenotype offers a natural mammalian model to examine metabolic, biochemical and physiological depression, hypothermia and tissue ischemia/reperfusion (I/R) (Carey et al., 2003). Geiser and Turbill (2009) have noted that hibernation generally results in a decreased extinction rate of a species since they can utilize a 'sit-and-wait' approach when environmental conditions are unfavorable, thereby minimizing food and water requirements and avoiding predators. This is unlike strict homeotherms that need to

maintain a high constant Tb at all times and therefore require a constant high food supply. Physiologically, in hibernating mammals, respiration is reduced from 100-200 to 4-6 breaths/min with bouts of apnea (McArthur & Milsom, 1991), renal functions are reduced or cease all together, the heart rate decreases from 200-300 to 3-5 beats/min (Zatzman, 1984) with epithelial transport in the digestive tract also being suppressed (Carey et al., 2001). These changes in metabolism, oxygen consumption, fuel selection, Tb and heart rate are thought to be mediated by metabolic depression, which result in decreased intracellular activity such as suppression of ion pumps, gene transcription and protein synthesis which can be achieved via chromatin remodeling (methylation, acetylation), mRNA and protein degradation and via changes in post-translational modifications (phosphorylation, SUMOylation, ubiquitination) (Andrews, 2007).

These intracellular events are preceded by preparatory changes that need to occur to set up the animal with the capacity to enter torpor; these occur during the late summer and autumn (e.g. building up body fat reserves) and are regulated by circannual environmental cues. Once the preparations are done, some species like ground squirrels withdraw to their burrows and start going through torpor-arousal cycles although these are short and shallow to start with. Although there is a "hard-wired" nature to torpor in obligate hibernators, there are still extra controls that are needed to regulate the actual descent into (and arousal from) each torpor bout. The importance of these other cues are highlighted by the fact that there are many facultative hibernators that also show circannual rhythms of fattening, food storage, other preparations, etc (e.g. chipmunks), but do not go into torpor unless the perceived stress (food running out, very cold winter) rises too high (Melvin & Andrews, 2009; Harlow & Frank, 2001).

Preparation for Hibernation:

In order for hibernation to be successful, fat-storing hibernators, such as ground squirrels, need to ingest sufficient food to give them enough calories to last over the winter and also for several weeks after spring emergence before food is readily available again. To do this, animals enter a period of hyperphagy during the late summer and early autumn and synthesize and store huge amounts of triglycerides, mainly in white adipose tissue (WAT), which is the primary energy source throughout hibernation (Dark, 2005). As a result of this fat storage, body mass may increase by 50-100%. Prior to dormancy, animals select an appropriate hibernaculum such as underground burrows, mines or caves in order to protect themselves from predators and temperature extremes. Some hibernators, such as hamsters and chipmunks also cache food in their hibernaculum, which is periodically ingested during hibernation (Humphries et al., 2003). Unlike fat-storing hibernators, food-storing species may compile up to 25-50 times the amount of energy they will need in the form of seeds but without the need to increase their physical mass (French, 1985).

The development of full torpor capacity is a gradual process (Figure 1.1). Early on in the hibernation season, the animal engages in a series of "test-drops" while sleeping, which results in Tb dropping by a few degrees and then returning to normal. Over time these torpor bouts deepen and lengthen, in part facilitated by the decline in ambient temperature of the hibernaculum as winter progresses. The prevailing hypothesis concerning the induction of a torpor bout is that a chemical opiate, similar to morphine, is probably responsible for the phenotype; however, this has yet to be proven (Schipke, 1995). Other endocrine regulatory candidates include iodothyronamine (Scanlan et al.,

2004), ghrelin (Gluck et al., 2006) and leptin (Nelson, 2004) since they are known to influence the duration of torpor. Although the mechanism of how environmental cues such as food scarcity and decreased ambient temperatures affects the induction of hibernation is unknown, it is clear that the entrance into dormancy is a tightly coordinated response, with the brain, particularly the hypothalamus, being important due to its regulation of Tb and of an organism's activity level (sleep and wakefulness) (Kalter & Folk, 1979).

Torpor:

Entry into torpor is caused by metabolic inhibition that reduces metabolic rate (oxygen consumption) and is followed by a consequent drop in Tb (Snyder & Nestler, 1989). Some small mammals such as hamsters, mice and shrews routinely use daily torpor; by allowing Tb to fall by a few degrees Celsius during their resting hours, they thereby reduce their total daily energy expenditure (Swoap, 2008). Seasonal hibernators greatly extend torpor bouts to last days or weeks. Metabolic inhibition is very strong as animals enter torpor and is accompanied by a decrease in the hypothalamic set-point for Tb and some vasodilatation that can dissipate heat. In some species, such as ground squirrels, the final metabolic rate in torpor is similar to the value that would be expected from the change in Tb (ie. most rates fall about 2 fold for every 10°C reduction in temperature, ie. $Q_{10} = 2$) whereas in other species, especially very small animals, the net change in metabolic rate between euthermia and torpor can be much greater, showing a Q_{10} of 3 or more (Geiser, 1988).

In hibernators, the entry and exit from torpor is a gradual process with bout length increasing in duration during midwinter and decreasing toward spring. As previously

stated, physiological systems involving the cardio-vascular and renal systems are suppressed during hibernation in order to minimize energy expenditure. Recently, von der Ohe and colleagues (2007) found that brain synapses were reduced to 50-60% of their normal size during torpor and regenerated during arousal, with changes in protein localization and their associations observed, but not their degradation. This gives great insight into the mechanism of the neuronal plasticity found in hibernators. By decreasing these functions, hibernators are able to survive over the winter by utilizing their fat stores in the white adipose tissue. Lipid oxidation via oxidative phosphorylation in mitochondria is the primary mechanism of energy production during hibernation and this is indicated by a respiratory quotient (ratio of CO_2 output to O_2 consumed) value of ~0.7, compared to values of ~1 for carbohydrate catabolism (Buck & Barnes, 2000). Even tissues, like brain, that normally depend almost exclusively on carbohydrate for fuel, can switch to partial lipid dependence during hibernation. Triglycerides cannot cross the blood-brain barrier but the liver produces ketone bodies from lipid hydrolysis which can and have been shown to be preferentially used by the brain during hibernation (Andrews et al., 2009).

An example of the regulatory mechanisms that contribute to the switch from carbohydrate to lipid metabolism can be seen by increased expression levels of pyruvate dehydrogenase kinase isoenzyme 4 (PDK4) during hibernation. PDK4 is responsible for inhibiting pyruvate dehydrogenase (PDH), which regulates pyruvate entry into the tricarboxylic acid (TCA) cycle (Buck et al., 2002, Andrews et al., 1998). As a consequence of PDK4 action, PDH activity decreased dramatically in tissues during torpor, effectively blocking carbohydrate catabolism. Other glycolytic regulatory

enzymes also show suppressed activity during hibernation in order to favor lipid catabolism, including liver glycogen phosphorylase, phosphofructokinase, and pyruvate kinase; like PDH, the mechanism is also reversible phosphorylation (Storey, 1987). Other changes that facilitate lipid metabolism in torpor include elevated levels of triacylglycerol lipase (pancreatic isoform) in some tissues (Squire et al., 2003) and upregulation of the intracellular fatty acid binding proteins that move fatty acids in the cytoplasm (Hittel & Storey, 2001). Although torpor is not continuous over the entire hibernation cycle, it is the stage where the majority of energy savings occurs due to the reorganization of the animal's physiological and metabolic priorities.

Arousal:

One aspect of hibernation that still intrigues scientists in terms of its necessity, is the periodic arousals from torpor that interrupt dormancy. Arousal from torpor usually lasts 6 to 24 hours during which the animal raises its Tb and physiological functions back to their euthermic values. These interbout arousals require a huge increase in oxygen consumption to support high levels of heat production by nonshivering thermogenesis in brown adipose and shivering thermogenesis in skeletal muscle and are responsible for utilizing up to 80% of the total fuel consumption during the entire winter hibernation period (Dark & Miller, 1998). The reasons for these costly arousal bouts are still not clear, but many scientists have speculated based on current information. Arousals may be needed to allow recovery of physiological functions that degenerate during prolonged torpor such as replenishing proteins damaged by oxidative stress, renewing immunological defenses, refreshing memory circuits during slow-wave sleep (ie. torpor is not a sleep state) (Daan et al., 1991), and in facultative hibernators allowing time to eat

and drink (Humphries et al., 2003).

The change from hypothermia to euthermia produces drastic changes in a hibernator. For example, the kidney goes from not producing any urine during torpor, by preventing filtration through their glomerulus, to producing hypotonic urine (Deavers & Musacchia, 1980). This shift in renal function is believed to be mediated by changes in arterial blood pressure (drop by 50% in hibernation) and results in the structural integrity of the kidney being maintained (Tempel et al., 1977; Zancanaro et al., 1999). Dramatic changes in blood pressure, body temperature and heart rate are known to accompany arousal from torpor; for example, in thirteen-lined ground squirrels, these variables respectively changed from 60/30 to 170/90 mmHg, 2 to 36°C and 3 to 450 beats/min (Lyman et al., 1982). These changes require a coordinated physiological and metabolic reorganization in order to ensure that vital functions can resume properly without damage. Furthermore, the disruption of blood throughout arousal is not uniform. Instead, at the onset, blood flow is largely confined to the thoracic region, with the anterior and posterior portions of the animal only starting to receive major increases in blood flow once the heart rate reaches 100 beats/min and 200 beats/min, respectively (Bullard & Funkhouser, 1962). This focuses blood flow on the thoracic brown adipose (generating heat), the lungs (providing the oxygen needed for thermogenesis) and the heart (circulating the oxygen and heat), thereby warming and restoring normal functions to this part of the body first (Wells, 1971).

A variety of metabolic changes accompany arousal as well. For example, hyperactivation of protein synthesis occurs during arousal in certain tissues (Zhegunov et al., 1988) reversing the strong suppression of protein translation during torpor (Storey,

2003). Gluconeogenesis is partially restored in the early phases of arousal to help refresh glucose/glycogen pools that were depleted (Galster & Morrison, 1975). Nelson and colleagues (2009) performed metabolite studies examining differences between the torpor-arousal cycles and found that dynamic changes occur that affect enzyme cofactors as well as purine, pyrimidine and amino acid metabolism, with arousal and torpor having increased and decreased levels, respectively. Expression changes for genes involved in fatty acid metabolism, cardiac contractility, circadian rhythms, molecular transport, detoxification, growth and apoptosis, gluconeogenesis, muscle atrophy and RNA and protein protection were also found to be different during the torpor-arousal cycle (Yan et al., 2008).

Oxidative Stress:

Oxidative stress is a natural occurring phenomenon that effects all organisms exposed to environmental oxygen. Oxidative stress occurs when the antioxidant capacity of the cell cannot buffer against redox changes within the organism leading to oxidation of biomacromolecules (Adibhatla & Hatcher, 2010). This damage is mediated by free radicals that contain one or more unpaired electrons in their outer orbital, making them highly reactive and more likely to undergo a chemical reaction. The majority of naturally occurring free radicals are Reactive Oxygen Species (ROS), meaning their unpaired electron is located on an oxygen atom; these include superoxide $O_2^{\cdot -}$ and hydroxyl radicals $OH^{\cdot -}$, with hydrogen peroxide H_2O_2 and ozone O_3 being nonradical ROS (Valko et al., 2007). Although oxidative stress can damage DNA, proteins, lipids and cause cell death; the role of some ROS in cellular signaling is also becoming well-known, and therefore a balancing act between the deleterious and essential functions of ROS must

occur *in vivo* to ensure survival (Droge, 2002). Oxidative stress damage has been associated with a variety of pathological conditions including diabetes (Kaneto et al., 2010), chronic inflammatory diseases (Ferguson, 2010), cancer (Ralph et al., 2010), Parkinson's disease (Schapira & Tolosa, 2010), Alzheimer's disease (McCaddon & Hudson, 2010) and ischemia/stroke (Forder & Tymianski, 2009; Allen & Bayraktutan, 2009), which is why it is important to understand how hibernators cope with this stress and minimize tissue damage by ROS during prolonged periods of torpor and/or during the arousal process. During arousal, a huge increase in oxygen consumption is needed to support thermogenesis and this also causes a corresponding increase in ROS production.

Superoxide radicals are a naturally occurring by-product of cellular respiration which are formed when oxygen gas is only partially reduced near the inner mitochondrial membrane at the ubiquinone and NADH-dehydrogenase sites of the electron transport chain (ETC) (Muller et al., 2004). Approximately 1-4% of molecular oxygen destined for oxidative phosphorylation is converted into superoxide radicals instead of water. Superoxide radicals and hydrogen peroxide are not very toxic in the cell; however, they can interact with Fe^{2+} and Cu^{+} *in vivo* resulting in the production of potent hydroxyl radicals via the Fenton reaction. Other endogenous sites of ROS production include xanthine oxidase, cytochrome P450 enzymes, NADPH oxidases, heavy metals (iron, copper, cobalt) and lipid oxidation of polyunsaturated fatty acids (PUFAs) (Krivoruchko & Storey, 2010; Martinon, 2010). ROS have important roles in the immune response, apoptosis, cellular senescence, detoxification of chemicals and induction of the mitogenic response (Bashan et al., 2009).

There are a variety of methods that an organism can utilize in order to minimize

the deleterious effects of ROS and oxidative stress. These protective mechanisms include the use of both constitutively expressed and inducible metabolites, enzymes and proteins. Overall, the antioxidant defense strategies utilize either preventative mechanisms to minimize ROS formation, detoxification methods to breakdown ROS, repair mechanisms to fix damage from ROS, and/or degradation mechanisms to catabolize damaged macromolecules (Valko et al., 2007). One of the most widely studied antioxidant enzymes is superoxide dismutase (SOD), which converts superoxide radicals into hydrogen peroxide and comes in three isoforms in mammals: the cytoplasmic copper-zinc SOD (CuZn-SOD), the mitochondrial manganese form (Mn-SOD) and extracellular SOD (EC-SOD). The hydrogen peroxide product is lipid soluble and can transverse throughout the cell where it is normally decomposed. However, it can also undergo the Fenton reaction with Fe^{2+}, producing highly reactive hydroxyl radicals with the resulting Fe^{3+} being susceptible to reduction back to Fe^{2+} by superoxide radicals (setting up a catalytic cycle of iron-mediated ROS generation) (Kong & Lin, 2010; Valko et al., 2006). Other key antioxidant enzymes include catalase, glutathione peroxidase, glutathione S-transferases and peroxiredoxins (Morin & Storey, 2007), whereas low molecular weight nonenyzmatic antioxidants include thioredoxin, glutathione, ascorbic acid, β-carotene, and lipoic acid, among others (Kharrazi et al., 2008).

Although there a variety of strategies a cell can utilize in order to minimize oxidative stress, studies have shown that a number of transcriptional changes occur in the hibernating ground squirrel, which conveys a high degree of protection against oxidative stress. This is of particular interest since these changes normally occur during a time of severe metabolic depression when adenosine triphosphate (ATP) use during transcription

and translation is strongly suppressed; this indicates that specific enhancement of antioxidant gene/protein expression is of great importance to hibernation (Storey, 2010). Redox sensitive signaling pathways involving ROS are well known to be involved in stimulating growth, differentiation, proliferation and apoptosis related genes under the regulation of multiple transcription factors including nuclear factor (NF) κB, the phosphoinositide 3 kinase (PI(3)K)-Akt pathway, p53, NF-E20-related factor-2 (Nrf2), heat shock factor 1 (HSF1) and hypoxia-inducible factors (HIF) (Ji, 2008; Liu et al., 1996). The MAPK (Zhu et al., 2005), Nrf2 (Morin et al., 2008B; Ni & Storey, 2010), p53 (Fleck & Carey, 2005) and HIF-1 (Morin & Storey, 2005) cascades have been identified as mediating differential tissue responses involved in oxygen and ROS metabolism during hibernation. The present thesis evaluates the role of the NF-κB transcription factor in antioxidant defense of the hibernator.

NF-κB:

NF-κB was discovered in 1986 by Sen and Baltimore when they found a unique binding protein in B-cells of the immune system with the sequence GGGGACTTTCC of the κ region. Since then, much research has gone into elucidating its structure, function and regulation, all of it demonstrating that NF-κB has a central role in cell homeostasis. NF-κB stimulates the expression of a variety of genes with diverse functions including cytokines, immune receptors, stress response genes, transcription factors and regulators, growth factors and cellular adhesion molecules (Pahl, 1999). Cytokines (Shalom-Barak et al., 1998), pathogenic bacteria (Medina et al., 2002), oxidative stress (Schreck et al., 1991), ER-overload (Yamazaki et al., 2009), environmental stressors such as hypoxia (Greenberg et al., 2006), growth factors (Biswas et al., 2000) and variety of other factors

are all known to influence NF-κB expression. Furthermore, disregulation of NF-κB is implicated in pathologies including rheumatoid arthritis (Okamoto, 2006), muscle wasting (Hasselgren, 2007B), diabetes (Eldor et al., 2006), heart disease (Valen et al., 2001), stroke (Herrmann et al., 2005), cancer (Lee et al., 2007), Parkinson's disease (Soos et al., 2004), Alzheimer's disease (Collister & Albensi, 2005), inflammatory bowel disease (Atreya et al., 2008) and many more.

The multiple functions of NF-κB within cells has led to much research into understanding the complexity and intricacies of its response and regulation, with upstream and downstream players and their functions still being elucidated today. Under normal cell conditions, the NF-κB dimer is sequestered in the cytoplasm with its inhibitor protein, IκBα, bound to it. When an upstream inducing event occurs, signals converge on NF-κB regulatory protein kinase, IκB kinase (IKK), which is composed of IKKα, IKKβ and NEMO subunits. The NEMO subunit is primarily responsible for controlling the activation of the NF-κB pathway (Herscovitch et al., 2008), with IKKα and IKKβ both being protein kinases. IKKβ and IKKα are activated by the presence of different substrates with IKKβ being responsible for the major and rapid pro-inflammatory response associated with cytokines such as those caused by tumor necrosis factor alpha (TNFα) and lipopolysaccharides (LPS), which result in the phosphorylation of IκBα (Hacker & Karin, 2006). IKKα rarely phosphorylates IκBα; instead it acts as a nucleokinase to help activate gene expression or activates the noncanonical pathway (d'Abusco et al., 2010). For example, IKKα can phosphorylate histone H3 residues, mediating their subsequent acetylation and causing the κB promoter region in genes to become exposed, allowing for increased gene transcription (Yamamoto et al., 2003).

IκBα is phosphorylated by IKKβ at Ser-32 and Ser-36 which allows it to be targeted by an SCF-type E3 ubiquitin ligase, resulting in the subsequent proteasomal degradation of the inhibitor protein. The freed NF-κB dimer (consisting of p50/p65 subunits) is then able to translocate into the nucleus, where it can bind to its κB promoter region and selectively upregulate a variety of target genes (Figure 1.2). Modulation of the activity and duration of signaling by this pathway can occur at many points and involves a variety of modifications, including induction of IκBα synthesis, hyperphosphorylation of IKK, phosphorylation of NF-κB, and altered processing of NF-κB precursors (Karin & Ben-Neriah, 2000).

NF-κB is a unique transcription factor due to its redox sensitivity, meaning that it shows differential activation during times of ROS accumulation. Oxidative stress normally activates NF-κB whereas antioxidants inhibit it, although these responses are known to vary according to cell type (Li & Karin, 1999). There are a variety of signals within the NF-κB signaling cascade which are redox sensitive and are known to activate NF-κB by phosphorylating IκBα serine sites; these include the protein kinases Akt, double stranded RNA-activated serine-threonine protein kinase, MEKKK1, NF-κB-inducing kinase (NIK), and p90RSK (Ma, 2010). Hypoxia/reoxygenation and H_2O_2 are also known activators of NF-κB, with the displacement of IκBα being mediated by the phosphorylation of its Tyr-42 via c-Src kinase, with the inhibitor being subsequently degraded by calpain proteases (Lluis et al., 2007). Post-translational modification of the NF-κB dimer has been found to mediate and modify signal specificity in relation to oxidative stress, for example, phosphorylation and ubiquitination of the p65 subunit is required for full activation of the pathway (Kefaloyianni et al., 2006). Inhibition of the

NF-κB pathway can also occur during oxidative stress by altering Cys-179 of IKKβ via S-nitrosylation or S-glutathioylation, rendering it non-functional (Janssen-Heininger et al., 2009). Therefore, much still has to be elucidated pertaining to the regulation of IκBα, NF-κB and the IKK complex members with respect to differing stimuli, such as oxidative stress, in various tissues and organisms, with a particular emphasis on post-translational modifications since these alternations attenuate, specify and integrate the cellular cross-talk that results in altered gene expression.

NF-κB has a variety of downstream targets, which include genes encoding cytokines (Mori & Prager, 1996), stress-responsive proteins (Ammirante et al., 2008), surface receptors (Kitamure et al., 2005), antioxidants (Rojo et al., 2004), pro-apoptosis proteins (Grimm et al., 2005), IκBα (Hoffmann et al., 2002) and many others. Two downstream targets of NF-κB that are of particular interest with respect to oxidative stress are heme oxygenase 1 (HO-1) (Lin et al., 2007) and MnSOD (Kiningham et al., 2008). HO-1 is a stress-inducible enzyme which is activated in the presence of anoxia, ischemia/reperfusion, ROS, UV light, oxidants, xenobiotics, Nrf2, MAPK and many more. It is responsible for the breakdown of heme into biliverdin, Fe^{2+} and carbon monoxide (Ryter & Choi, 2002, 2005; Ohlmann et al., 2003). Its regulation during times of oxidative stress is essential since biliverdin, its secondary metabolite bilirubin, and carbon monoxide are antioxidants, whereas both free heme and the Fe^{2+} released from heme can catalyze the production of hydroxyl radicals by the Fenton reaction (Wang & Chau, 2010). The free iron produced from heme metabolism is not normally as deleterious as the free heme group since its production stimulates ferritin H chain expression, which can bind to ferritin L chain to form a high Fe-storing complex, capable

of holding approximately 45,000 Fe atoms per ferritin and thereby ameliorating the Fenton reaction (Knovich et al., 2009). Therefore, it is not surprising that HO-1 expression and deregulation has been associated with diseases such as cardiovascular disease, cancer (Jozkowicz et al., 2007), diabetes (He et al., 2010) and neurodegenerative conditions (Schipper et al., 2009) since its byproducts are cytoprotective and are anti-apoptotic/pro-survival in nature but also proinflammatory (Frank et al., 2008).

MnSOD is another antioxidant target of NF-κB during times of oxidative stress (Djavaheri-Mergny et al., 2004). MnSOD catalyzes the dismutation of superoxide radicals formed in mitochondria into H_2O_2 and oxygen. The enzyme is a homotetramer and is essential for maintaining cellular homeostasis, its over- or under- expression being associated with tumor suppression and promotion, respectively (Bag & Bag, 2008). MnSOD is under the control of variety of a redox sensitive transcription factors and signaling cascades including NF-κB, AP-1, TNFα, Sp1, AP-2, STAT3, Akt and many more (Warner et al., 1996; Wei et al., 2008; Jung et al., 2009; Banerjee Mustafi et al., 2009). Expression of MnSOD has protective effects against many disease states that are associated with oxidative stress including diabetes (Chen et al., 2005), cancer (Delhalle et al., 2002) and neurodegenerative conditions (Xu et al., 2002). Like HO-1, the intricacies of MnSOD regulation with respect to oxidative stress are still an active area of research; however, its role as a cytoprotectant during times of stress has been clearly demonstrated (Perry et al., 2010).

Model Organism:

During intermittent arousals from torpor, the hibernating ground squirrel encounters a wide range of physiological, biochemical and metabolic changes that can

lead to oxidative stress. A primary one derives from the huge increase in uncoupled respiration by brown adipose tissue during arousal; indeed, oxygen consumption of ground squirrels rises rapidly by as much as 36-fold compared with the rate in torpor and is 3-fold higher than the resting rate of euthermic summer animals (Muleme et al., 2006). Elevated oxygen consumption by the electron transport system goes hand-in-hand with a comparable rise in superoxide generation and not surprisingly antioxidant defenses respond quickly to this challenge. Indeed, plasma ascorbate is rapidly depleted as ground squirrels rewarm (Drew et al., 2002) and in hamsters, plasma SOD and catalase activities rise sharply by 3-4 fold during arousal (Okamoto et al., 2006; Ohta et al., 2006). Early studies by Buzadzic et al. (1990) of hibernator brown adipose tissue showed high constitutive activities of antioxidant enzymes and were among the very first studies to show adaptive enhancement of antioxidants in response to stress in an animal system.

The oxidative stress in the arousing hibernator may also be exacerbated by other factors. For example, various organs of the hibernator are under-perfused during torpor, potentially creating ischemic situations that are rapidly reversed by reperfusion when arousal occurs. This reperfusion event is quite dramatic in the peripheral and splanchnic organs, which have their blood supply shunted to more critical organs including heart, lungs, adipose tissue and brain during torpor (Carey et al., 2003A). Reperfusion events are well-known to be accompanied by oxidative stress; indeed, much of the metabolic damage associated with heart attack and stroke occurs during the reperfusion stage as a response to ROS generated when the reduced state of mitochondrial cytochromes is rapidly reversed when oxygen is reintroduced (Wang et al., 2010). Oxidative stress in hibernators can also be related to the high levels of PUFAs that are present in hibernator

membrane and triglyceride depots. These are necessary to maintain lipid fluidity at a lower Tb values and one of the important pre-hibernation metabolic adjustments shown by hibernators is an increase in the relative amounts of linoleic and α-linolenic acid in their lipids. Indeed, PUFAs are an important factor in determining the duration and frequency of torpor bouts and overall winter survival (Frank et al., 2008), although they elevate susceptibility to oxidative stress because they can be attacked by ROS causing peroxidation of the lipids and generating alkoxyl radicals ($LO^{\cdot}$), alkyl peroxyl radicals ($LOO^{\cdot}$) and alkyl hydroperoxides (LOOH) (Gerson et al., 2008). Therefore the hibernating ground squirrel is a vital model for studying cellular defense mechanisms to oxidative stress, caused by ischemia/reperfusion events, since it is able to survive repeated assaults without any apparent consequence to its overall health and survival (Ma et al., 2005).

In the past decade, researchers have started investigating a variety of antioxidant defense strategies that hibernators utilize in order to get a better understanding of how they protect themselves from the I/R oxidative stress that they encounter. This oxidative stress can manifest itself in a shift to the oxidized form of GSH, GSSG (Carey et al., 2003B), an increased amount of conjugated dienes within tissues and activation of redox sensitive transcription factor such as NF-κB (Carey et al., 2000). These I/R events have been known to cause more damage in non-hibernating organisms when compared to aroused euthermic animals (Carey et al., 2006). Other antioxidants and signaling cascades utilized during hibernation to minimize tissue damage include increased ascorbate acid concentration (Drew et al., 2002), Nrf2 activation of some antioxidant genes (Ni & Storey, 2010), upregulation of peroxiredoxins (Morin & Storey, 2007), MAPK activation

(MacDonald & Storey, 2005), and increased SOD expression (Petrovic et al., 1983).

Objectives and Hypotheses:

The above information all argues for the importance of good antioxidant defenses to hibernation success and it is known that this includes both constitutive and inducible defenses. Hence, transcription factors such as NF-κB, the regulatory proteins that control NF-κB, as well as the antioxidant enzymes and proteins whose expression is regulated by NF-κB, will have critical roles to play in dealing with multiple forms of oxidative stress to achieve successful hibernation.

Hypothesis: The redox sensitive transcription factor NF-κB is activated during hibernation and this leads to upregulation of downstream antioxidant enzymes.

Chapters 3 and 4 of this thesis test this hypothesis by examining the regulation of NF-κB including the expression of the NF-κB dimer proteins (p50, p65), the IκBα inhibitory subunit, and the IKK complex in the skeletal muscle and liver of 13-lined ground squirrels, *Spermophilus tridecemlineatus*, over the course of the torpor-arousal cycle. Two key downstream antioxidant targets of NF-κB, HO-1 and MnSOD, are also analyzed in skeletal muscle and the liver. Reverse-transcription (RT)- polymerase chain reaction (PCR) and Western blotting techniques were used to examine both gene and protein expression levels and a DNA binding affinity assay using a modified ELISA was utilized to determine if there was a change in binding affinity of NF-κB during hibernation in skeletal muscle.

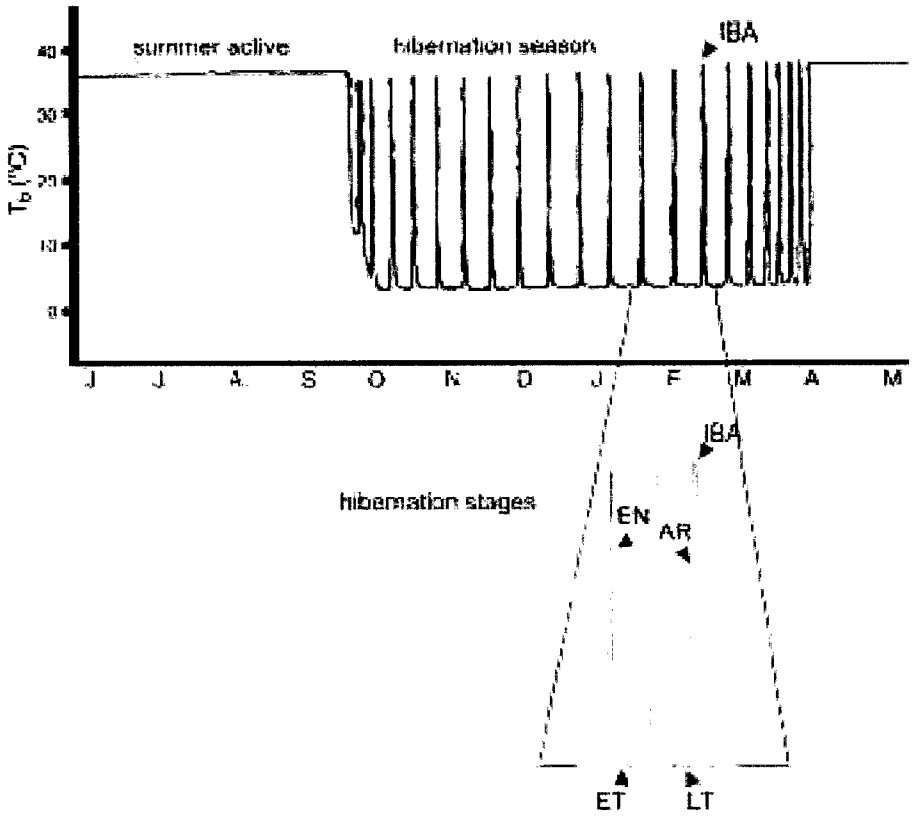

Figure 1.1: Body temperature (Tb) of a gold-mantled ground squirrel (*Spermophilus lateralis*) as a function of time over a one year period, including the winter hibernation season. The enlargement shows a region encompassing significant time points: entrance into torpor (EN) which lasts up to 12 hours, early torpor (ET) within 48 hours of entering torpor, late torpor (LT), arousal (AR) with a duration of ~2 hours, and finally interbout arousal (IBA) with a duration of ~20 hours. Taken from Carey et al. 2003A).

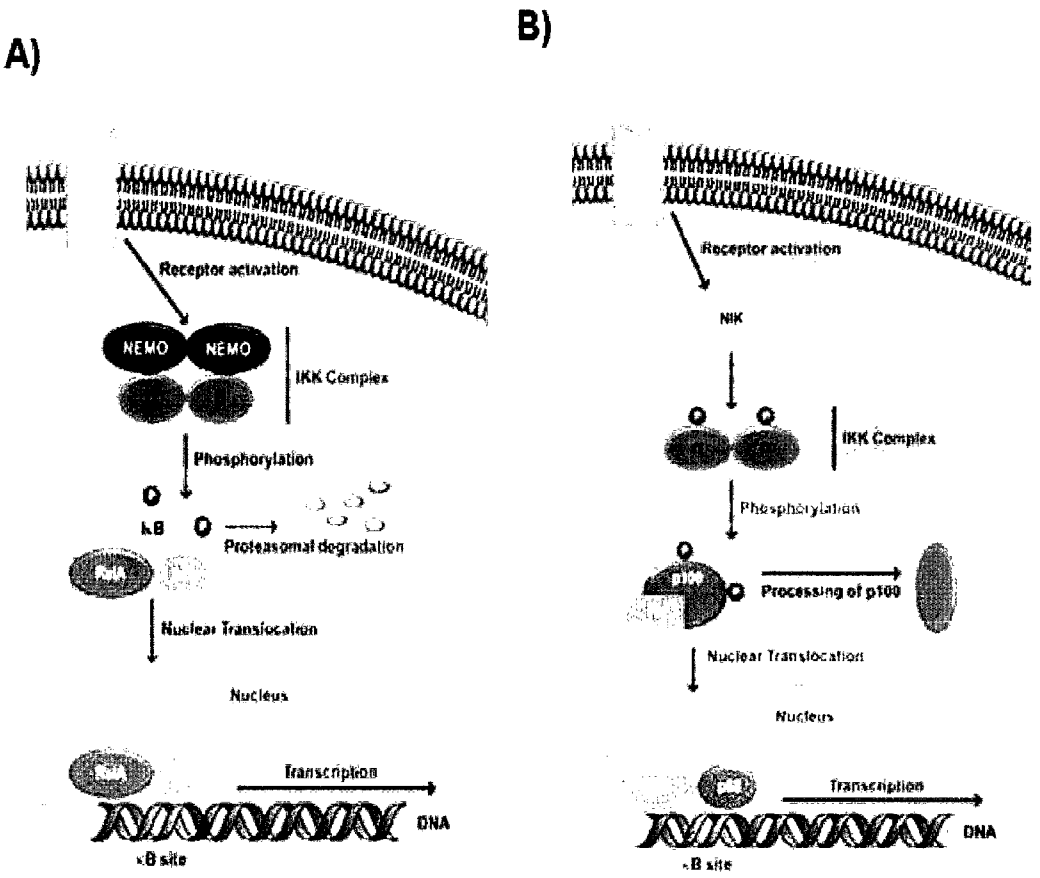

Figure 1.2: NF-κB signaling cascade. A) Canonical pathway: Activation of IKK by a signaling molecule results in the phosphorylation of IκBα that then dissociates and allows the p50/ RelA (p65) dimer to translocate into the nucleus where it can selectively upregulate its target genes. **B)** Non-canonical pathway: NIK activates IKKα, causing it to phosphorylates p100 which then dissociates from RelB/p52 allowing the dimer to subsequently translocate into the nucleus and upregulate its target genes. Images obtained from Hooper, 2010.

Chapter 2

Materials and Methods

Animal Experiments

Thirteen-lined ground squirrels, *S. tridecemlineatus*, weighing 130-180 g were captured by licensed trappers (TLS Research, Michigan) and transported to the Animal Hibernation Facility, National Institute of Neurological Disorders and Stroke, NIH, Bethesda, MD. Hibernation experiments were conducted by the laboratory of Dr. J.M. Hallenbeck. Animals were kept in shoebox cages, held at 21°C and fed *ad libitum* until they gained sufficient lipid stores (mass rose to 220-240 g) to enter hibernation. Animals were fitted with a sensor chip (IPTT-200; Bio Medic Data Systems) injected subcutaneously under isofluorane anesthesia in order to monitor body temperature (Tb). To induce hibernation, animals were transferred to cold chambers at 4-6°C in cages containing wood shavings. Tb was monitored and used to determine the stage of hibernation. Most animals settled into torpor after 2-3 days, and were sacrificed by decapitation at various points over torpor-arousal bouts; tissue samples were quickly excised and immediately frozen in liquid nitrogen. Samples were delivered to Carleton University on dry ice and stored at -80°C until use. Skeletal muscle and liver samples were retrieved from the following conditions: (1) active in the cold room (ACR); these interbout euthermic squirrels had not yet reentered torpor after 3 days in the cold room and showed continuous Tb values of 36-38°C, (2) early entrance into torpor (ENT): characterized by decreasing Tb (ranging from 31 to 12°C), (3) early-hibernation (EHIB): animals showed a stable T_b of 5-7°C for less than 24 hours, (4) late-hibernation (LHIB): animals were in continuous torpor for at least 3 days with a stable T_b of 5-7°C, (5) early-arousal (EAR): squirrels exhibited a rising T_b of about 12°C after at least 3 days of constant torpor, and (6) late-arousal (LAR): full interbout arousal with a T_b of 37°C for at

least 18 hours.

Total RNA Isolation and Quality Assessment

All materials and solutions were treated with 0.1% v/v diethylpyrocarbonate (DEPC) and autoclaved prior to use, with four samples from each time point being extracted separately. Total RNA was extracted from skeletal muscle and liver using Trizol™ reagent (Invitrogen), according to manufacturer's instructions. Briefly, 100 mg samples of tissue were homogenized in 1 mL Trizol using a Polytron homogenizer. Subsequently, 200 μL of chloroform was added to each sample and centrifuged at 12,000 rpm for 15 min at 4°C in the BHG Hermle Z 360 K (Mandel Scientific Co. LTEE/LTD) centrifuge. Total RNA was removed and precipitated in isopropanol (500 μL) for 10 min at room temperature, followed by a 15 min centrifugation at 12,000 rpm at 4°C. The total RNA pellet was washed with 1 mL of 70% ethanol, centrifuged at 12,000 rpm for 5 min and the supernatant was discarded. The pellet was air-dried for 15 min and then resuspended in 50 μL of DEPC treated water. RNA concentration was determined by reading absorbance at 260 nm on a GeneQuant Pro spectrophotometer (Pharmacia), and the ratio of absorbance at 260/280 nm was used as an indicator of RNA purity. RNA was brought up to a final concentration of 1 μg/μL in DEPC distilled water and its quality was examined by native agarose gel electrophoresis (1% ethidium bromide) to check the integrity of the 18S and 28S ribosomal RNA (rRNA) bands.

cDNA Synthesis and PCR Amplification

First strand cDNA synthesis followed the manufacturer's protocol using 3 μg aliquots of total RNA (1 μg/μL) from skeletal muscle and liver. The RNA was diluted in

7 μL of DEPC treated water with 1 μL of oligo-dT (200 ng/μL). Following the addition of oligo-dT (5'-TTTTTTTTTTTTTTTTTTTTTTV-3'; V= A or G or C) (Sigma Genosys), which anneals to the mRNA polyA tail, the samples were placed in a PCR machine (Mastercycler, Eppendorf) for 5 min at 65°C and then chilled rapidly on ice for 5 min. A 4 μL of 5X first strand buffer, 2 μL 10 mM dithiothreitol (DTT), 1 μL dNTPs and 1 μL Superscript II reverse transcriptase (all Invitrogen) were combined with the samples for a total volume of 19 μl. The mixture was incubated at 42°C for 1 h and then held on ice. Serial dilutions of the cDNA in DEPC water were prepared ($10^{-1} - 10^{-4}$) and were used to amplify all genes of interest, including *α-tubulin* which was used for normalization.

Primers for *p50*, *p65*, *MnSOD* and *HO-1* were designed using the Primer Design program, v.3 (Scientific and Educational Software) based on consensus mammalian sequences of the target genes. The primer sequences were as follows:

1) *p65* forward 5'- TGGCTTCTATGAGGCTGARC-3' and reverse 5'-ATCCGGTGRCGATCGTCTG-3', R= A/G
2) *p50* forward 5'-CTGGAAGCACGRATGACAGA-3' and reverse 5'-TCTTTYTGAACYTTRTCACA-3',
3) *H0-1* forward 5'- MGGYTTYAAGCTGGTGATGG-3' and reverse 5'-TGAGCAGGAACGCAGTCTTR-3', M= A/C
4) *MnSOD* forward 5'-CAGCCTGCRYTGAAGTTCAA-3' and reverse 5'-GGRATAAGRCCTGTKGTTCC-3',
5) *α-tubulin* forward 5'-AAGGAAGATGCTGCCAATAA-3' and reverse 5'-GGTCACATTTCACCATCTG-3'.

PCR was performed by mixing 5 µl of cDNA sample (dilution 10^{-1}-10^{-4}), 15.5 µL of DEPC treated water, 0.5 µL of 10 PCR buffer (Invitrogen), 1.25 µL of 50 mM $MgCl_2$ (Invitrogen), 0.5 µL dNTPs, 1 µL of Taq Polymerase (Invitrogen) and 1.25 µL of primer mixture (0.3 nmol/µL forward and 0.3 nmol/µL reverse) for a total volume of 25 µL. The PCR cycles consisted of the following steps: initial denaturation at 95°C for 7 min, 40 cycles of denaturing at 94°C for 1 min, annealing at 53.2-60.5°C for 1 min and elongation at 72°C for 1.5 min, followed by a final elongation step at 72°C for 10 min. The optimal number of cycles was 40 for skeletal muscle and liver, with the optimized annealing temperature being 53.2, 53.2, 53.2, 60.8 or 54°C for *p65*, *p50*, *MnSOD*, *HO-1* or *α-tubulin,* respectively. PCR products were separated on 1.0% agarose gels prepared by adding 2.0 g agarose to 200 mL of 1 x TAE buffer; the latter was prepared by mixing 4 mL of a 50x TAE stock (242 g Tris base, 57.1 mL concentrated acetic acid, 100 mL of 0.5 M ethylenediaminetetraacetic acid (EDTA) in 1 L of water, adjusted to pH 8.5) with 196 mL of ddH_2O. A 2 µL aliquot of ethidium bromide (0.2 mg/200 mL) was added to the mixture which was subsequently heated and then cooled in a gel casting tray. A 3 µL aliquot of xylene blue loading dye was added to each PCR reaction and then 14 µl of the total volume was aliquoted onto the agarose gel. The gel was run at 130 V for 18 min in 1 x TAE buffer and examined under UV light. To ensure product saturation did not occur during quantitative runs, the most dilute cDNA samples that produced visible product bands were used.

Samples of *p65*, *p50*, *MnSOD* and *HO-1* samples were excised from the agarose gel and were prepared for sequencing by the freeze/squeeze method. Briefly, samples were frozen in liquid nitrogen for approximately 5 min, thawed, and then crushed twice,

followed by a centrifugation at 7 min at 7,000 rpm while being passed through a filter cap. The purified cDNA samples were then sent to DNA Landmarks (St-Jean Richelieu, QC) for sequencing, with the resulting sequence identity confirmed using the BLASTN sequence comparison program. Figure 2.1 illustrates a representative agarose gel of the *p50* mRNA expression levels.

Protein Extraction and Nuclear Extract Preparation

Samples of frozen hind leg skeletal muscle or liver tissues were crushed under liquid nitrogen and then homogenized 1:3 w:v using a Polytron P10 homogenizer in 1 mL of homogenization buffer (20 mM HEPES, 200 mM NaCl, 0.1 M EDTA, 10 mM NaF, 1 mM Na_3VO_4, 10 mM β-glycerol-phosphate, pH 7) with 1 mM phenylmethylsulfonyl fluoride (PMSF) and 1 µl of protease inhibitor cocktail (BioShop Canada Inc.) added just prior to homogenization. The samples were centrifuged at 4°C for 15 min at 12,000 rpm, supernatants were removed, and soluble protein concentrations were quantified using the Coomassie blue dye-binding assay with the Bio-Rad prepared reagent (BioRad Laboratories, Hercules, CA). Supernatants were then adjusted to a concentration of 4 µg/µL by addition of small amounts of homogenization buffer and mixed 1:1 v:v with 2 X sodium dodecyl sulfate (SDS) loading buffer (100 mM Tris-base, 4% w/v SDS, 20% v/v glycerol, 0.2% bromophenol blue, 10% v/v 2-mercaptoethanol) to give a final concentration of 2 µg/µL. Samples were boiled for 5 min and then cooled on ice, aliquoted and frozen at -40°C.

Separate tissue samples were used to make cytoplasmic and nuclear fractions. Briefly, tissue was homogenized using ~20 piston stokes of a Dounce homogenizer in 1:2 w:v of homogenization buffer (10 mM HEPES, pH 7.9, 10 mM KCl, 10 mM EDTA, 10

mM DTT, 1.5 μL protease inhibitor cocktail [Sigma]) and then centrifuged 10,000 rpm for 10 min at 4°C. Supernatants (cytoplasmic fractions) were collected, and then pellets (nuclear fractions) were resuspended in 150 μL of extraction buffer (10 mM HEPES, 10 mM EDTA, 10 mM KCl, 20 mM β- glycerol phosphate, 10 mM DDT and 1.5μL protease inhibitor cocktail) per gram of tissue used. Nuclear fractions were then placed on ice and allowed to rock for 1 h with mixing of the sample every 10 min throughout the incubation. Samples were centrifuged at 10,000 rpm at 4°C for 10 min and the supernatant was saved. Protein concentration in both cytoplasmic and nuclear fractions was quantified with the Bio-Rad assay. Samples were adjusted to a concentration of 5 μg/μL with extraction buffer and then mixed with 1:1 v:v with 2 X SDS loading buffer, processed and stored as described above. Samples were then used for Western blotting as described below. To assess the efficiency of separation of nuclear versus cytoplasmic fractions, immunoblots were also run using an antibody (1:2000 dilution) for a protein located only in the nuclei (histone H3) (Cell Signaling); the secondary antibody was anti-rabbit at a dilution of 1:4000.

Western Blotting

Two gels were ran simultaneously, with each requiring two glass plates; a short and spacer plate. The plates were put together with the short plate facing outwards, slid into a green casting frame and then secured. The frame was then placed onto a casting stand with grey gasket and secured. The presences of leaks were determined by placing water between the plates and checking if the level decreased following a 5 minute incubation. If no leaks were present the water was poured off and the resolving gel was prepared. The resolving gels were composed of 8-12% acrylamide gels, with the amount

of water and 30% acrylamide aliquoted into the gels differing depending on the desired concentration. One 10% acrylamide gel (5mL total) was composed of 2.0 mL water, 1.7 mL 10% acrylamide, 1.3 mL 1.5 M Tris (pH 8.8), 50 µL 10% SDS, 50 µl 10% APS and 3µL TEMED. Gel mixtures were poured into the glass plates with 90% butanol added on top to speed up the reaction and destroy air bubbles. Following 30 minutes (or until polymerization finished) the butanol was removed and the top of the gel was washed with ddH_2O. The upper stacking gel mixture (approximately 1 mL) was poured onto the lower gel and was composed of 0.68 mL of water, 0.17 mL 30% acrylamide, 0.13 mL 1.0 M Tris (pH 6.8), 10.0 µL 10% SDS, 10.0 µL 10% APS and 1.0 µL of TEMED. Well combs were placed into the resolving gel which was allowed to polymerize for 30 min. Well combs were removed following polymerization, with the gel plates being removed from the casting frame and placed into electrode assembly cassettes.

Equal amounts of sample protein (30 µg/well) for each tissues were aliquoted into the wells of the 8-12% polyacrylamide gels and samples were separated at 180 V for 55 min in running buffer (0.3% Tris-base, 1.9% glycine, 1% SDS). Proteins were then transferred to PVDF membrane by electroblotting at 160 mA for 90 min using transfer buffer (25 mM Tris pH 8.5, 192 mM glycine, 10% v/v methanol). Membranes were blocked with 5.0 % skim milk in TBST (20 mM Tris, pH 7.6, 140 mM NaCl, and 0.05% v/v Tween-20) for 15 min, washed in TBST 3 times for 5 min, and then probed with their respective primary antibody for 24 h at 4°C. The membranes were washed 3 times for 5 min in TBST and then incubated with secondary antibody at room temperature for 1 h. The primary antibodies used are shown in Table 1. Primary antibodies were all made from rabbit and so the secondary antibody in all cases was HRP-linked anti-rabbit IgG

[Bioshop] (1:6000 v:v dilution in TBST). Bands were visualized by enhanced chemiluminescence (H_2O_2 and Luminol) with the blots being subsequently restained using Coomassie blue to visualize all protein bands. Figure 2.2 illustrates a representative blot of MnSOD in the liver.

Table 2.1: List of primary antibodies used with their dilution factor (in brackets), expected molecular mass (kDa) of the protein that the antibody detects, and the commercial source.

Primary Antibody (& dilution)	**Size (kDa)**	**Company**
Anti- NF-κB-p65 (1:6000)	~65	Cell Signaling
Anti-NF-κB-p50/p105 (1:2000)	~ 50/105	Cell Signaling
Anti-MnSOD (1:5000)	~24	Stressmarq
Anti-HO-1 (1:5000)	~32	Stressgen
Anti-IKKα (1:4000)	~85	Cell Signaling
Anti-IKKβ (1:4000)	~87	Cell Signaling
Anti-Phospho-IKKα/β (Ser176/180) (1:1000)	~ 85 / 87	Cell Signaling
Anti- IκBα (1:4000)	~39	Cell Signaling
Anti-Phospho-IκBα (Ser32) (1:1000)	~40	Cell Signaling

Transcription factor (TF) ELISAs

Binding of NF-κB to its DNA element was assessed with an ELISA-type assay that uses 96-well microplates coated with the double-stranded oligonucloeotide corresponding to the DNA binding element that is recognized by NF-κB.

DNA probes were based on consensus sequence of the NF-κB p65 promoter binding region and synthesized by Sigma Genosys. The sequences were as follows:

NF-κB 5' –Biotin-CACAGTTGAGGGGACTTTCCCAGGC-3'

NF-κB Complement 5'GCCTGGGAAAGTCCCCTCAACTGTG-3'

Single-stranded probes were diluted in sterile H_2O to 500 pmoles/μL each.

A test run was performed to ensure that the signal was due to transcription factor binding and not to a nonspecific background signal, with the following: no DNA control, no protein control, no primary antibody control, and the sample nuclear extract. Nuclear extracts were prepared as stated previously with the exception that samples were not treated or boiled with 2X SDS; instead they were made up to their final volume using extraction buffer following protein quantification to 5 μg/μL. A quantification run was then performed using the same conditions as the successful test run using the nuclear extracts from the ACR, ENT, EHIB, LHIB and EAR time points. Briefly, a 10 μL aliquot of the biotinylated p65 oligo was mixed with 10 μL of its complement, incubated for 10 min at 94°C, and then allowed to cool gradually to produce double-stranded probe of 250 pmoles/μL. The wells of a streptavidin-coated microplate (R&D Systems) were then incubated with 40 pmoles of double stranded (ds) DNA probe (in phosphate buffered saline (PBS)) for one hour. The plate was washed 2X with wash buffer (1X PBS, 0.1% Tween-20), followed by a wash with PBS. Aliquots of nuclear extracts were then added

to the TF-binding buffer [10 mM HEPES, pH 7.9, 50 mM KCl, 0.5 mM EDTA, 3 mM $MgCl_2$, 10% v:v glycerol, 0.5 mg/mL BSA, 0.50% v:v NP-40, 0.5 mM DDT, 0.02 μg/μL salmon sperm DNA, NaCl (variable amounts of NaCl were added to the buffer based on the volume of nuclear extract to be added, final concentration was always 60 mM)] with 20 μg of skeletal muscle extract in 60 μL added to each well. Samples were allowed to incubate for 1 h at room temperature; while shaking at 100 rpm.

The plate was washed 4X with wash buffer (as above) coated with 60 μl of the anti-rabbit pAb NF-κB p65 primary antibody (GenScript) diluted 1:1000 v:v in PBST (PBS with 0.05% Tween-20) and allowed to incubate for 1 h. Following 4 washes with wash buffer, 60 μl of HRP-linked anti-rabbit IgG secondary antibody (1:2000 v:v dilution in PBST) was placed in each well and allowed to incubate for 1 h. The plate was washed 5X with wash buffer, and each well was then coated with 60 μl of TMB (3,3',5,5'-tetramethylbenzidine). Once a blue color had developed (approximately 5-10 min), 60 μl of 1M HCl was added to stop the reaction and then samples intensities were determined by measuring absorbance at 450 nm (with a reference wavelength of 655 nm) on a Multiskan spectrum microplate spectrophotometer (Thermo Electron Corporation).

Quantification and Statistics

Band densities on the chemiluminescent immunoblots and ethidium bromide stained agarose gels were visualized using the Chemi-Genius BioImaging system (Syngene, Frederick, MD) and quantified using Gene Tools software. Band densities for *p50*, *p65*, *MnSOD* and *HO-1* PCR products were normalized against the corresponding *α-tubulin* band amplified from the same cDNA sample. Immunoblots were normalized

against the summed intensities of a group of Coomassie-stained proteins in the same lane as the sample; these bands were chosen since they were not close to the band of interest and their intensities did not change between control and experimental stress states. ELISA absorbance values were normalized by subtracting the mean of the negative controls from the experimental values. Data are expressed as means ± standard error of the mean (SEM), n = 3-4 independent samples. Statistical testing of normalized band intensities used one-way ANOVA and a post-hoc test (Student-Newman-Keuls).

α-tubulin was used as the normalization gene as multiple experiments have demonstrated the levels remain constant throughout the torpor-arousal cycle. During hibernation the *α-tubulin* controls are constant relatively to the other known constant genes that can be used for normalization (see Table 1 in Appendix 1 for complete list). Three constant bands were used as the normalization and loading controls for the Westerns blots. A variety of proteins have been found experimentally to have a constant expression pattern over the torpor-arousal cycle (see Table 2 in Appendix 1 for complete list).

A summary of all results can be found in Appendix 2.

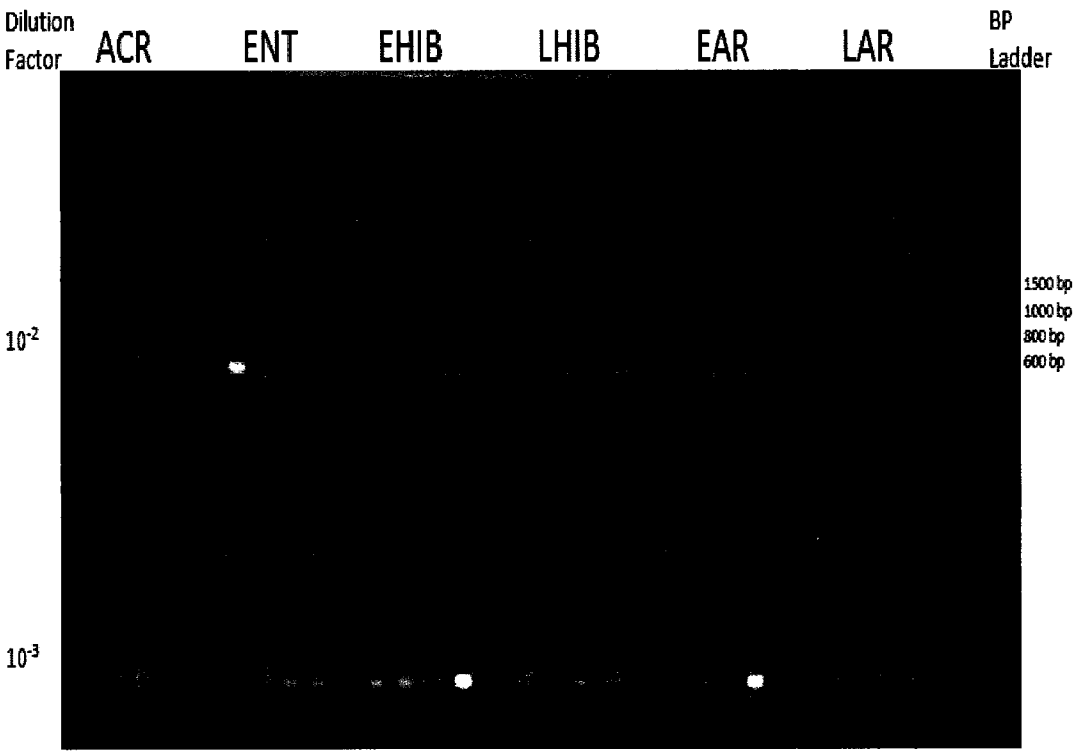

Figure 2.1: Representative agarose gel of *p50* mRNA expression levels using RT-PCR in the liver. Different time points throughout the torpor-arousal (n=4) cycle were examined at various dilutions of cDNA, with a base pair (BP) ladder included for all lanes as a control. The 10^{-2} dilution was used to quantify *p50* expression since it was the lowest dilution that produced bands in the majority of time points.

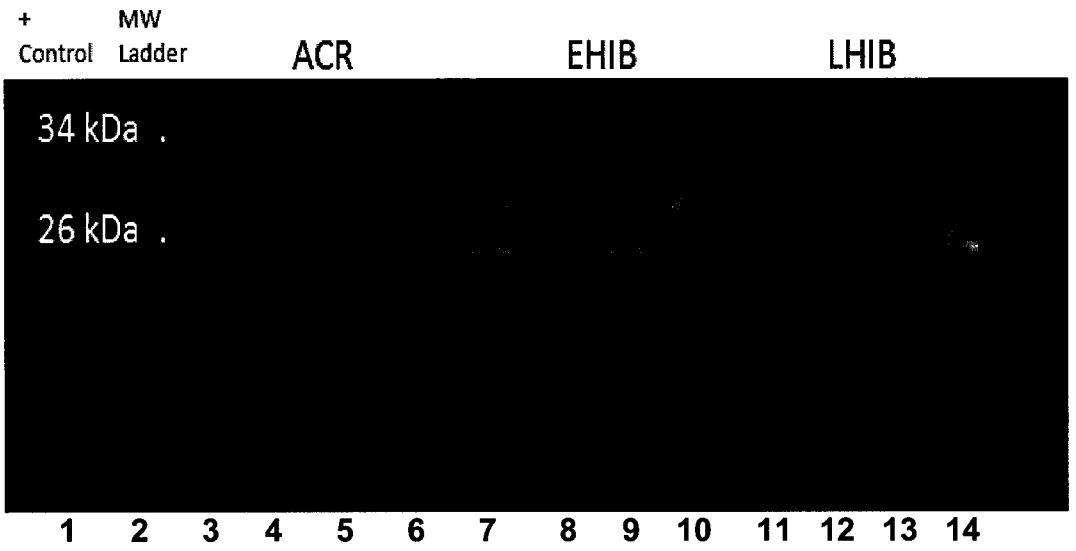

Figure 2.2: Representative Western blot of MnSOD protein expression levels in the liver. Shown here are n=4 different samples for each of ACR (lane 3-6), EHIB (lane 7-10) and LHIB (lane 11-14) along with a positive control (lane 1) (Active Room Temperature *S. tridecemlineatus*) and a Molecular Weight (MW) ladder (lane 2). Based on location and absence of other bands, this band was quantified to determine the expression level of MnSOD.

Chapter 3

NF-κB Regulation in Skeletal Muscle

Introduction:

Skeletal muscle is an extremely important tissue in all organisms since it provides them with the mechanical force needed for locomotion and other movements. Upon exit from torpor, it is critical that the skeletal muscles of hibernators are still fully functional in order to allow them to resume all of the essential tasks of euthermic life. Metabolic functionality of skeletal muscles is also critical to the arousal process itself since shivering thermogenesis by muscle is one of the two sources of heat (the other being nonshivering thermogenesis in brown adipose tissue). During torpor, muscles go unused for many days or even weeks at a time and such a situation in humans and nonhibernating mammals would cause muscle disuse atrophy. However, this does not appear to be the case in hibernators; studies have found little or no atrophy of muscles during hibernation (Malatesta et al., 2008). Another issue for hibernator muscle is ischemia/reperfusion (I/R) – how unused, hypoperfused muscles in the torpid animal deal with the very rapid and large increase in perfusion, oxygen consumption and ROS generation that accompanies arousal and shivering thermogenesis. This chapter looks at some of the signaling and regulatory events involved in dealing with increased oxidative stress associated with the I/R events of the torpor/arousal cycle.

Unlike many tissues, muscle has the unique characteristic of being highly plastic; meaning that its composition and metabolic activity can change according to functional demands placed upon it, such as during exercise or prolonged disuse. All vertebrate skeletal muscle arises from embryonic myoblasts that fuse to form nucleated myotubes, subsequently differentiating into adult myofibers. Muscle consists of many parallel myofibrils which are connected to bones via tendons. Myofibres are composed of

sarcomeres, which are arranged end-to-end (bordered by z-line) and composed of thin actin filaments and thick myosin filaments that results in distinctive banding patterns depending on their composition. For example, the A band is composed of interdigited thick and thin filaments while also encompassing the M line and H zone, with the former being important in energy metabolism due the presence of the enzyme creatine kinase. Muscle contraction relies on the presence of ATP in order to facilitate myosin head movement along the actin filaments. This ATP is produced from carbohydrate (glucose) and lipid (triglycerides) catabolism, drawing these fuels from either endogenous stores in the form of glycogen reserves or lipid droplets in cells or taking them up from the circulatory system (Luther, 2009; Boateng & Goldspink, 2008).

A variety of factors are known to influence muscle atrophy including muscle length, fiber type, age, rate of protein synthesis/degradation, oxidative stress and duration/type of immobilization (Kondo et al., 1991). By using mammalian hibernators and other naturally occurring models of muscle inactivity, such as estivating frogs, scientists are starting to understand the protective mechanisms against muscle atrophy that are used during natural states of prolonged dormancy (Hudson & Franklin, 2002). During muscle atrophy, the catabolism of myoglobin (the oxygen storage protein) in muscle releases iron from its heme group and this iron can catalyze the Fenton reaction, thereby accelerating ROS damage (Kondo et al., 1993). Not surprisingly, fast-twitch muscle fibers receive less oxidative damage than slow twitch muscle due to their lesser dependence on aerobic metabolism and greater reliance on anaerobic glycolysis (Pette & Spamer, 1986). Antioxidant defenses against oxidative stress appear to be one of the main mechanisms that protect muscle from atrophy mediated by ROS. This protection

comes in the form the upregulation of antioxidants and the decreased metabolic rate, which directly lowers the production of ROS during hibernation (Grundy & Storey, 1998; Kondo et al., 1991; Sen et al., 1997).

NF-κB activation has been found to lead to muscle atrophy in a variety of non-hibernating organisms by inducing the expression of pro-inflammatory cytokines, augmenting the ubiquitin-proteasome degradation of muscle specific proteins and interfering with myogenic differentiation (Li et al., 2008). IL-1-β, IL-6 and TNFα are a few of the pro-inflammatory cytokines that are known to be up-regulated by NF-κB during atrophy; in turn, these are all potent activators of NF-κB. This positive feed-back loop is believed to be a major problem in muscular dystrophy, since this chronic inflammation leads to further destruction of the muscle fibers (Kumar et al., 2004), with the p50 subunit and Bcl3 (a member of the IκB family) being essential components of this inflammatory response (Hunter & Kandarian, 2004). Muscle RING finger protein 1 (MuRF1), an E3 ubiquitin ligase, is also upregulated by NF-κB in skeletal muscle during atrophy, and exacerbates the wasting condition by targeting muscle proteins for proteasomal degradation (Cai et al., 2004). The role of NF-κB during myogenesis is complex since its effect varies with the differentiation process. It has been proposed that NF-κB activation in the early phases of development inhibits myogenic differentiation, while it is needed once developed to promote skeletal muscle homeostasis and growth (Bakker et al., 2008).

The complexity of NF-κB signaling which can give rise to opposing messages makes this transcription factor an interesting protein to examine during hibernation, especially since muscle atrophy is known to be limited in hibernator models.

Results:

Analysis of NF-κB protein levels

Levels of NF-κB subunits (p50 and p65) in skeletal muscle were measured by immunoblotting comparing control animals that had not yet entered a bout of cold torpor (ACR) and five time points on the torpor-arousal cycle: entrance into torpor (ENT), early-hibernation with Tb 5-7°C for less than 24 h (EHIB), late-hibernation with continuous torpor for at least 3 d (LHIB), early-arousal with rising Tb (EAR), and late-arousal with Tb returned to ~37°C for at least 18 h (LAR). Each antibody crossreacted with a single band on immunoblots at the expected molecular mass for the p50 and p65 subunits at 50 and 65 kDa, respectively. As compared with ACR controls, p50 total protein increased significantly in EHIB (by 2.3 fold, $p< 0.05$) and remained elevated through EAR (1.7 fold higher, $p<0.05$) and LAR (1.6 fold higher, $p<0.05$) (Figure 3.1). Compared to ACR controls, p65 total protein was increased significantly at all time points except for LHIB: levels in ENT, EHIB, LAR, and EAR were 1.4, 1.2, 1.2 and 1.2 fold higher than ACR, respectively ($p< 0.005$).

Analysis of IκBα and P-IκBα

Total and phosphorylated forms of IκBα, an inhibitor protein that binds to NF-κB, were analyzed in skeletal muscle by immunoblotting, again comparing a pre-hibernation control (ACR) and five time points on the torpor-arousal cycle; ENT, EHIB, LHIB, EAR and LAR (Figure 3.2). The antibodies used crossreacted with a single band on immunoblots at the expected molecular mass of IκBα and P-IκBα of approximately 39 and 40 kDa, respectively. When compared to the ACR control, IκBα expression was

found to increase significantly during EAR, by ~2.6 fold ($p < 0.05$) while levels in ENT, EHIB and LHIB remained low. For p-IκBα, values peaked in ENT at 2-fold greater than ACR ($p<0.05$), then were reduced during torpor and rose again to about control levels during arousal.

Analysis of HO-1 and MnSOD

HO-1 and MnSOD are the two downstream target genes that are regulated by NF-κB which code for antioxidant enzymes. Protein levels of both were measured in skeletal muscle over the time course of torpor and arousal (Figure 3.3). The antibodies cross reacted with single bands on immunoblots at the expected molecular masses of 24 and 32 kDa for MnSOD and HO-1, respectively. As compared to the ACR controls, the amount of HO-1 decreased during ENT by 54% and remained low during EHIB and LHIB (38 and 51% lower than ACR, respectively). HO-1 rose again to its maximal expression level during EAR to 1.51-fold higher than ACR ($p < 0.05$), an increase of 3-fold over the LHIB level that preceded it. As compared to ACR, the amount of MnSOD protein increased strongly when animals entered torpor, with values during EHIB and LHIB being 2.19 and 1.96-fold higher, respectively ($p < 0.005$) than in ACR. Levels remained elevated during arousal at about 1.6-fold higher than in ACR.

Analysis of P-IKK, IKKα, IKKβ

IKK is a protein kinase that phosphorylates and regulates IκBα. The levels of two isoforms (α and β) of IKK were assessed as well as the relative amount of phosphorylation of IKK on Ser176/180 (Figure 3.4). The antibodies all crossreacted with

single bands on the immunoblots at the expected molecular masses of 85, 87 and 85/87 for IKKα, IKKβ and P-IKK, respectively. When compared to the ACR control, P-IKK levels were elevated at all time points (significantly for EAR), except for LHIB; levels during ENT, EHIB, EAR and LAR were respectively 1.24, 1.15, 1.55 ($P<0.05$), 1.14 fold higher than the ACR value. P-IKK content in LHIB was 91% of the value of the ACR control ($p<0.05$). IKKα levels, when compared to ACR, did not change significantly. Protein levels of IKKβ were relatively constant with a significant increase found during EAR (2.04 fold higher) compared to ACR ($p< 0.05$).

Analysis of *p50* and *p65* transcript levels

The primers for *p50* and *p65* were used in RT-PCR to assess relative mRNA transcript levels of the two genes in skeletal muscle over the torpor-arousal course. Figure 3.5 shows *p50* and *p65* expression levels. Transcript levels of *p50* decreased strongly when squirrels entered torpor, stayed low throughout torpor and decreased even further in fully aroused animals; levels in ENT, EHIB, LHIB and LAR were, respectively, 48.1, 66.2, 72.6 and 27.4% of the ACR maximum ($p< 0.05$). Transcript levels of *p65* behaved differently and were unchanged during ENT but increased strongly during EHIB, by 1.75 fold, when compared to the ACR control ($p<0.005$). Subsequently, levels decreased below ACR for the remainder of the torpor-arousal cycle.

Analysis of *HO-1* and *MnSOD* transcript levels

The primers for *HO-1* and *MnSOD* were used in RT-PCR to assess relative mRNA transcript levels in skeletal muscle over the torpor-arousal course. Figure 3.6

shows *HO-1* and *MnSOD* expression levels. The transcript levels for *HO-1* decreased 45% during ENT and was sustained during torpor and EAR, with LHIB and EAR being respectively 59 and 66% of the ACR value ($p < 0.05$). Transcript levels rose slightly above control levels during LAR. *MnSOD* transcript levels were significantly decreased during torpor with respect to the ACR controls, with levels in EHIB LHIB, EAR and LAR being 52, 52, 50 and 50%, respectively, of the control value ($p<0.01$).

Analysis of p65 DNA-binding affinity

The amount of nuclear NF-κB p65 binding to its promoter was measured using an ELISA comparing nuclear extracts of skeletal muscle from control conditions (ACR) with 4 time points on the torpor-arousal cycle: ENT, EHIB, LHIB, and EAR (Figure 3.7). The antibody (anti-p65, Genescript) used cross-reacted with DNA bound nuclear p65 samples. As compared to ACR, the amount of nuclear p65 DNA binding to its promoter increased 1.36-fold in ENT ($p < 0.005$) values and decreased below control levels through the remainder of torpor. The amount of p65 bound to DNA in the nucleus was slightly lower in EHIB, with a significant decrease also found during LHIB and EAR, being 59 and 19%, respectively, of the ACR value ($p < 0.05$).

Analysis of p50 and p65 nuclear translocation

Figure 3.8 depicts p50 and p65 distribution between cytoplasmic and nuclear fractions of skeletal muscle. In the cytoplasmic fraction, p50 protein levels decreased significantly during torpor, with the value in LHIB being just 37% of the ACR control ($p < 0.01$). However, p50 levels did not change in the nucleus during torpor. Conversely,

p65 levels were unchanged in the cytoplasm during torpor but increased significantly (by 1.14 fold) in the nuclear fraction of skeletal muscle during hibernation compared to the ACR control ($p < 0.01$).

Sequencing results for *p50, p65, HO-1* and *MnSOD*

Figure 3.9-3.12 show sequencing results for the PCR products that were amplified for each of the target genes and had their amino acid sequence deduced. Each product was confirmed as being the correct gene by nucleotide sequence comparisons using the BLAST search engine with highest percent identities found with the homologous gene from other mammals; for example, ground squirrel nucleotide sequence identity compared with the human sequence was 92.8, 93.9, 81.6 and 86.0 % for *p50, p65, HO-1* and *MnSOD*, respectively, for the segment of the gene segment that was amplified.

Figure 3.9 depicts the deduced amino acid multiple alignment, homology tree and homology matrix for the partially amplified *p50* gene product. The partial sequence of the squirrel coded for 88 of the total 968 amino acid residues known to occur in human, with a 98% homology found between these species. The squirrel had a 90% sequence similarity between it and the mouse and rat. The squirrel had 1 unique amino acid substitution between it and all the other organisms within the partial sequence, resulting in a glycine replacing arginine-42. The partial sequence was found to amplify a region containing parts of the immunoglobulin-like fold, Plexins, Transcription factor (IPT) domain and the N-terminal subdomain of the Rel homology domain (RHD) of p50.

The deduced amino acid multiple alignment, homology tree and homology matrix for the partially amplified *p65* gene are depicted in Figure 3.10. The partial sequence of

the squirrel coded for 178 of the total 551 amino acid residues known to occur in human, with a 99% homology found between these species. Squirrel had a 94% sequence similarity between it and the mouse and rat. There were no unique amino acid substitutions found between the squirrel and the other mammals for this partial sequence. The partial sequence was determined to encompass parts of the N-terminal subdomain of the RHD and the IPT domain of p65.

Figure 3.11 depicts the deduced amino acid multiple alignment, homology tree and matrix for the partially amplified *HO-1* gene. The partial sequence of the squirrel coded for 145 of the total 288 amino acid residues known to occur in human. A 70% sequence homology was found between the squirrel and the other mammals. There were 28 unique amino acids substitutions found between the squirrel and the other mammals. The partial sequence was determined to encompass 3 of the 8 heme binding pockets of the HemeO domain in HO-1.

The deduced amino acid sequence, multiple alignment, homology tree and homology matrix for the partially amplified *MnSOD* gene are depicted in Figure 3.12. The partial sequence of the squirrel coded for 73 of the total 222 amino acid residues known to occur in human, with an 88% homology found between these species. Squirrel had an 89% sequence similarity between it and the mouse and rat. There were 6 unique amino acids substitutions found between the squirrel and the other mammals. The partial sequence was determined to code for the iron/manganese superoxide dismutase c-terminal domain in MnSOD.

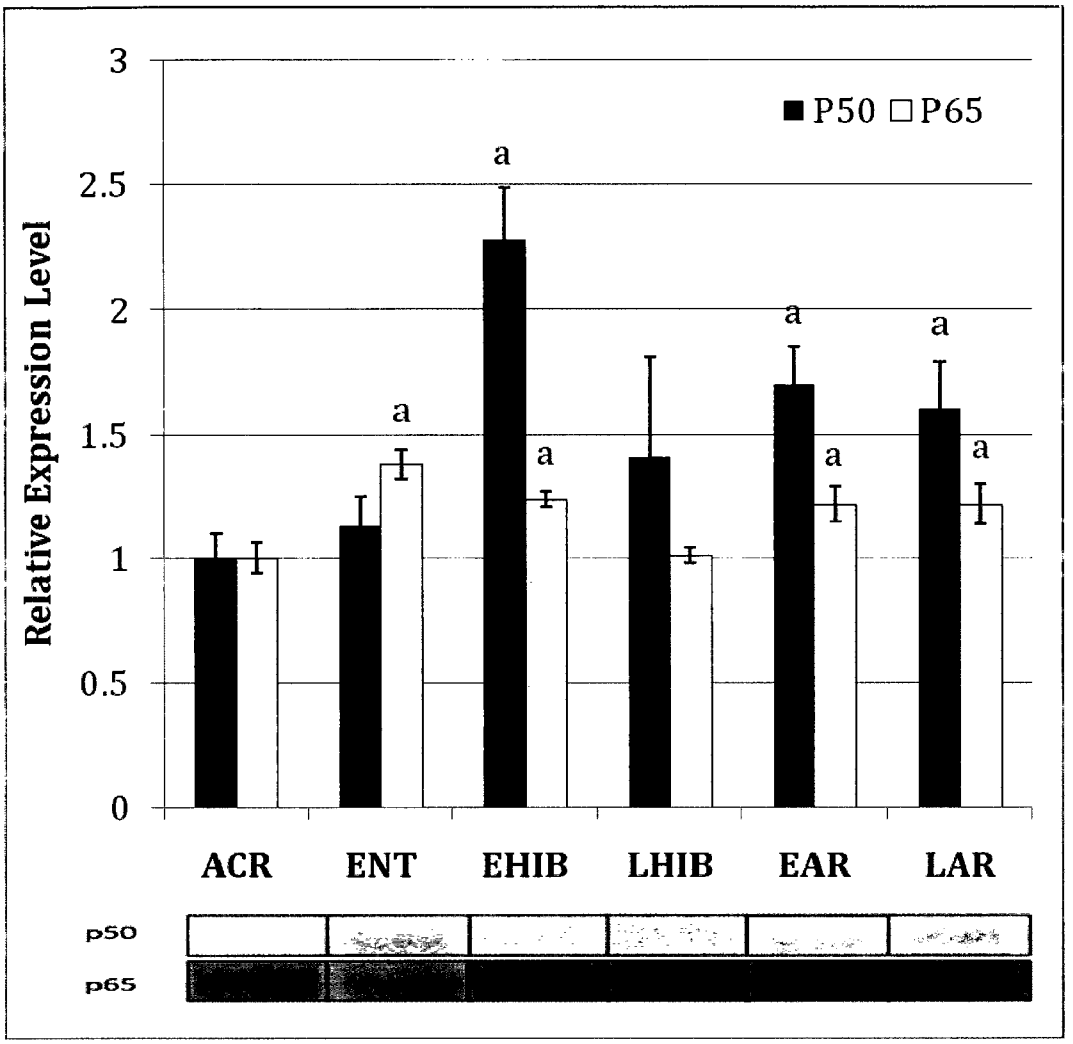

Figure 3.1: Changes in the protein levels of NF-κB transcription factor p50 and p65 subunits over the course of a torpor-arousal cycle in skeletal muscle of *S. tridecemlineatus*. Sampling points are: active in the cold room (ACR), entrance into torpor (ENT), early hibernation (EHIB), late hibernation (LHIB), early arousal (EAR) and late arousal (LAR). See Materials and Methods for more extensive definitions. Representative blots are shown along with histograms showing mean normalized band densities (± S.E.M., n=3- 4 independent trials on tissue from different animals). Data were analyzed using analysis of variance with a post hoc Student-Newman-Keuls test; **a** - denotes values which are significantly different from the ACR controls, $P<0.05$.

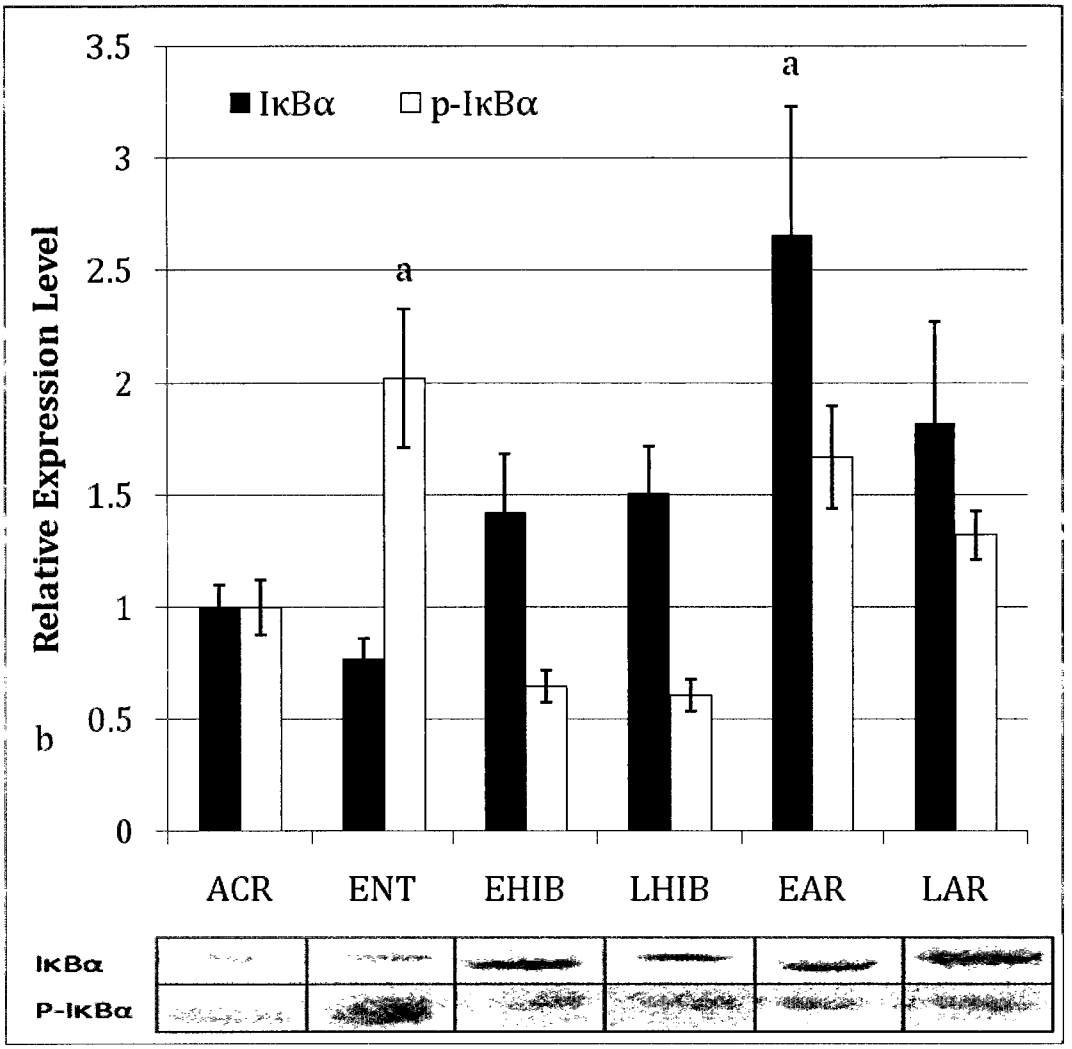

Figure 3.2: Changes in the protein levels of total and phosphorylated IκBα subunits over the course of a torpor-arousal cycle in skeletal muscle of *S. tridecemlineatus*. Sampling points are: active in the cold room (ACR), entrance into torpor (ENT), early hibernation (EHIB), late hibernation (LHIB), early arousal (EAR) and late arousal (LAR). See Materials and Methods for more extensive definitions. Representative blots are shown along with histograms showing mean normalized band densities (± S.E.M., n=3-4 independent trials on tissue from different animals). Data were analyzed using analysis of variance with a post hoc Student-Newman-Keuls test; **a** - denotes values which are significantly different from the ACR time point, $P<0.05$.

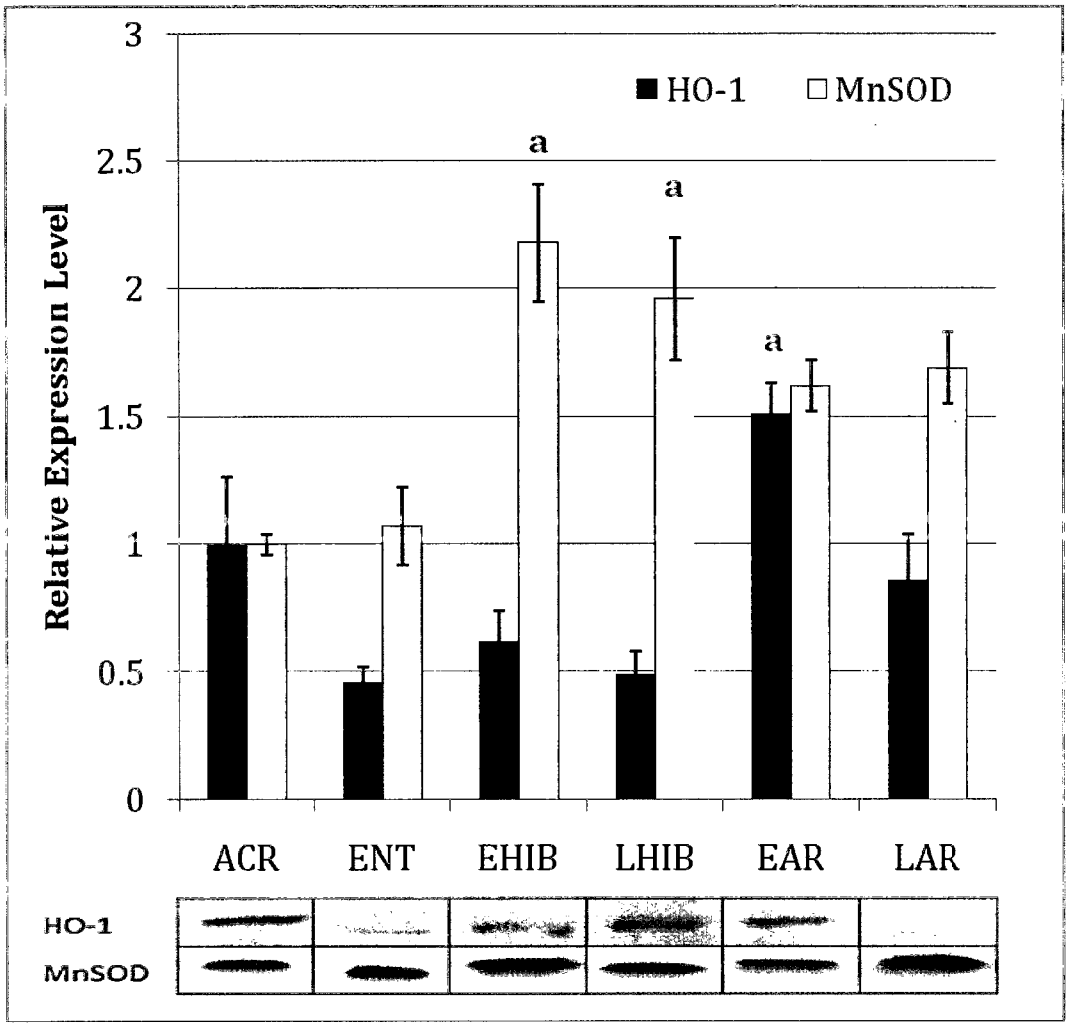

Figure 3.3: Changes in the protein levels of MnSOD and HO-1 over the course of a torpor-arousal cycle in skeletal muscle of *S. tridecemlineatus*. Sampling points are: active in the cold room (ACR), entrance into torpor (ENT), early hibernation (EHIB), late hibernation (LHIB), early arousal (EAR) and late arousal (LAR). See Materials and Methods for more extensive definitions. Representative blots are shown along with histograms showing mean normalized band densities (± S.E.M., n=3-4 independent trials on tissue from different animals). Data were analyzed using analysis of variance with a post hoc Student-Newman-Keuls test; **a** -denotes values which are significantly different from the ACR controls, $P<0.05$.

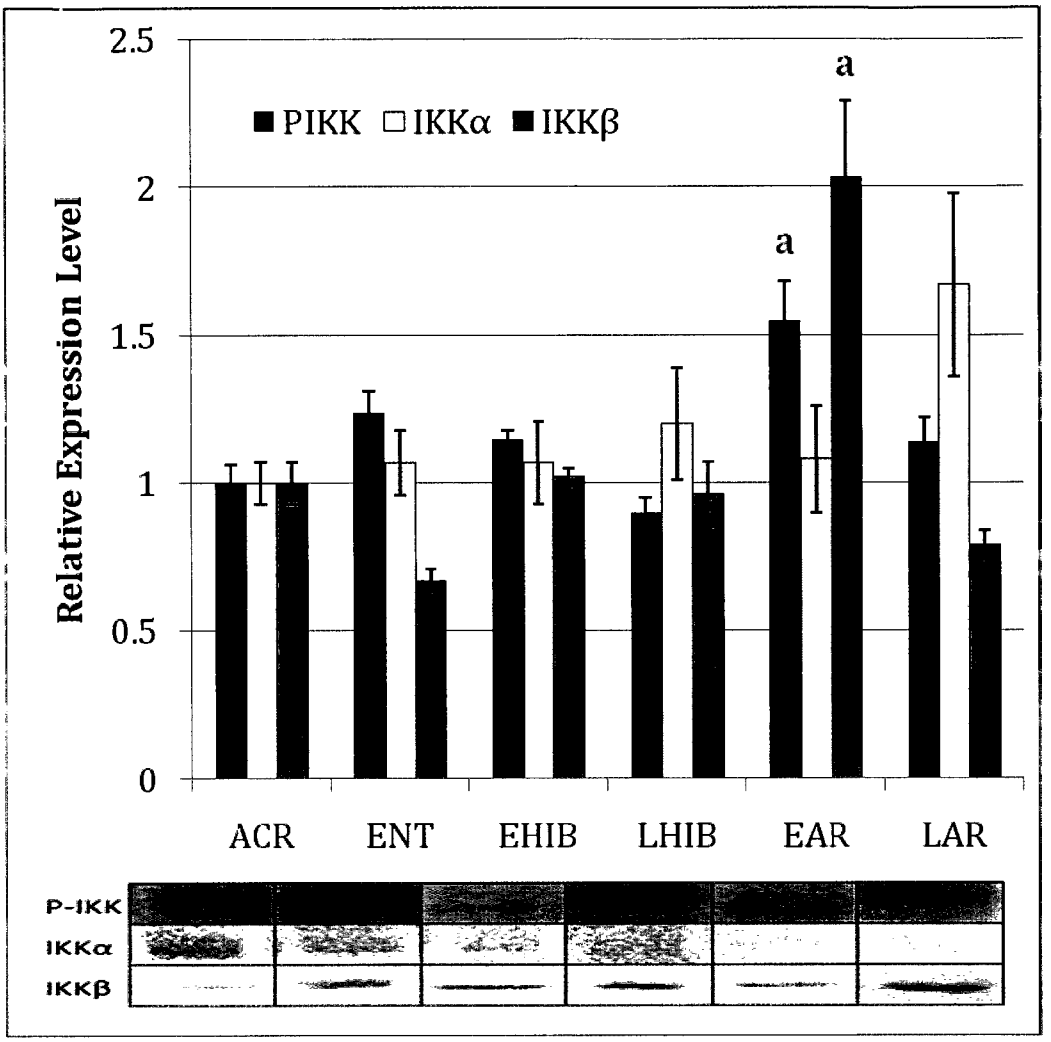

Figure 3.4: Changes in the protein levels of phosphorylated IKK and its two subunits (α and β) over the course of a torpor-arousal cycle in skeletal muscle of *S. tridecemlineatus*. Sampling points are: active in the cold room (ACR), entrance into torpor (ENT), early hibernation (EHIB), late hibernation (LHIB), early arousal (EAR) and late arousal (LAR). See Materials and Methods for more extensive definitions. Representative blots are shown along with histograms showing mean normalized band densities (± S.E.M., n=3-4 independent trials on tissue from different animals). Data were analyzed using analysis of variance with a post hoc Student-Newman-Keuls test; **a** - denotes values which are significantly different from the ACR controls, $P<0.01$.

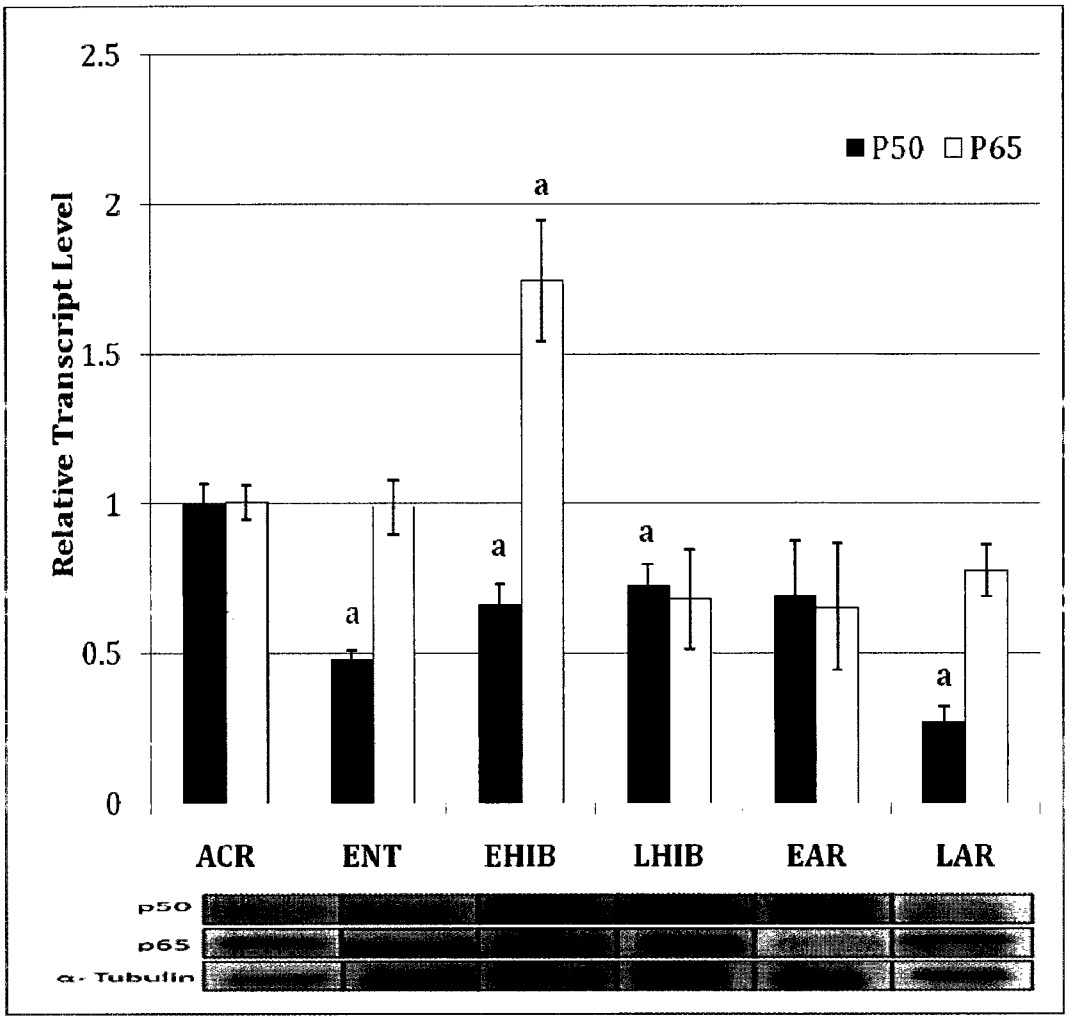

Figure 3.5: Changes in NF-κB *p50* and *p65* mRNA transcript levels in skeletal muscle of *S. tridecemlineatus* over the torpor-arousal cycle. Shown are representative bands on agarose gels (and bands for *α- tubulin* that was used for normalization) and histograms of means (± S.E.M., n=4-8 semi-independent trials on separate RNA isolations from different animals) for six sampling points. Data were analyzed using analysis of variance with a post hoc Student-Newman-Keuls test; **a** - denotes values which are significantly different from the ACR control, $P<0.05$.

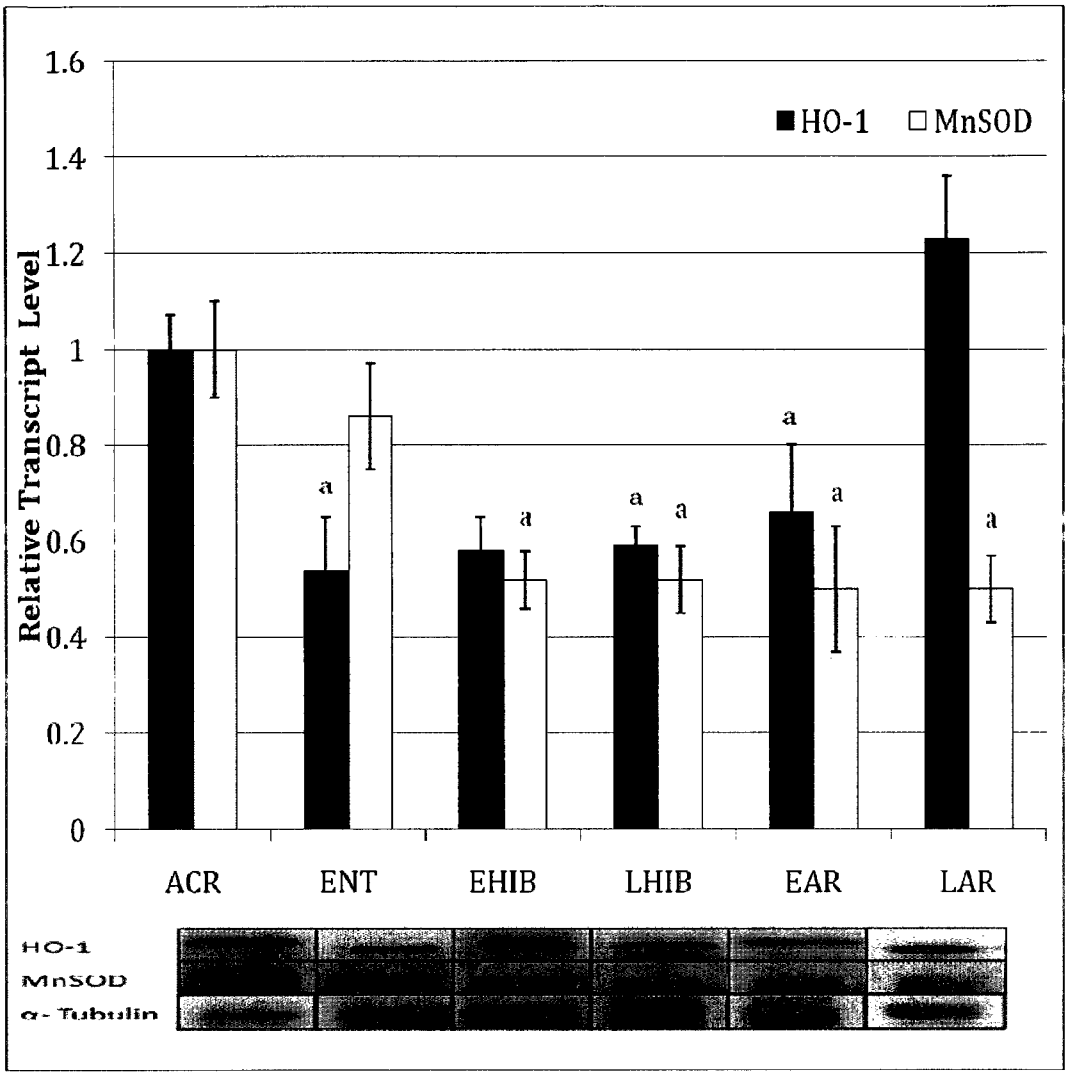

Figure 3.6: Changes in *HO-1* and *MnSOD* mRNA transcript levels in skeletal muscle of *S. tridecemlineatus* over the torpor-arousal cycle. Shown are representative bands on agarose gels (and bands for *α- tubulin* that was used for normalization) and histograms of means (± S.E.M., n=4-8 semi-independent trials on separate RNA isolations from different animals) for six sampling points. Data were analyzed using analysis of variance with a post hoc Student-Newman-Keuls test; **a** - denotes values which are significantly different from the ACR control, $P<0.05$.

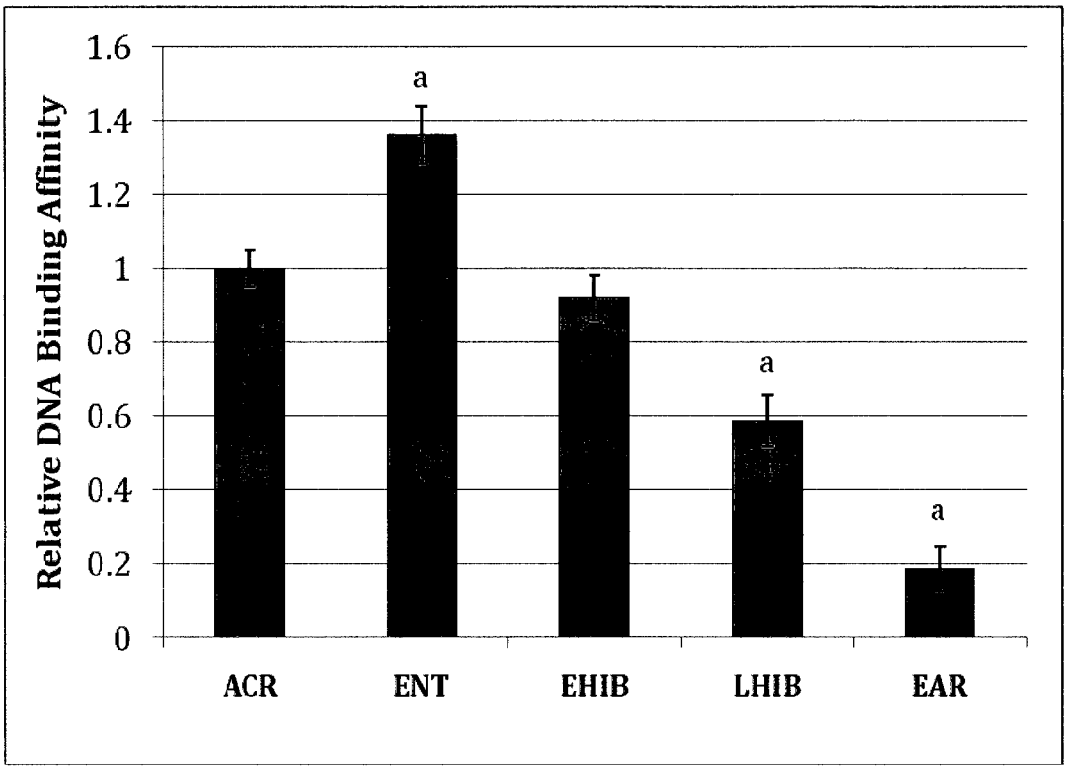

Figure 3.7: Changes in the amount of p65 DNA binding in skeletal muscle of *S. tridecemlineatus* over the torpor-arousal cycle. Histograms of normalized means (± S.E.M., n=4 independent trials on tissue from different animals) for five sampling points. Data were analyzed using analysis of variance with a post hoc Student-Newman-Keuls test; **a** - denotes values which are significantly different from the ACR time point, $P<0.005$.

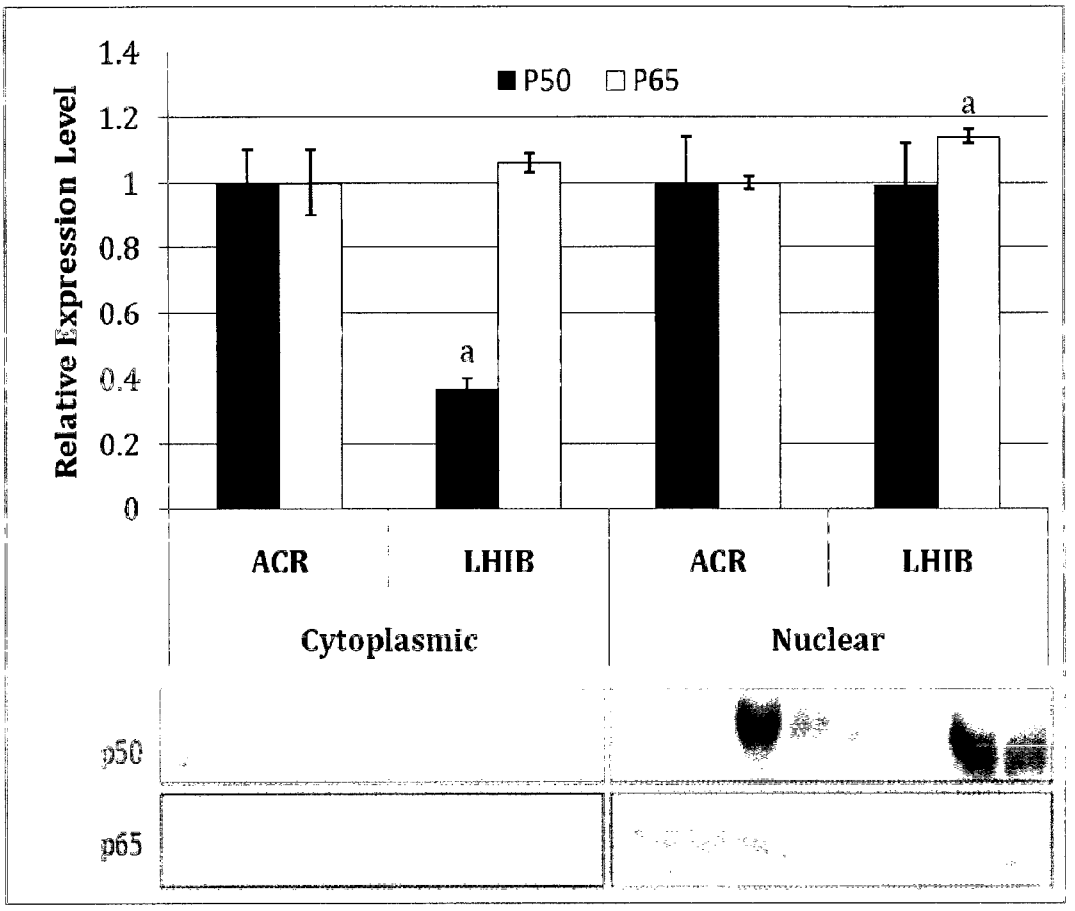

Figure 3.8: Distribution of p50 and p65 between the cytoplasm and nucleus in skeletal muscle of *S. tridecemlineatus* under control (ACR) and hibernation (LHIB) conditions. Representative Western blots are shown along with histograms showing mean normalized band densities (± S.E.M., n=3 independent trials on tissue from different animals). Data were analyzed using analysis of variance with a Student's t-test; **a** - denotes values which are significantly different from the respective ACR control for the same subcellular fraction, $P<0.01$.

A)

```
Squirrel   1   LTDREKELIRQAALQQTKEMDLSVVRLMFTAFLPDSTGSFTGRLEPVVSDAIY
Human      188 -g-----------------------------------------r----------
Mouse      186 -------i-----v-----------------------------r----------
           186 -------i-----------------------------------r----------

Squirrel   54  DSKAPNASNLKIVRMDRTAGCVTGGEEIYLLCDKV
Human      241 ----------------------------------
Mouse      239 ----------------------------------
Rat        239 ----------------------------------
```

B)

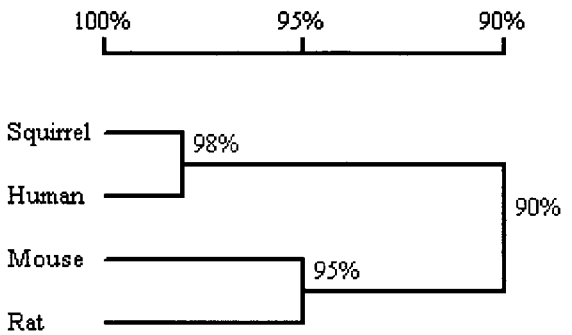

C)

Homology matrix of 4 sequences

```
Squirrel          100%
Human             97.7%  100%
Mouse             96.6%  84.0%  100%
Rat               97.7%  83.5%  95.0%  100%
```

Figure 3.9: Sequencing results for the *p50* gene product that was amplified from the ground squirrel, *S. tridecemlineatus*, skeletal muscle. The full length *Homo sapiens p50* gene codes for a polypeptide that is 968 residues in length. **A)** Multiple alignment showing the partial deduced amino acid sequence of *S. tridecemlineatus* compared to three other mammalian species: human (*Homo sapiens*, accession number: NP_001158884.1), mouse (*Mus musculus*, accession number: NP_032715) and rat (*Rattus norvegicus*, accession number: XP_342347.2). Amino acid sequences are numbered on the left. Dashed lines represents identical amino acids as found in the ground squirrel, with unique amino acids substitutions in the ground squirrel being depicted in bold and underlined. **B)** Cladogram prepared with DNAMAN depicting amino acid identity compared to other mammalian species: **C)** Homology matrix of the four sequences.

A)

```
Squirrel    1   VKKRDLEQAISQRIQTNNNPFQVPIEEQRGDYDLNAVRLCFQVTVRDPSGRPLCLP
Human       119 ----------------------------------------------------r--
Mouse       119 ----------------------h-----------------------------a----l-t
Rat         119 ----------------------------------------------------r-t

Squirrel    59  PVLSHPIFDNRAPNTAELKICRVNRNSGSCLGGDEIFLLCDKVQKEDIEVYFTGPG
Human       177 ------------------------------------------------------------
Mouse       177 ------------------------------------------------------------
Rat         177 ------------------------------------------------------------

Squirrel    113 WEARGSFSQADVHRQVAIVFRTPPYADPSLQAPVRVSMQLRRPSDRELSEPMEFQ
Human       231 ---------------------------------------------------------
Mouse       231 ---------------------------------------------------------
Rat         231 ---------------------------------------------------------

Squirrel    169 YLPDTDDRHR
Human       288 ----------
Mouse       288 ----------
Rat         288 ----------
```

B)

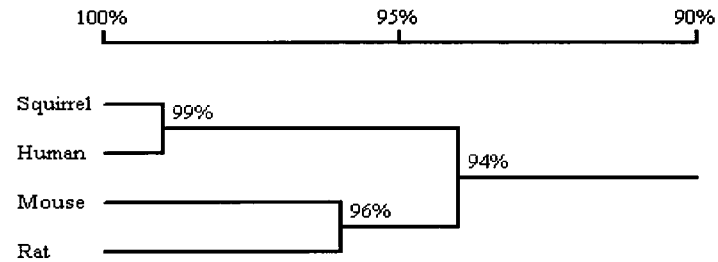

C)

Homology matrix of 4 sequences

```
Squirrel            100%
Human               99.4% 100%
Mouse               97.8% 88.9% 100%
Rat                 98.9% 90.2% 96.2% 100%
```

Figure 3.10: Sequencing results for the *p65* gene product that was amplified from ground squirrel, *S. tridecemlineatus*, skeletal muscle. The full length *Homo sapiens p65* gene codes for a polypeptide that is 549 residues in length. **A)** Multiple alignments showing the partial deduced amino acid sequence for *S. tridecemlineatus* compared to three other mammalian species: human (*Homo sapiens*, accession number: NP_068810.3), mouse (*Mus musculus*, accession number: NP_033071.1) and rat (*Rattus norvegicus*, accession number: NP_954888.1). Amino acid sequences are numbered on the left. Dashed lines represents identical amino acids as found in the ground squirrel, with unique amino acids substitutions in the ground squirrel being depicted in bold and underlined. **B)** Cladogram prepared with DNAMAN depicting amino acid identity compared to other mammalian species: **C)** Homology matrix of the four sequences.

A)

```
Squirrel    1  QIEHNTDNPVFAPLYFPEELHHRATLEQDMAFWYRPCWQQAVPYTAGMLRGSGRLQQ
Human      64  --r-kes-----v--------rk-a----l----g-r--evi---pa-q-yvk--he
Mouse      64  --r-kq---y----------r--a---------g-h--eii-c-patqhyvk--he
Rat        64  --r-kq---y----------r--a---------g-h--e-i---patqhyvk--he

Squirrel   58  VERREPEMLVAHAYTHYLGNLSRGQVLKKITHKALDLPSSREGLAFFTFPKVASA
Human     121  -g-t---l-------r---d--g-------aq--------g---------ni---
Mouse     121  -g-th--l-------r---d--g-------aq--ma----g---------nid-p
Rat       121  -ggth--l-------r---d--g-------aq--ma----g---------sidnp

Squirrel  112  TKFKQLYHSLMNTLEMTPEVRQRVIKEAKTAFLL
Human     175  -------r-r--s-----a------e--------
Mouse     175  -------rar----------kh--te--------
Rat       175  -------rar----------kh--te--------
```

B)

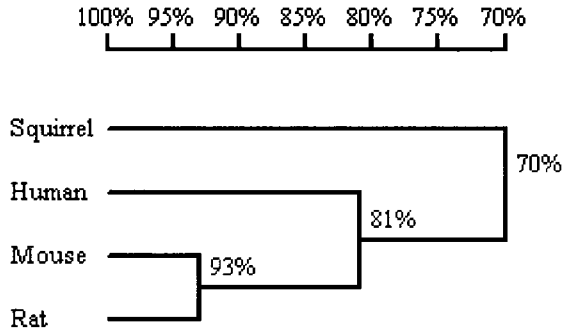

C)

Homology matrix of 4 sequences

```
Squirrel            100%
Human               73.3% 100%
Mouse               68.5% 82.3% 100%
Rat                 68.5% 80.2% 93.4% 100%
```

Figure 3.11: Sequencing results for the *HO-1* gene product that was amplified from skeletal muscle of the ground squirrel, *S. tridecemlineatus*. The full length *Homo sapiens HO-1* gene codes for a polypeptide that is 288 residues in length. **A)** Multiple alignments showing the partial deduced amino acid sequences from *S. tridecemlineatus* compared to three other mammalian species: human (*Homo sapiens*, accession number: NP_002124.1), mouse (*Mus musculus*, accession number: NP_034572.1) and rat (*Rattus norvegicus*, accession number: NP_036712.1). Amino acid sequences are numbered on the left. Dashed lines represents identical amino acids as found in the ground squirrel, with unique amino acids substitutions in the ground squirrel being depicted in bold and underlined. **B)** Cladogram prepared with DNAMAN depicting amino acid identity compared to other mammalian species: **C)** Homology matrix of the four sequences.

A)

```
Squirrel    1   SVLMGGGEPKGELLEAIKRDFGSFDKFKEKLTTVSAGVQGSGWGWLGFNKEQGRLQ
Human       105 lspn----------------------------aa-v---------------r-h--
Mouse       105 lspk--------------------e-------a--v--------------------
Rat         105 lspk--------------------e-------a--v--------------------

Squirrel    57  IAACANQDPLQGTTGLI
Human       161 ----p------------
Mouse       161 ----s------------
Rat         161 ----s------------
```

B)

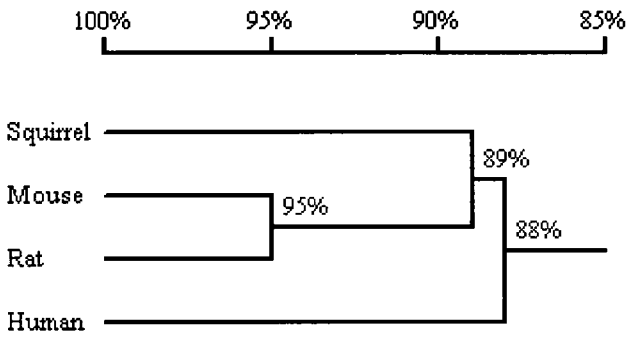

C)

Homology matrix of 4 sequences

```
Squirrel            100%
Human               86.3% 100%
Mouse               89.0% 90.1% 100%
Rat                 89.0% 87.8% 95.0% 100%
```

Figure 3.12: Sequencing results for the *MnSOD* gene product that was amplified from the ground squirrel, *S. tridecemlineatus*, skeletal muscle. The full length *Homo sapiens MnSOD* gene codes for a polypeptide that is 222 residues in length. **A)** Multiple alignments showing the partial deduced amino acid sequence from ground squirrel compared to three other mammalian species: human (*Homo sapiens*, accession number: NP_000627), mouse (*Mus musculus*, accession number: NP_038699) and rat (*Rattus norvegicus*, accession number: NP_058747.1). Amino acid sequences are numbered on the left. Dashed lines represents identical amino acids as found in the ground squirrel, with unique amino acids substitutions in the ground squirrel being depicted in bold and underlined. **B)** Cladogram prepared with DNAMAN depicting amino acid identity compared to other mammalian species: **C)** Homology matrix of the four sequences.

Discussion:

Skeletal muscle is a vital organ in ensuring the survival of hibernators during their arousal periods from torpor due to its role in raising Tb to euthermic values via shivering thermogenesis. Hibernation results in the immobilization of the organism for prolonged periods of time and a high degree of oxidative stress. Unlike non-hibernators which would have severe muscle atrophy due to disuse and damaging ROS, hibernators mitigate these problems by upregulating certain protective mechanisms and by decreasing their metabolic rate and oxygen consumption in a regulated, coordinated manner (Tessier & Storey, 2010). Although there are a variety of mechanisms, which can minimize this damage, the differential regulation of transcription factors is of great importance since they can change the expression of a variety of downstream targets in a coordinated fashion, resulting in substantial changes in the proteome during times of metabolic depression. Numerous transcription factors have already been implicated as having a role in muscle atrophy including NF-κB, C/EBP (CCAAT/enhancer binding protein) and FOXOs (Forkhead box O) (Hasselgren, 2007A).

During times of exercise, ROS production increases, activating NF-κB, which selectively upregulates target genes, such as MnSOD and HO-1, in order to protect muscle and minimize damage caused by oxidative stress. Although there are a variety of other redox sensitive signaling pathways that can mediate antioxidant responses such as MAPK, PI(3)K/Akt, p53 and the heat shock response, NF-κB has been found to be one of the most important in determining the amount of protection from oxidative stress (Ji et al., 2007). The complexity of NF-κB activation which results in both antioxidant and

proinflammatory response being turned on has been the topic of much research concerning muscle atrophy since these competing messages can result in either destruction or maintenance of cell integrity. Recently it has been shown that both the canonical and noncanonical NF-κB signaling pathways can be employed in an atypical or alternative way during immobilization and atrophy, suggesting significant roles for both pathways in mediating the pathology (Bar-Shai et al., 2008). Therefore, understanding NF-κB regulation during hibernation may result in a better understanding of how these conflicting signals are integrated to produce a protective response during sustained immobilization, which minimizes the amount of muscle atrophy endured.

In this present study, NF-κB was found to be activated during the early phases of torpor in skeletal muscle, followed by a decrease in its activity during late torpor and arousal. This activation was evident by the increased level of p65 within the nucleus binding to its promoter during ENT (~1.4 fold increase), which was followed by a constant decrease in levels during EHIB, LHIB and EAR (Figure 3.7). The increases in p65 binding levels were accompanied with an increased amount of p65 nuclear translocation during hibernation (Figure 3.8). Since transcription factor activation normally results in a change in the subcellular location of the protein (either into or out of the nucleus), it is reasonable to assume that NF-κB is activated in skeletal muscle during hibernation and this is based upon the observation that translocation into the nucleus increases, as does binding to its promoter.

The activation that occurs in skeletal muscle appears to be the result of the canonical NF-κB signaling pathway since p65 appears to be mediating the response due to it being released from P-IκBα (Dejardin, 2006). This is evident by the fact that the

increased DNA binding during ENT was accompanied by a dramatic increase in P-IκBα (2-fold), while the observed subsequent decrease in binding was correlated with decreased phosphorylation levels of the inhibitor (Figure 3.2). This increase in P-IκBα level during ENT indicates that the nuclear translocation and activation of NF-κB is a result of IκBα being phosphorylated and then being degraded by the ubiquitin-proteasomal pathway, which allows the p50 and p65 subunits to enter the nucleus and selectively upregulate NF-κB target genes.

In order to assess whether the activated NF-κB upregulated its target genes, their expression levels were examined and assessed. By examining Figure 3.1 it is evident that following ENT, there is an increased expression of p50 which is sustained throughout the remainder of torpor and arousal whereas p65 levels only increased marginally but were also sustained throughout hibernation. It is important to note that p50 contains a κB promoter in its upstream regulatory region which allows for auto-upregulation during canonical NF-κB signaling (Ten et al., 1992). These data suggest that NF-κB is binding to its promoter and upregulating its target genes during ENT since p50 levels had increased expression following the nuclear translocation of the transcription factor due to P-IκBα induced dissociation (Cogswell et al., 1993). This temporal delay in protein expression following promoter binding is essential since it takes time for the transcription factor to bind, alter transcription and then have its mRNA product translated. P65 levels were highest during ENT, which suggests that its expression was being regulated by other transcription factors such as Sp1 prior to NF-κB activation, since it lacks a κB promoter region (Ueberla et al., 1992). Therefore, the differential regulation of the NF-κB subunits by the canonical NF-κB signaling pathway, with p50 expression increasing following

ENT suggest that the transcription factor is binding to its promoter during ENT and selectively upregulating its target genes.

As previously stated, NF-κB negatively regulates itself by upregulating its inhibitor, IκBα, thereby ensuring the response is specific, concise and controlled. By examining Figure 3.2, it is evident that the amount of IκBα increases dramatically following ENT, peaking at EAR. This suggests that NF-κB is binding to its κB promoter upstream of the *IκBα* gene (Scott et al., 1993) during ENT into torpor and results in the increased expression of its inhibitor during torpor and arousal. The increased expression of its inhibitor during late torpor and arousal also correlates well with the decreased amount of p65 binding in the nucleus during these time points. Therefore, these data show that NF-κB is activated during ENT, which is a result of IκBα being phosphorylated and freed from the transcription factor, thereby allowing it to translocate into the nucleus and upregulate its target genes, including p50 and IκBα. The synthesis of its inhibitor during hibernation is essential to the organism's survival since it provides a regulatory mechanism with which to limit NF-κB activation, thereby ensuring the correct amount of proinflammatory and antioxidant gene products are produced to protect the skeletal muscle from atrophy and oxidative stress.

The antioxidant downstream targets, MnSOD and HO-1, showed differential expression levels throughout torpor-arousal that were similar to those seen for p50 and IκBα. Figure 3.3 shows that MnSOD expression increased dramatically in EHIB and sustained levels were greater than the control throughout the remainder of the torpor-arousal cycle. Unlike MnSOD, HO-1 levels decreased during the entry into torpor, increased dramatically during EAR, but then subsequently decreased once again.

Therefore, both of these antioxidant downstream targets showed dramatic increases over the torpor-arousal period subsequent to NF-κBs activation and entry into the nucleus. The increase in expression at different times would suggests that NF-κB upregulates its varying target genes at various points along the torpor-arousal cycle, which is probably due to changes in promoter accessibility via chromatin remodeling (Morin et al., 2008A). The differential expression of these target genes could also be a result of microRNAs interacting with the mRNAs transcripts of the downstream targets, thereby also regulating their expression at the translational level during torpor and arousal (Morin & Storey, 2009). From these results, it is clear that antioxidant enzymes are differentially upregulated during hibernation across the torpor-arousal cycle and that this regulation may be influenced by the redox sensitive transcription factor NF-κB.

In order to gain a better insight into the regulation of the antioxidant downstream targets, RT-PCR was performed to assess the relative levels of mRNA for each species. Figure 3.6 depicts the changes in mRNA expression for *HO-1* and *MnSOD*. Overall, a substantial decrease in mRNA was found to accompany entry into hibernation for *HO-1*, which gradually grew in levels until LAR, when it dramatically increased. *MnSOD* transcripts were high in ACR, decreased during entry into torpor and then remained at a constant lower level from EHIB through LAR. Given that torpor-arousal bouts are cyclical in nature over the hibernation season, the increased *MnSOD* transcript level during ENT, when compared to EHIB, LHIB, EAR and LAR, correlates with the dramatic increase in MnSOD protein levels seen during EHIB and sustained throughout arousal. Therefore, although the transcript level decreases during hibernation, relative to the ACR control, there is an increase during ENT relative to the other torpor-arousal time

points, which correlates with the increased MnSOD protein level suggesting NF-κB may be regulating its expression.

HO-1 transcript levels showed a different expression pattern in which the level was sustained throughout entrance and torpor with a gradual increase that led to a dramatic increase during LAR. Unlike MnSOD, transcript levels of *HO-1* did not correlate well with protein expression data, meaning the maximal mRNA expression level did not precede the maximal protein level. This is not a cause for alarm since mRNA and protein expression patterns do not always correlate with one another since many other factors including chromatin remodeling, translational regulation, degradation pathways and post-translational modifications can affect the expression level of a protein (Guo et al., 2008). Also, other transcription factors could cause this spike in *HO-1* transcripts during hibernation, such as Nrf2 (Morin et al., 2008B). Although a correlation was not evident for HO-1, the results do indicate that the target genes show differential regulation over the torpor-arousal cycle and that antioxidant genes play an important role in ensuring the survival of the ground squirrel via their differential regulation by transcription factors.

The mRNA levels of *p50* and *p65* were also examined with each showing differential expression patterns (Figure 3.5). The *p50* subunit transcript levels decreased substantially during entry into torpor; however these levels then slightly rose and were sustained until LAR, where they decreased once again. This gradual increase in mRNA during torpor correlated with the increased protein expression seen during torpor and arousal suggesting that NF-κB may be upregulating expression of its own subunit. On the other hand, *p65* transcripts increased dramatically early in torpor and then decreased and

maintained this level during LHIB and arousal. Although the spike in transcript levels did not correlate with a spike in protein expression levels, the continual expression of *p65* mRNA during torpor-arousal may be sufficient to account for the increased amount of p65 protein over the torpor-arousal cycle. Since NF-κB does not regulate *p65* gene transcription, the reason for this variability will not be addressed further.

The final group of proteins to be examined in the skeletal muscle of hibernating ground squirrels was the IKK complex and its components (Figure 3.4). The expression pattern of IKKα did not change throughout the torpor-arousal cycle, which is not surprising since this component is not necessary for the phosphorylation of IκBα. However, IKKα is essential for allowing the full activation of NF-κB downstream genes by influencing the acetylation/phosphorylation of histone H3 residues around their κB promoter. Therefore, these data indicate that the amount of IKKα, which is sustained at control levels throughout hibernation, is adequate for the skeletal muscle to avoid atrophy during this state of metabolic depression. Interestingly, both P-IKK and IKKβ showed similar expression patterns; levels were maintained at about the control value with a dramatic significant increase seen during EAR. This dramatic increase in the activated form, P-IKK, and the kinase responsible for phosphorylating IκBα, IKKβ, during EAR, suggests that NF-κB is activated during arousal, with the level of activity decreasing again upon re-entry into torpor. The increase in the amount of P-IKK was correlated with increased amounts of P-IκBα during arousal which peaked during ENT. Therefore, this suggests that NF-κB is regulated in a cyclical pattern based on the hibernator's torpor-arousal cycle: activating kinases are maximally expressed during arousal which results in increased P-IκBα levels throughout arousal and entrance into torpor, subsequently

causing NF-κB to translocate into the nucleus, maximally during ENT, where it can selectively upregulate its target genes for the next arousal period.

In order to ensure that the PCR gene products that were amplified encoded the genes of interest, DNA sequencing was performed on each sample from skeletal muscle. Figure 3.9-3.12 depict the deduced amino acid sequence for each gene, including the alignment of these protein sequences to known human, mouse and rat sequences. The ground squirrel amino acid sequences were highly conserved compared with those of the other mammals, with p50, p65, HO-1 and MnSOD showing respectively 90, 94, and 70 and 88% mean identity when all 4 species were considered together. These values indicate that the genes amplified were the proper targets and that they were highly conserved between the four mammalian species.

In conclusion, it was determined that NF-κB is regulated in a cyclical pattern which is based upon the torpor-arousal cycle that ground squirrels experience during the winter hibernation season. Starting from arousal and going to entrance into torpor, the amount of P-IKK increases which subsequently results in elevated amounts of P-IκBα. This leads to P-IκBα being degraded and allows the NF-κB dimer to translocate into the nucleus where it binds to its κB promoter, upregulating its target genes, which ensures that their products are expressed and ready for arousal. Following entry into torpor the level of NF-κB activation decreases from the ENT maximal value until it returns to this elevated point during the subsequent torpor-arousal cycle. Therefore, the regulation of NF-κB is important in maintaining skeletal muscle integrity during hibernation and this is seen by its time dependant activation and deactivation which results in the selective upregulation of its target genes, including antioxidants and its own inhibitor. This high

expression and activation of NF-κB during late arousal and entry into torpor ensures that the antioxidant products needed to compensate for the oxidative stress associated with elevated oxygen consumption and increased metabolic rate during arousal from torpor are available and sufficient to mitigate possible tissue damage and muscle atrophy.

Chapter 4

NF-κB Regulation In The Liver

Introduction:

The liver is an essential organ that is responsible for many functions including the detoxification of metabolites, production of digestive enzymes, glycogen/glucose storage/release and the regulation of many other aspects of the body's metabolism. The liver also acts as a gland by controlling the secretion of angiotensinogen and insulin-like growth factor (IGF) thereby regulating aldosterone levels, blood pressure, growth and metabolism (Neo et al., 2010; Breuhahn & Schirmacher, 2008). Gluconeogenesis, glycogenolysis, glycogenesis, protein synthesis and degradation, bile production, cholesterol metabolism, iron storage and conversion of ammonia to urea are only a few of the essential tasks that the liver performs (Li & Chiang, 2009; Friedman, 2008; Suh et al., 2007). Due to the high metabolic activity of the liver, and in particular its major role in detoxification processes, hepatocytes have high amounts of cytoprotectants in order to limit cellular damage by secondary metabolites or other by-products (Crichton et al., 2002). This and the fact that the liver has the ability to regenerate itself makes it an excellent and unique model of cell proliferation control and tissue damage, growth and repair (Michalopouloslm, 1990).

NF-κB is involved in many vital functions within the liver including the degradation of microbial pathogens, proliferation of hepatocytes when hepatic mass decreases due to injury, and protecting hepatocytes from TNFα-induced cell death (Chakraborty & Mann, 2010). For example, mice defective in the IKK subunit, NEMO, developed spontaneous chronic hepatitis that is characterized by liver inflammation, compensatory hepatocyte proliferation, and increased hepatocyte apoptosis, leading to hepatocellular carcinomas (Paspatrakis, 2009; Luedde et al., 2007). This dramatic change

in liver homeostasis is not surprising given mice lacking p65, IKKβ or NEMO die *in utero* due to degeneration of the fetal liver via TNFα induced apoptosis (Tanaka et al., 1990; Schmidt-Supprian et al., 2000).

Although complete ablation of NF-κB function results in liver pathogenesis, some studies have found that selected ablation of key components, for example IKKβ, can result in a significantly reduced amount of liver necrosis and inflammation during times of I/R injury (Luedde et al., 2005). I/R events produce liver dysfunction by causing a biphasic inflammatory response in which Kupffer cells initiate the cascade by producing ROS. This leads to NF-κB activation in hepatic parenchymal and non-parenchymal cells, with subsequent recruitment and activation of neutrophils via inflammatory mediators, leading to an ever increased level of ROS production (Kuboki et al., 2007) and hepatocyte injury. However, the activation of NF-κB is known to decrease the amount of hepatic damage, and is thought to be mediated though an alternative signaling pathway using other machinery such as peptidyl-prolyl isomerase, which is a DNA binding regulator (Kuboki et al., 2009).This alternative signaling pathway also results in different posttranslational modifications of IκBα such as tyrosine phosphorylation, but is also influenced by components of the canonical IKK complex, such as IKKβ (Wullaert et al., 2007).

By examining the different cell types in the liver, scientists have been able to elucidate the differing signaling pathways and found that hepatocytes use the alternative pathway whereas Kupffer cells utilize the classical pathway. During I/R, the hepatocytes encounter ROS due to drastic changes in oxygen consumption, resulting in c-Src activation and subsequent phosphorylation of tyrosine residues on IκBα. This

phosphorylation results in IκBα being released, but not subsequently ubiquitinated and degraded by the proteasome; however, gene transcription of protective genes still occurs by the freed p50/p65 dimer. This upregulation of cytoprotective genes by the alternative pathway ceases during prolonged ischemia and ROS production due to the increase of GSSG (oxidized glutathione), which is a potent inhibitor of NF-κB, and possibly by the increased activity of an *in vivo* tyrosine phosphatase which leads to dephosphorylation of tyrosine phosphorylated IκBα. The pro-inflammatory genes are believed to be produced by nonparenchymal cells whose NF-κB is activated by TNF or LPS (Figure 4.1) (Llacuna et al., 2009). Therefore, in the future, researchers must try to examine specific cells types individually when examining I/R events in the liver since the exact mechanism and intricacies between cell types still need to be elucidated.

The dichotomy of NF-κB activation leading to antioxidant and proinflammatory activation during I/R in the liver is only further complicated by the fact that other transcription factors such as AP-1 and HSF1 also modulate transcription during I/R events which can influence IL-6 expression, thereby influencing NF-κB activity (Tacchini et al., 2006). HO-1 (Xue et al., 2007) and MnSOD (Pardo et al., 2008), are known to be induced during I/R events in the liver to provide protection against oxidative stress, with EC-SOD and catalase also known to mitigate tissue damage when present (He et al., 2006). Age has also been found to be factor in NF-κB activation and protection, with younger mice surviving I/R events more readily due to their proteasome being more efficient at degrading phosphorylated and ubiquitinated IκBα as compared to older mice. This increased activation was suggested to be mediated by the proteasomal degradation component, PSMD4 (proteasome subunit, non-ATPase 4), due to an increase

in its expression in young livers during I/R (Huber et al., 2009).

The protective mechanisms that hibernators utilize in order to reduce hepatic injury during cold I/R events is of interest since they provide a natural model of effective cytoprotection. Lindell and colleagues (2005) have done some preliminary studies in which they observed reduced liver damage that was associated with decreases in Kupffer cell activation leading to maintained mitochondrial respiration and bile production between hibernating (aroused and torpor) and summer active ground squirrels. The known role of NF-κB as a modulator of liver growth/regeneration (Taub, 1996) and antioxidant defense during I/R events (Fan et al., 1999; Yuan et al., 2005) in mouse models suggests that this transcription factor is a key signaling molecule during oxidative stress. This implies that NF-κB would probably change its expression/activation pattern over the course of torpor-arousal cycles in hibernating animals in order to protect the structural integrity of the liver.

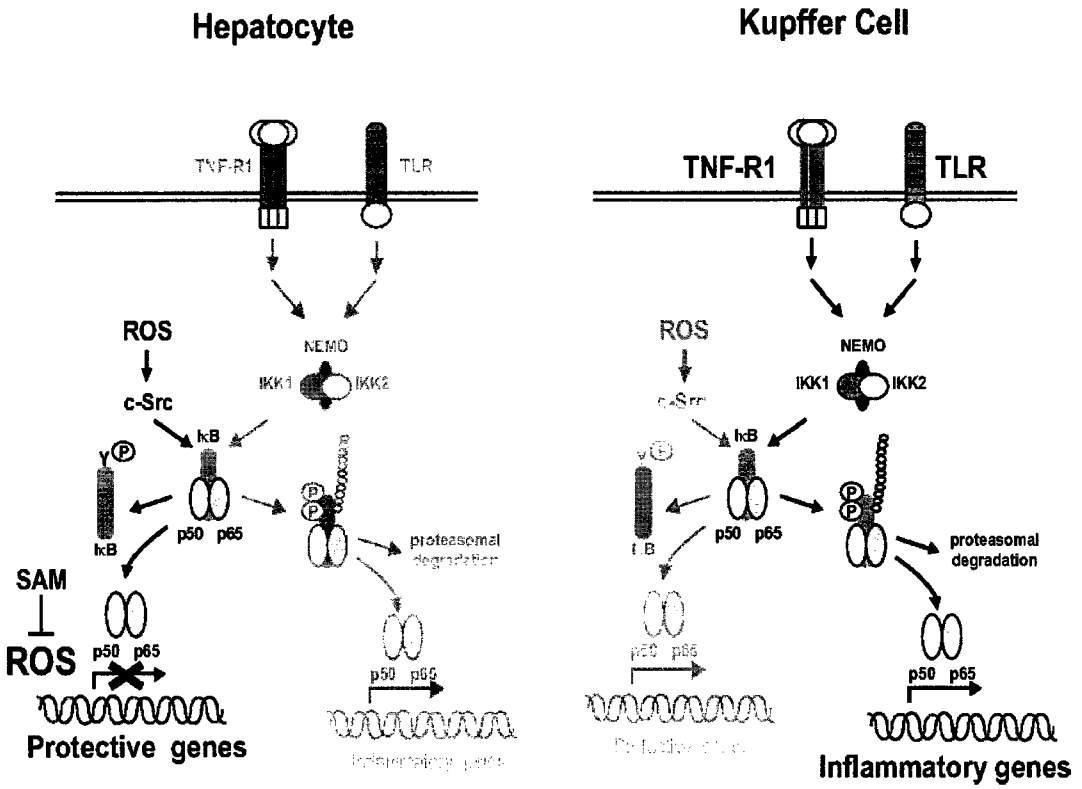

Figure 4:1: Differing NF-κB signaling pathways induced by ischemia/reperfusion in the liver. In hepatocytes, ROS initially results in the activation of c-Src, which subsequently phosphorylates IκB at a tyrosine residue, allowing the p50/p65 subunits to translocate into the nucleus and trigger the upregulation of protective genes. The alternative pathway is utilized until ROS overwhelm the system. In Kupffer and other nonparenchymal cells the classical pathway is utilized. This results in IκB being phosphorylated on two serine residue by the IKK complex and subsequently ubiquitinated and then degraded by the proteasome allowing for the expression of inflammatory genes. Image from Llacune et al., 2009.

Results:

Analysis of NF-κB protein levels

Levels of NF-κB subunits (p50 and p65) in the liver were measured by immunoblotting comparing a pre-hibernation control (ACR) and five time points on the torpor-arousal cycle: ENT, EHIB, LHIB, EAR and LAR (Figure 4.2). Each antibody crossreacted with a single band on immunoblots at the expected molecular mass for the p50 and p65 subunits at 50 and 65 kDa, respectively. Compared to ACR, both p50 and p65 had significantly higher protein levels during LHIB, with a respective 3.4 and 3.6-fold increase observed ($p<0.05$), followed by a return to near control values for the remainder of arousal.

Analysis of IκBα and P-IκBα

Total and phosphorylated forms of IκBα were measured in the liver over the time course of torpor-arousal (Figure 4.3). The antibodies crossreacted with a single band on immunoblots at the expected molecular mass of the dephosphorylated and phosphorylated (Ser 32) IκBα forms, respectively, at approximately 39 and 40 kDa. Compared with ACR, a strong decrease in IκBα occurred during ENT and then levels remained low throughout torpor and then rose again to near control values during arousal. ENT, EHIB and LHIB were respectively 32, 63 and 62% of the ACR maximum value ($P<0.05$). The amount of phosphorylated IκBα Ser32 showed a similar, but not as dramatic a decrease during ENT (68% of ACR value $P<0.005$), followed by a return to near control values during EHIB. During LHIB and LAR, strong increases in the amount

of the phosphorylated protein were observed with respectively a 2.1 and 2.2-fold increase with respect to ACR ($P<0.005$), followed by a return to control values during EAR.

Analysis of HO-1 and MnSOD

Protein levels of the downstream gene targets of NF-κB, HO-1 and MnSOD, were measured over the torpor-arousal cycle (Figure 4.4). The antibodies cross reacted with a single band on immunoblots at the expected molecular mass of 24 and 32 kDa for MnSOD and HO-1, respectively. The amount of HO-1 stayed near control value throughout torpor and arousal, expect for the dramatic increase seen during LHIB, which had a 3-fold greater expression level when compared to the ACR control ($P<0.05$). When compared to ACR, MnSOD expression levels dramatically increased 2.4-fold during ENT ($P<0.05$) and subsequently decreased to below or near the control values for the reminder of hibernation.

Analysis of P-IKK, IKKα, IKKβ

The protein kinase that regulates IκBα, IKK, was analyzed by measuring the levels of both subunits (α and β) as well as the overall phosphorylation state of the Ser176/180 residues (Figure 4.5). The antibodies cross reacted with a single band on the immunoblots at the expected molecular mass of 85, 87 and 85/57 kDa for IKKα, IKKβ and P-IKK, respectively. P-IKK expression levels were dramatically increased 2.8-fold during ENT ($P< 0.005$), followed by a decrease and stabilization over the remainder of the torpor-arousal cycle, at a level that was above the ACR value. Values in LHIB, EAR and LAR were respectively 1.7, 1.45 and 2-fold higher than the ACR control ($P< 0.005$).

A similar expression pattern was seen for IKKα; during ENT a strong increase was seen, followed by a subsequent decrease, then stabilization at expression levels above the ACR value. The expression levels in ENT, LHIB, EAR and LAR were respectively 1.5, 1.5,1.5 and 1.6-fold larger, with respect to the ACR control, whereas EHIB was 68% of the ACR value ($P< 0.05$). The IKKβ expression pattern was different then the other IKK components, with reduced levels seen throughout the entire torpor-arousal cycle. ENT, EHIB, LHIB, EAR and LAR were, respectively, 68, 45, 72, 70 and 65% of the ACR value ($P<0.005$).

Analysis of *p50* and *p65* transcript level

The primers for *p50* and *p65* were used in RT-PCR to assess relative mRNA transcript levels in liver over the torpor-arousal course. Figure 4.6 shows *p50* and *p65* expression levels. As compared with ACR, *p50* transcript levels increased strongly during ENT (by 2.7 fold, $P<0.05$) and remained elevated through EHIB, LHIB and EAR being 1.3, 1.6, and 1.2-fold higher than ACR values, respectively. During LAR, levels were reduced to 65% of the ACR value. *P65* transcript levels also rose significantly during ENT (by 2.2 fold, $P<0.005$) and remained significantly elevated though EHIB, LHIB, EAR and LAR being respectively 1.4, 2.1, 1.8 and 1.5-fold higher than the ACR value ($P<0.05$).

Analysis of *HO-1* and *MnSOD* transcript level

The primers for *HO-1* and *MnSOD* were used in RT-PCR to assess relative mRNA transcript levels in liver over the torpor-arousal course. Figure 4.7 shows *HO-1*

and *MnSOD* expression levels. Compared to the ACR controls, *HO-1* transcript levels increased significantly during ENT and remained high over the remaining sampling points resulting in levels in ENT, EHIB, LHIB, EAR and LAR that were, respectively, 1.7, 2, 1.7, 1.8 and 1.6-fold higher than ACR ($p< 0.05$). *MnSOD* transcript levels also rose significantly during ENT by 1.6- fold ($P< 0.005$), but in contrast to *HO-1*, levels were reduced again to values similar to ACR over the remainder of the hibernation course.

Analysis of p50 and p65 nuclear localization

Figure 4.8 shows the distribution of p50 and p65 between cytoplasmic and nuclear fractions, comparing the ACR and LHIB conditions. P50 protein levels increased significantly in both the cytoplasmic and nuclear fractions of liver during torpor compared to the corresponding ACR control value for the same subcellular fraction with respective 1.4 and 1.7-fold increases ($p< 0.01$). P65 protein levels also increased significantly in both subcellular fractions during hibernation with a 2.1 ($p< 0.05$) and 1.3-fold ($p< 0.01$) increase compared to the ACR controls for the cytoplasmic and nuclear fractions, respectively.

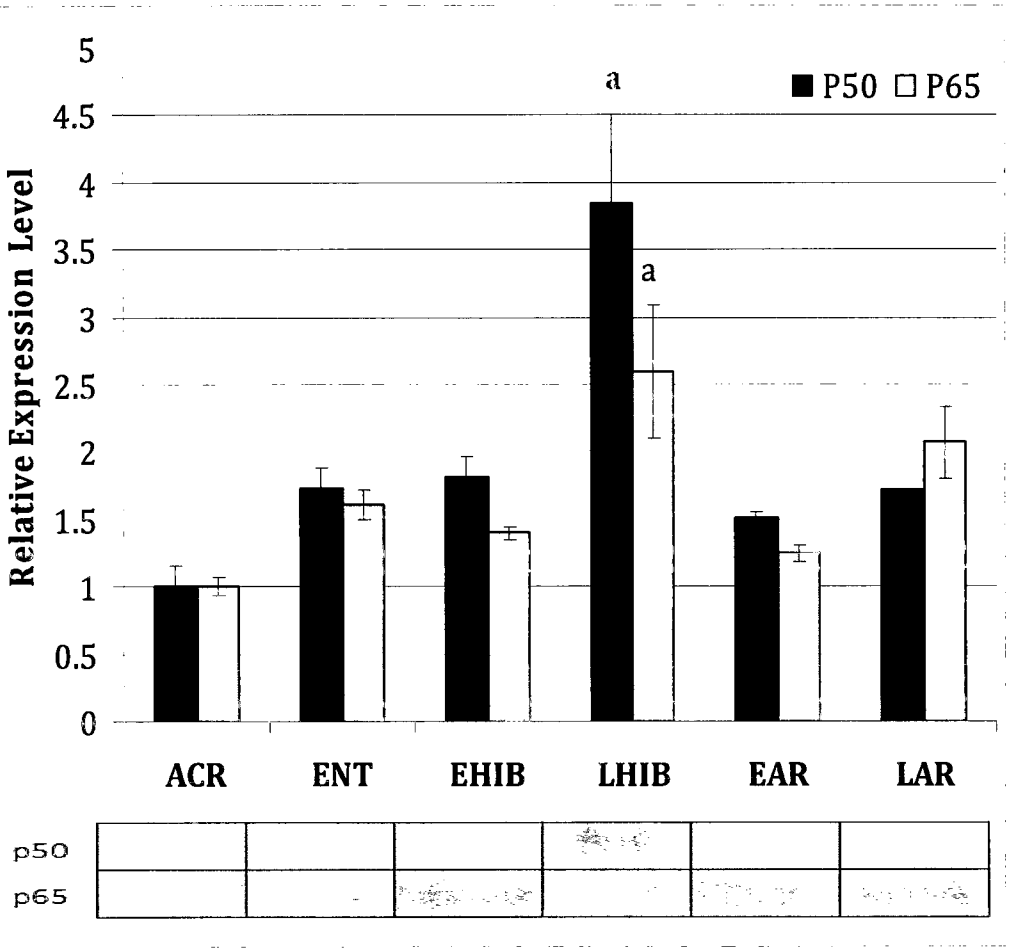

Figure 4.2: Changes in the protein levels of NF-κB transcription factor p50 and p65 subunits over the course of a torpor-arousal cycle in liver of *S. tridecemlineatus*. Sampling points are: active in the cold room (ACR), entrance into torpor (ENT), early hibernation (EHIB), late hibernation (LHIB), early arousal (EAR) and late arousal (LAR). See Materials and Methods for more extensive definitions. Representative blots are shown along with histograms showing mean normalized band densities (± S.E.M., n=3 -4 independent trials on tissue from different animals). Data were analyzed using analysis of variance with a post hoc Student-Newman-Keuls test; **a** - denotes values which are significantly different ACR control, $P<0.05$.

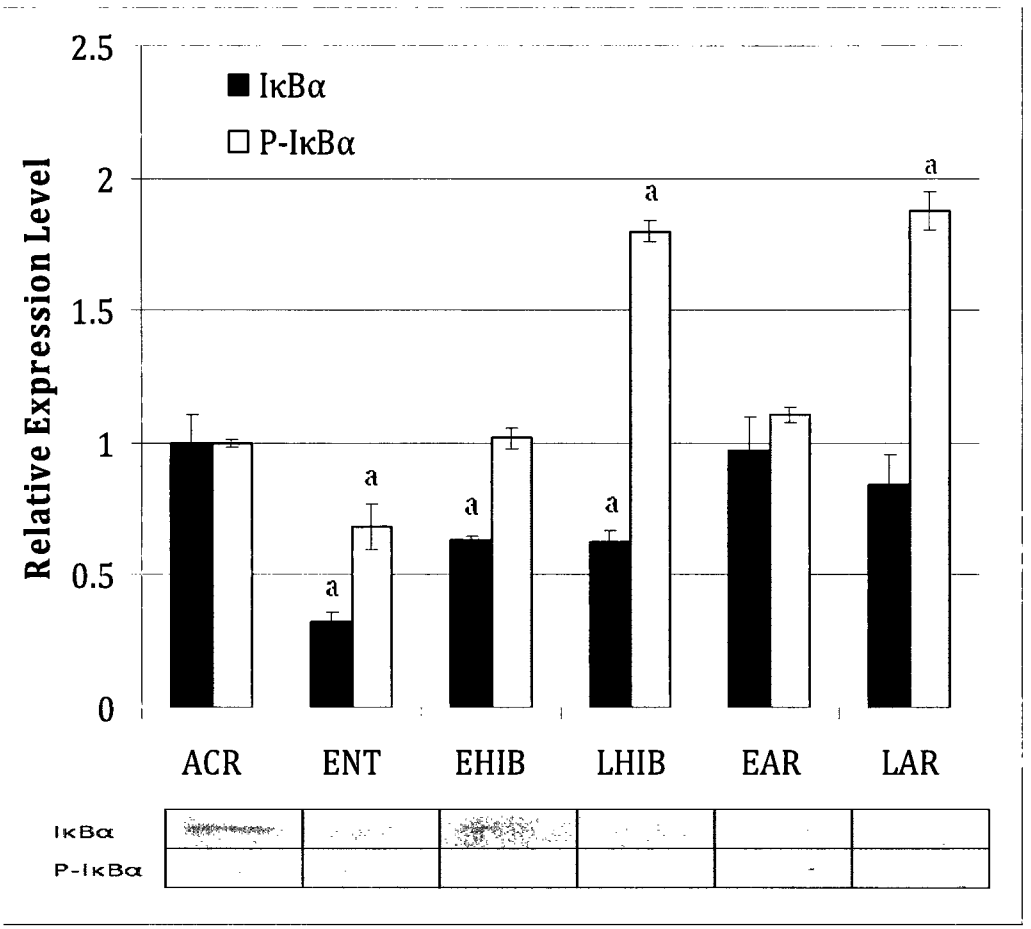

Figure 4.3: Changes in the protein levels of total and phosphorylated IκBα (Ser32) subunits over the course of a torpor-arousal cycle in liver of *S. tridecemlineatus*. Sampling points are: active in the cold room (ACR), entrance into torpor (ENT), early hibernation (EHIB), late hibernation (LHIB), early arousal (EAR) and late arousal (LAR). See Materials and Methods for more extensive definitions. Representative blots are shown along with histograms showing mean normalized band densities (± S.E.M., n=3-4 independent trials on tissue from different animals). Data were analyzed using analysis of variance with a post hoc Student-Newman-Keuls test; **a** - denotes values which are significantly different from each other with respect to the ACR control, $P<0.05$.

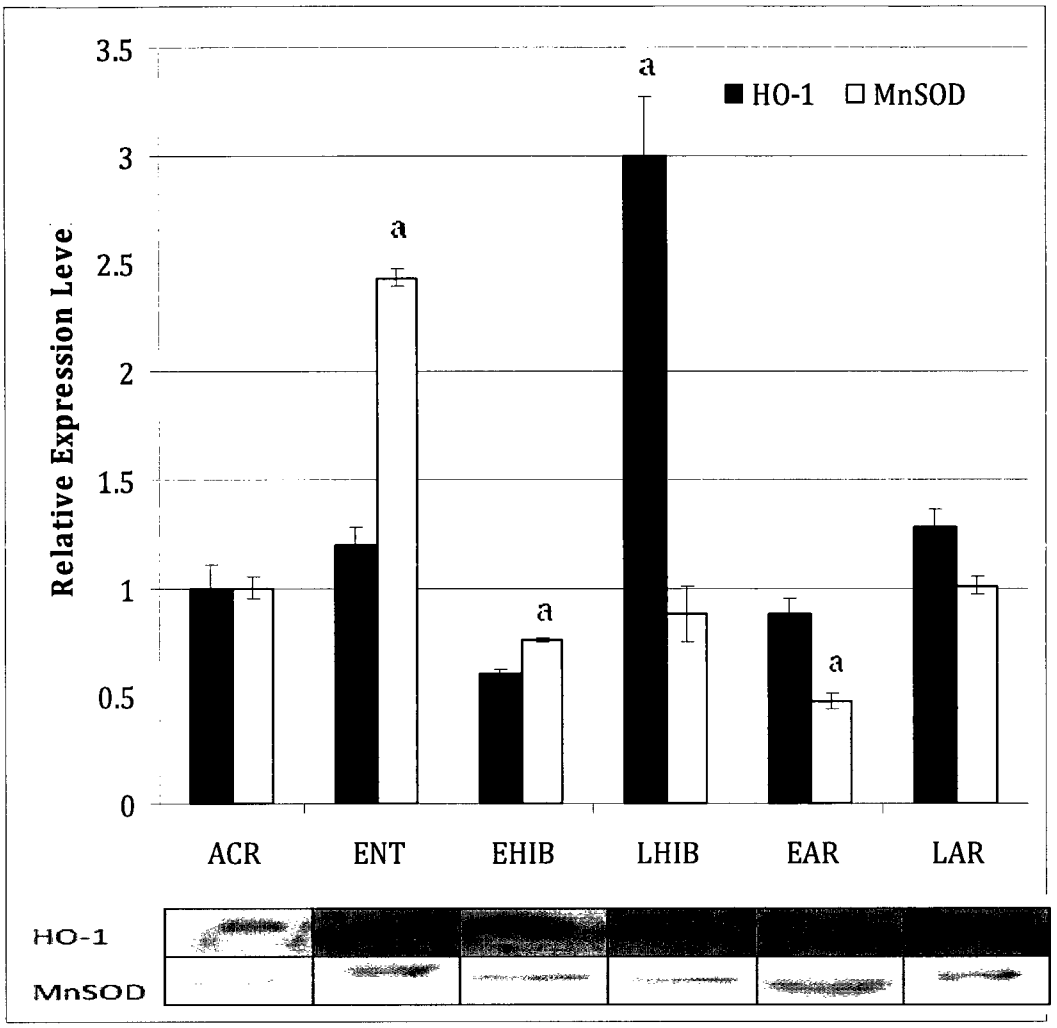

Figure 4.4: Changes in the protein levels of HO-1 and MnSOD over the course of a torpor-arousal cycle in liver of *S. tridecemlineatus*. Sampling points are: active in the cold room (ACR), entrance into torpor (ENT), early hibernation (EHIB), late hibernation (LHIB), early arousal (EAR) and late arousal (LAR). See Materials and Methods for more extensive definitions. Representative blots are shown along with histograms showing mean normalized band densities (± S.E.M., n=3-4 independent trials on tissue from different animals). Data were analyzed using analysis of variance with a post hoc Student-Newman-Keuls test; **a** - denotes values which are significantly different from each other with respect to the ACR control, $P<0.05$.

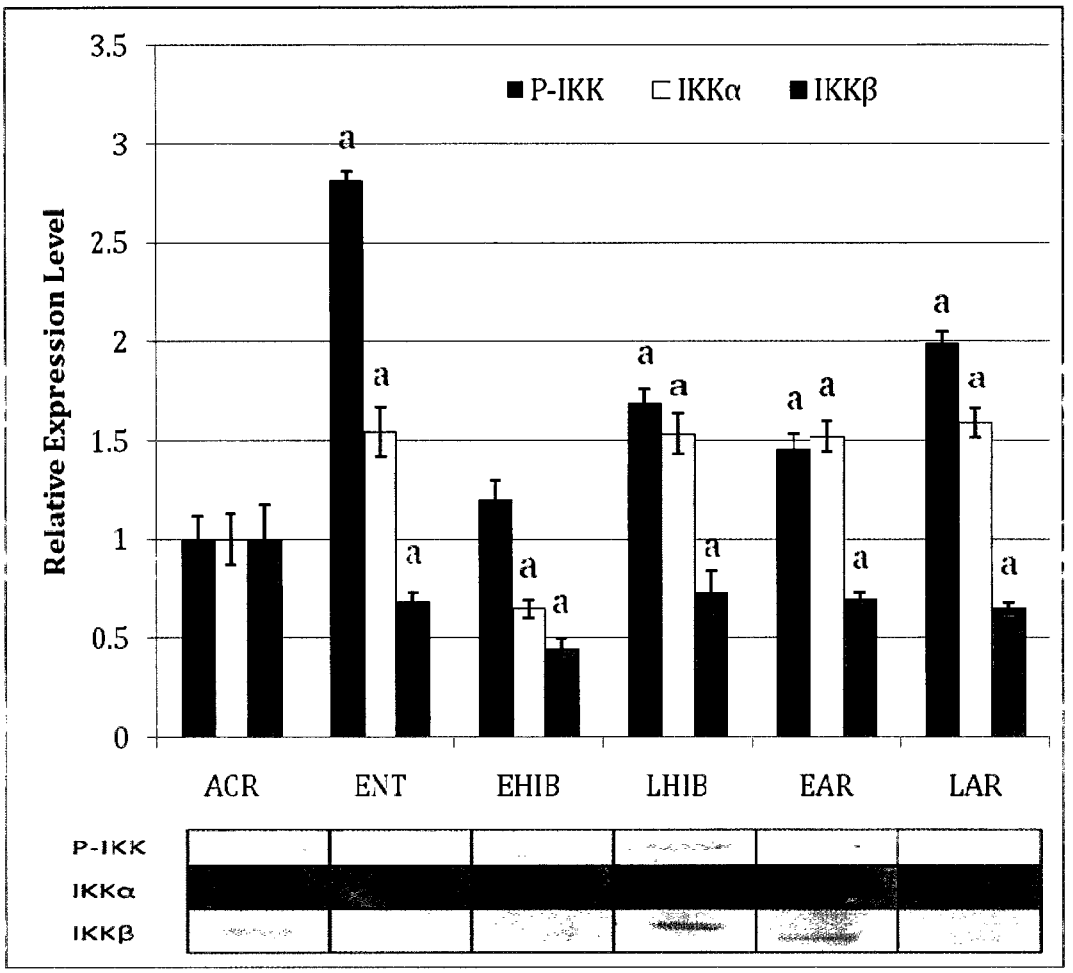

Figure 4.5: Changes in the protein levels of phosphorylated IKK and its two subunits (α and β) over the course of a torpor-arousal cycle in liver of *S. tridecemlineatus*. Sampling points are: active in the cold room (ACR), entrance into torpor (ENT), early hibernation (EHIB), late hibernation (LHIB), early arousal (EAR) and late arousal (LAR). See Materials and Methods for more extensive definitions. Representative blots are shown along with histograms showing mean normalized band densities (± S.E.M., n=3-4 independent trials on tissue from different animals). Data were analyzed using analysis of variance with a post hoc Student-Newman-Keuls test; **a** - denotes values which are significantly different from each other with respect to the ACR control, $P<0.05$.

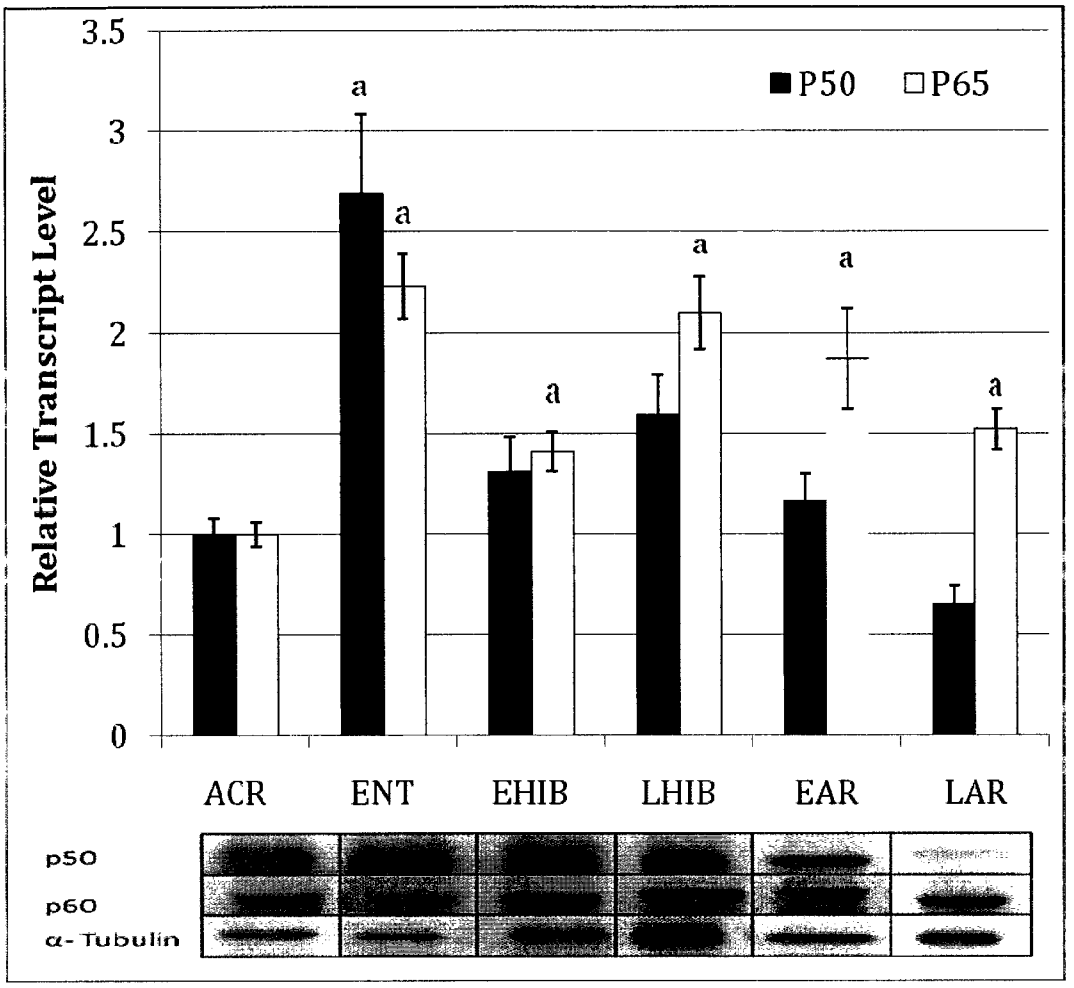

Figure 4.6: Changes in the levels of *p50* and *p65* mRNA transcript levels in liver of *S. tridecemlineatus* over the torpor-arousal cycle. Shown are representative bands on agarose gels (and bands for *α- tubulin* that was used for normalization) and histograms of means (± S.E.M., n=4-8 semi-independent trials on separate RNA isolations from different animals) for six sampling points. Data were analyzed using analysis of variance with a post hoc Student-Newman-Keuls test; **a-** denotes values which are significantly different from each other with respect to the ACR controls, $P<0.05$.

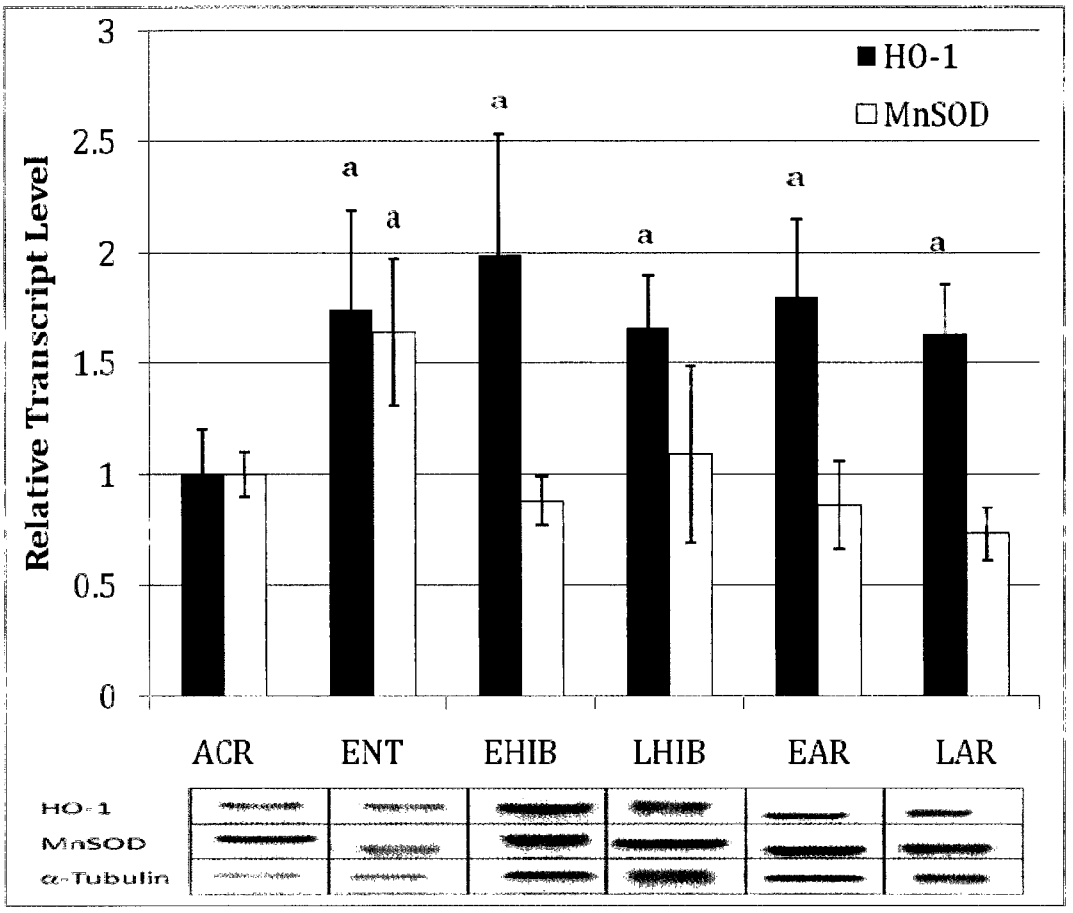

Figure 4.7: Changes in the levels of *HO-1* and *MnSOD* mRNA transcript levels in liver of *S. tridecemlineatus* over the torpor-arousal cycle. Shown are representative bands on agarose gels (and bands for *α- tubulin* that was used for normalization) and histograms of means (± S.E.M., n=4-8 semi-independent trials on separate RNA isolations from different animals) for six sampling points. Data were analyzed using analysis of variance with a post hoc Student-Newman-Keuls test; **a-** denotes values which are significantly different from each other with respect to the ACR control, $P<0.05$.

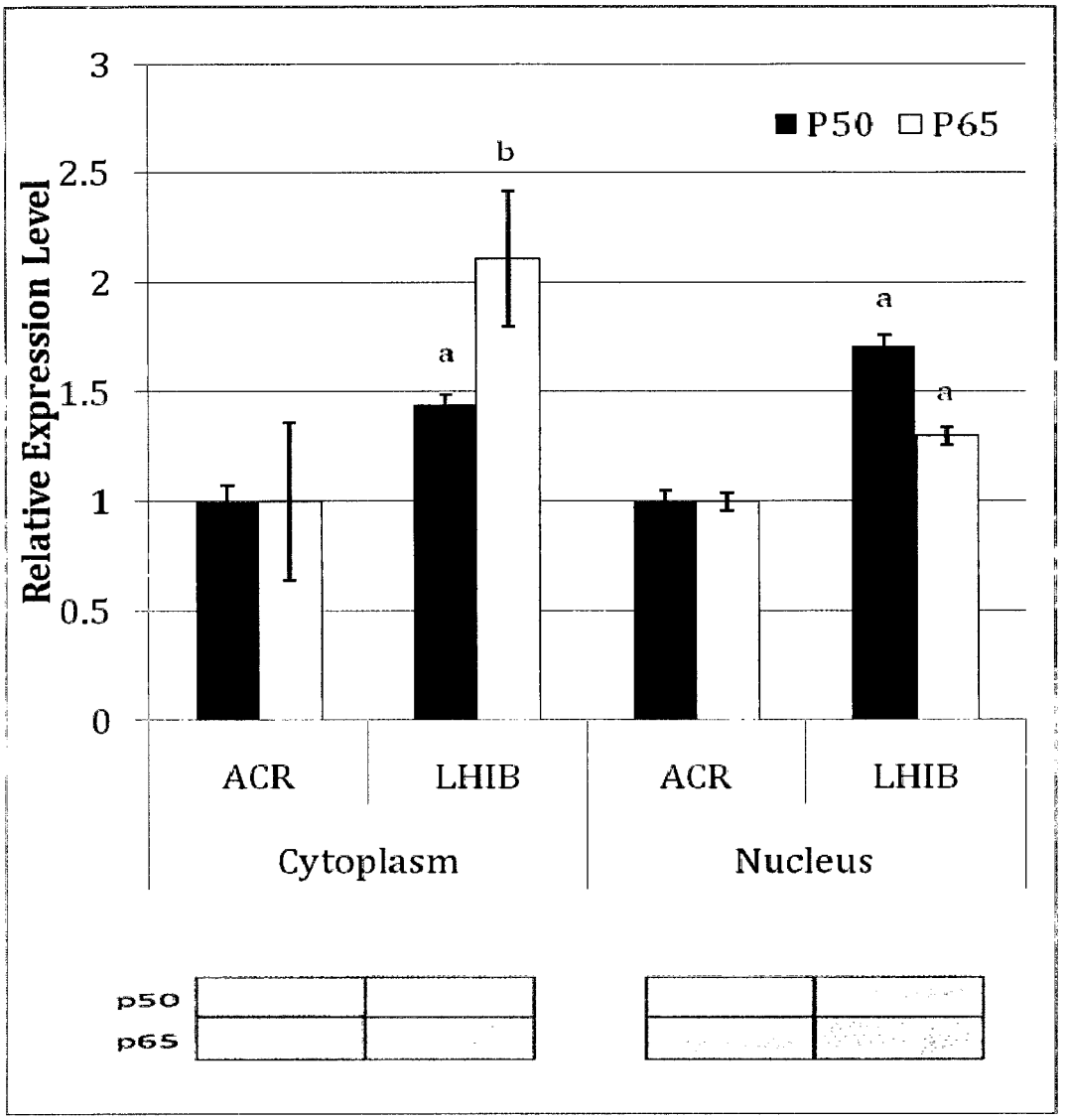

Figure 4.8: Distribution of p50 and p65 between the cytoplasm and nucleus in the liver of *S. tridecemlineatus* under control (ACR) and hibernation (LHIB) conditions. Representative Western blots are shown along with histograms showing mean normalized band densities (± S.E.M., n=3-4 independent trials on tissue from different animals. Data were analyzed using analysis of variance with a post hoc Student's t-test; **a** and **b** denotes values which are significantly different from each other with respect to ACR, respectively $P<0.01$ and $P< 0.05$.

Discussion:

Like the skeletal muscle, the liver performs vital functions during hibernation which ensure the survival of the organism. Its role as a metabolic hub is important since it provides the brain and other tissues with the fuels needed, in the form of ketone bodies and glucose, to maintain their basic cellular function during times of metabolic depression (Baker & van Breukelen, 2009). Previous studies have shown that post-translation modifications of key enzymes involved in glucose catabolism and oxidative phosphorylation are differentially regulated in the liver to ensure a successful reprioritization of energy use during hibernation (Storey, 1987). Differential activation of transcription factors have also been found to play roles in hibernation success (Mamady & Storey, 2008). Therefore, examining NF-κB regulation in the liver is advantageous since this transcription factor is known to be differentially regulated in the liver during I/R events and other stresses, with the extent of its activation determining the overall outcome for the tissue.

During I/R injury, the first wave of oxidative damage in the liver is mediated by the ROS produced by Kupffer cells during the initial reperfusion period. These ROS result in mild damage and the production of inflammatory cytokines and chemokines by hepatocytes and Kupffer cells which recruit neutrophils. The recruited neutrophils are then activated by these inflammatory signals which cause them to produce more ROS that can subsequently lead to the destruction of hepatocytes (Shin et al., 2008). In the liver it has been found that both the canonical and alterative pathways of NF-κB signaling are activated during I/R events with the classical pathway being primarily activated by

chemokines whereas the alternative pathway is activated by hypoxia (Fan et al., 2002). Interestingly, hibernators do not experience such hepatocyte destruction when encountering similar I/R events during their arousal from hibernation and this could be a result of increased antioxidant defenses and by limiting the inflammatory response (Toien et al., 2001), which is why NF-κB, which plays roles in both, is a redox transcription factor worth investigating.

By examining the amount of the IκBα inhibitor and its phosphorylated form one can determine the extent, if any, of NF-κB canonical activation within a tissue. Figure 4.3 depicts the change in levels of IκBα and P-IκBα over the torpor-arousal cycle. Compared to control values, both the total amount of IκBα and the phosphorylation state of the protein dropped dramatically during entry into torpor but subsequently rose again over the remainder or torpor and arousal. IκBα was maximally expressed during arousal, with a near return to ACR whereas P-IκBα levels were highest during late torpor and late arousal. The overall increase in P-IκBα during arousal is similar to results seen in the skeletal muscle and would suggest that this is the segment of the torpor-arousal cycle in which there would be a high degree of nuclear translocation due to the high amount of inhibitor-free NF-κB dimers.

In order to further elucidate how the regulation of NF-κB via its inhibitor IκBα occurs in the liver, the expression patterns of IKK complex components were also examined (Figure 4.5). Levels of the phosphorylated active kinase, P-IKK, were maximal during ENT, with a subsequent reduction over the remainder of the torpor-arousal course, although remaining elevated as compared with ACR. During late arousal, the amount of P-IKK increased again and this could be a precursor to another spike in P-IKK when the

animal once again enters torpor. This increase in P-IKK content during ENT and arousal correlates with the gradual increase seen of P-IκBα during late torpor and arousal, with both having substantially elevated levels during arousal. Interestingly, IKKα showed a similar expression pattern as P-IKK: increased during ENT, followed by a decrease in early torpor with a subsequent and sustained rise in levels throughout arousal. This increase in IKKα expression would suggest that chromatin remodeling (via acetylation and phosphorylation) is important in the liver during hibernation in order for NF-κB to fully activate its downstream targets. Also, increased IKKα protein levels could also suggest a larger role for the non-canonical pathway in attenuating and modifying the NF-κB signal since this kinase is essential in mediating that pathway and connecting it to the canonical signaling branch.

On the other hand, IKKβ showed a reduced and sustained expression level, as compared to ACR, throughout the torpor-arousal cycle. This implies that less IKKβ is needed in the liver in order to sufficiently phosphorylate IκBα and activate NF-κB during hibernation or could be a result of the other signaling pathways converging and resulting in NF-κB activation independently of the IKK complex. The alternative tyrosine phosphorylation pathway, which signals though PI(3)K and is carried out by c-Src kinase is one such pathway that could be mediating the activation of NF-κB and would lead to less IKKβ being needed in order to achieve the desired amount nuclear translocation and gene upregulation (Beraud et al., 1999). Therefore, these results would suggest that the canonical pathways, in association with other signaling cascades, are activated in the liver during hibernation, resulting in the phosphorylation of the NF-κB inhibitor during arousal and leading to nuclear translocation of the dimer where it can selectively upregulate its

target genes.

In order to elucidate whether nuclear translocation of the NF-κB dimer occurred, subcellular expression levels of its components were examined. Figure 4.8 depicts the relative cytoplasmic and nuclear expression levels of the p50 and p65 subunits. During hibernation both subunits showed elevated levels in the nucleus and cytoplasm, suggesting nuclear translocation was occurring. This increase in nuclear translocation correlates with the increased amount of P-IκBα seen during LHIB and suggests the canonical pathway is activated. This activation results in the increased phosphorylation of IκBα by P-IKK, allowing the freed NF-κB to translocate into the nucleus where it can bind to its κB promoter and upregulate its target genes.

The expression levels of the p50 and p65 subunits were also examined in the liver to gain more insight into NF-κBs regulation (Figure 4.2). Over the torpor-arousal cycle both p50 and p65 showed sustained elevated levels, as compared to the ACR control. P65 and p50 had relatively constant expression patterns with both showing a drastic maximal expression during late torpor, which subsequently decreased back to the previous level. Transcript levels were also examined for both subunits to gain further insight into their regulation. Figure 4.6 shows that *p50* was maximally expressed during ENT and then expression subsequently decreased steadily throughout the remainder of the torpor-arousal cycle. *P65* transcript levels showed a similar pattern with maximal expression again during ENT and with a progressive fall in expression levels over the remainder of the torpor-arousal course but always remaining higher than ACR.

The spike in levels of both transcripts during ENT (Fig. 4.6) correlates well with

the dramatic increase in protein expression seen during LHIB for both p50 and p65 (Figure 4.2). These data indicate that the increased protein levels seen for both subunits during the torpor-arousal cycle were sustained partially by an upregulation at the transcriptional level of these genes. Since *p50* has a κB promoter, the increase in transcript level could be a result of enhanced NF-κB binding to its promoter during late arousal and ENT, especially given that P-IκBα is maximally expressed during these times, allowing for increased nuclear translocation and target gene upregulation. To elucidate the mechanism of how p65 transcript and protein levels are increased, it would be advantageous to examine Sp1 since it is the only transcription factor known to have an essential upstream binding site needed for the transcriptional activation of the p65 gene (Yurochko et al., 1995). From these results it is clear that NF-κB is modulating gene expression over the torpor-arousal cycle in the liver and that its own expression is being regulated by upstream activators and by itself.

The two antioxidant enzymes, HO-1 and MnSOD, were evaluated at both the protein (Figure 4.4) and transcript (Figure 4.7) levels over the torpor-arousal cycle. With respect to protein levels, HO-1 showed a dramatic increase during LHIB, which was followed by sustained but significantly lower levels throughout the remainder of torpor and arousal. MnSOD showed a spike in protein levels during ENT which was subsequently followed by a similar significant decrease over the remainder of torpor and arousal. *HO-1* transcript levels were elevated throughout torpor and arousal at a sustained level with respect to ACR. *MnSOD* transcript levels showed a moderate increase during entrance into torpor, but a return to near ACR levels for the remainder of torpor and arousal.

The increase in mRNA transcripts at the onset of torpor for both genes correlates fairly well with the protein data. Both genes showed spikes in protein expression at differing times along the torpor-arousal cycle while the mRNA levels stayed relatively constant. MnSOD had a slightly higher transcript level during ENT with respect to other points in the torpor-arousal cycle, which could contribute to the larger amount of protein expressed at that time point. However, there are a variety of factors which could explain the increased protein expression during entry into torpor such as changes in the regulation of translation via microRNAs or via mRNA availability due to nuclear storage bodies or the modulation of degradation pathways (Storey, 2010). The slightly elevated level of HO-1 mRNA during EHIB correlates with the increased protein expression seen during LHIB suggesting that selective gene upregulation by NF-κB may be occurring. It is important to note that this spike in protein levels could also be due to the contribution of other transcription factors such as Nrf2, which is known to be activated during hibernation and also modulates HO-1 expression (Morin et al., 2008B; Ni & Storey, 2008). Therefore, these data suggest that antioxidant enzymes are regulated in a coordinated fashion during hibernation in the liver, with NF-κB being a contributor to this selective upregulation.

In conclusion, NF-κB is regulated throughout the torpor-arousal cycle in the liver of hibernating ground squirrels, resulting in an upregulation of its target genes. The activating kinase, P-IKK, was expressed throughout torpor and arousal, resulting in an increased amount of P-IκBα during arousal. This correlated with the increase in mRNA levels of downstream targets during entry into torpor, suggesting that nuclear translocation occurs maximally between these time points. This increased level of

transcript may have contributed to the upregulation of their respective protein levels during torpor via translation, with this process subsequently being repeated by the re-activation and nuclear translocation of NF-κB during the next arousal period. From this it can be concluded that NF-κB is regulated in a coordinated fashion in the liver, in order to ensure that the proper level of protective gene products are produced in order to cope with the drastic changes it encounters during hibernation. The increase in antioxidant proteins during arousal would protect hepatocytes from ROS produced from the I/R event which is characteristic of arousal from torpor. Although the canonical pathway appears to be a major player in the liver, as indicated by the high expression of P-IKK and serine phosphorylated IκBα, the alternative pathway in association with the non-canonical pathway may also influence the expression of NF-κB downstream targets due to the increased level of IKKα present throughout the torpor-arousal cycle.

Chapter 5

General Discussion

Hibernation is a remarkable adaptation that allows a variety of mammalian species to abandon homeothermy when environmental conditions become unfavorable in order to conserve energy. By limiting their energy expenditure through effectively suppressing the majority of their metabolic, biochemical and physiological activities in association with lowering their Tb, hibernators are able to survive in a state of dormancy for months with limited physical repercussions. The periodic arousals that intersperse their bouts of deep torpor allow physiological, biochemical and metabolic activities to return briefly to euthermic values, which drastically change oxygen consumption and concentration, tissue perfusion and energy consumption in a coordinated and regulated fashion. These changes in other mammals often lead to severe tissue damage as a result of ischemia/reperfusion which makes hibernators an excellent model to examine how reversible metabolic depression can be achieved successfully (Heldmaier et al., 2004; Humphries et al., 2003).

Of particular interest is how hibernators can deal with oxidative stress that they encounter due to the drastic changes in oxygen consumption accompanying torpor-arousal cycles. Uncoupled respiration in brown adipose tissue, increased susceptibility to radical formation due to elevated PUFA levels, and the drastic changes in oxygen consumption that accompany arousal from torpor are all potential producers of ROS during hibernation, yet hibernators display no tissue damage following their arousal from torpor. Enhancement of antioxidant defense has been known to accompany hibernation in a tissue and time dependant fashion over the torpor-arousal cycle in order to cope with the elevated level of oxidative stress encountered during this heterothermic state (Morin & Storey, 2009; Blagojevic, 2007; Eddy et al., 2005).

Current research is now focusing on specific antioxidants and other redox sensitive signaling cascades in order to elucidate how they achieve this coordinated metabolic depression with minimal tissue damage. In this thesis, the expression of the redox sensitive transcription factor, NF-κB, was examined over the torpor-arousal cycle in skeletal muscle and the liver. Both of these tissues are important in ensuring hibernation is a success due to their roles in shivering thermogenesis (skeletal muscle) and maintaining metabolic activities (liver). NF-κB plays important roles in the maintenance, survival and destruction of both these tissues due to its products being pro-survival and/or proinflammatory depending on the upstream activators (Li et al., 2008; Papa et al., 2009). Due to the opposing signals produced and its sensitivity to the redox status within in the cell, I hypothesized that NF-κB would be differentially regulated during hibernation in order to ensure that the appropriate survival signals were produced while at the same time minimizing destructive inflammatory and apoptotic signals.

From my research, it was determined that NF-κB does show differential regulation across the torpor-arousal cycle with variations seen between tissues. In both tissues, NF-κB showed a general activation during arousal and entry into torpor, which was followed by upregulation of its downstream targets and subsequent deactivation. The extent of upregulation at the protein and mRNA level of the downstream targets showed variance between tissues with the upstream signaling molecules also showing variable expression patterns over the torpor-arousal cycle. Although differences arose, common themes of transcriptional changes over hibernation and the upregulation of antioxidant enzymes in preparation for oxidative stress were evident. These results concur with previous studies that have shown NF-κB to be differentially regulated in other hibernator

tissues (e.g. active in intestinal mucosa but not in brown adipose), with maximal translocation occurring during entry into torpor in order to minimize subsequent oxidative assaults (Carey et al., 2000, 2003A).

The transcriptional changes that occur during hibernation are providing valuable insight into how these organisms minimize damage and survive long-term hypothermia. Since hibernation is characterized by suppression of the rates of transcription and translation, gene upregulation would only occur if the product was necessary for the survival of the organism (Frerichs et al., 1998; Malatesta et al., 2008). General trends in the type of genes upregulated during hibernation reveal that antioxidant defenses, protein chaperones and other protective mechanisms for macromolecules are key players in minimizing damage associated with this state of dormancy (Storey, 2010). Indeed, NF-κB was found to be active during the end of interbout arousal with expression of its protective target genes being upregulated in time for the subsequent arousal from torpor.

This strategy of using redox sensitive transcription factors during hibernation makes sense since it allows for the secondary messengers (ROS), which are natural products of the oxidative stress, to be encountered in a cyclical pattern throughout the torpor-arousal cycle leading to these modulators of gene expression being regulated in a similar way. Depending on the mode of action and the downstream targets of the redox sensitive transcription factors and signaling cascades, various outcomes in terms of the products produced and their abundance can occur. In this study, antioxidant genes and the inhibitor of NF-κB were upregulated during torpor and into arousal. MnSOD and HO-1 are both potential negative regulators of NF-κB, thereby downregulating potentially harmful inflammatory events. MnSOD and HO-1 both modulate NF-κBs response

through interactions with the TNF-mediated signaling pathway components by modulating ROS intermediate signaling molecule availability and altering p65 post-translational modifications, respectively (Seldon et al., 2007; Manna et al., 1998). These negative regulators (IκBα, MnSOD and HO-1) of NF-κB, in association with the ROS produced during hibernation, help to specify its response in the various tissues. This fine tuning is essential since prolonged activation of NF-κB can result in a positive feedback loop becoming activated in which inflammatory cytokine stimulate an inflammatory response that can lead to necrosis and apoptosis of the cells in the area (Pasparakis, 2009; Loukili et al., 2010). Therefore, the results suggest that NF-κB is regulated in a coordinated, tissue specific manner, in order to optimize its protective roles during hibernation while at the same time minimizing its potential detrimental effects.

In both liver and skeletal muscle, sustained NF-κB activation has been linked to destruction of these tissues due to its role in mitigating the inflammatory response. Although the present results do not elucidate the exact mechanism and intricacies of this response in the selected tissues, they do provide evidence that a sustained activation does not occur, thereby protecting the liver and skeletal muscle from hepatocyte apoptosis and muscle atrophy, respectively (Li et al., 2008; Papa et al., 2009). Some insight into the regulatory mechanism of NF-κB in the various tissues can be gained by examining the differences between them, particularly the extent to which P-IKK was activated and the difference in ratios between IκBα and P-IκBα. These differences are important since they give insight into how the canonical pathway is altered during hibernation, since the antibodies used in this study were for the specific serine phosphorylated forms of IκBα and P-IKK (IKKα and IKKβ), which are characteristic of this pathway.

One of the major differences between the muscle and liver was the extent and duration of IκBα and P-IκBα expression. In the skeletal muscle (Figure 3.2) there was an obvious sinusoidal wave pattern of NF-κB activation and deactivation that was dependent on the cyclical expression pattern of the inhibitor and its phosphorylated form and which normally changed opposite to one another (as one increased the other decreased and vice versa). In liver (Figure 4.3), a similar cyclical expression pattern was found, however the extent and change in IκBα expression was not as dramatic and never increased above P-IκBα. The differences seen in expression levels of the inhibitor and its phosphorylated forms indicate that regulation of NF-κB varies according to tissue and is probably due to the different extracellular and intracellular signals that these tissues receive, resulting in differing outcomes from the resultant cross-talk between signaling cascades *in vivo* (Imbert et al., 1996). Therefore, the variable expression in the inhibitor and its various forms indicate that the active canonical NF-κB pathway has its intensity and duration of activation modified by various other cellular components and signaling cascades. It would be of interest in the future to study this further since this would allow for a better understanding of how gene transcription by NF-κB is modulated during hibernation.

The other indicator that cross-talk between pathways is occurring and is resulting in differential expression is the difference in the expression of P-IKK complexes throughout torpor-arousal. The IKK complex is one of the main sites where upstream effectors converge in order to modulate the expression of NF-κB (Shifera, 2010A, 2010B). Therefore, the differential expression of the components of these complexes could suggest that different upstream effectors are being utilized. In the skeletal muscle and the liver, a continuous increase and subsequent decrease in P-IKK expression was

found to occur in a cyclical pattern based on the torpor-arousal cycle, although durations of these phases were unique among the tissues. The major difference between the tissues was where and the maximal expression of P-IKK peaked, with liver (Figure 4.5) and skeletal muscle (Figure 3.4) showing maximum phosphophorylation of IKK during ENT and EAR, respectively. These spikes at different times indicate that canonical NF-κB activation is needed at differing points along the torpor-arousal cycle depending on the tissue. Therefore, in the future it would be advantageous to look at specific components of the alternative and noncanonical pathways in association with upstream effectors in order to determine if they follow similar cyclical expression patterns over the course of the torpor-arousal cycle and how these changes may affect NF-κB-regulated gene expression in these tissues.

The tight regulation of NF-κB observed is essential since uncontrolled activation can lead to damaging chronic inflammation via NF-κB regulatory control over cytokines, chemokine and adhesion molecules, which are essential components of the innate and adaptive immune response (Lawrence & Fong, 2010). During hibernation, animals can experience hypoxia and I/R events that drastically change oxygen levels and concentration. This can lead to the activation of kinases, transcription factors and other apoptosis-related genes via ROS second messengers, with their resultant downstream effects depending on the species identity, duration, intensity and cell type (Azad et al., 2008). This potential inflammatory event is mitigated even though hypoxia and ROS are present throughout the torpor-arousal cycle and are known mediators of inflammation via NF-κB activation (Safronova & Morita, 2009). By ensuring proper activation and deactivation of NF-κB during hibernation, the destructive consequences of inflammation

are minimized with other signaling cascades, transcription factors, epigenetic, transcriptional and translation controls contributing to this regulation in a tissue specific manner (Nathan & Ding, 2010).

The proper regulation of NF-κB is essential in all organisms since deregulation can lead to chronic inflammation, tissue-damage, necrosis and apoptosis, which accompanies many disease states including Alzheimer's, Crohn's disease, cancer and rheumatoid arthritis depending on the location and extent of these alterations (Tak & Firestein, 2001; Danese & Mantovani, 2010). Although NF-κB is known to induce inflammation, recent studies have also shown that it also performs essential tasks in terms of the upregulation of anti-inflammatory genes such as IL-10 when inflammation needs to be ended (Tomczak et al., 2006). Therefore, using NF-κB as a target for pharmacological intervention has proven difficult since there are multiple signaling players that converge and regulate its expression and the inherent diversity in dimer combinations due to the numerous proteins within the NF-κB family make it difficult to modulate a response with the goal of a specific outcome. The fact that NF-κB connects the immune responses to other tissues and responds to oxidative stress make it an interesting protein to examine during hibernation and other states of metabolic depression since the outcome of its response is directly related to its physiological, biochemical and metabolic environment (Fialkow et al., 2007).

In conclusion, it was determined that the redox sensitive transcription factor NF-κB showed differential regulation over the torpor-arousal cycle in a tissue dependant fashion during hibernation. The activation of NF-κB occurred at specific intervals throughout dormancy and this ensured that the appropriate amount of antioxidants, pro-

survival and proinflammatory downstream targets were produced. In the future it would be advantageous to examine the cellular components involved in the noncannonical and alternative pathways in association with their subcellular distribution in order to gain insight into how these pathways may be modulated over torpor/arousal and influence the canonical pathway. Other downstream targets of NF-κB should also be examined to determine the extent of their activation during hibernation; these could include cytokines, chemokines and pro-apoptotic products since differential expression patterns of these products would also impact the organism's ability to survive prolonged dormancy. Therefore, this research indicates that redox sensitive transcription factors perform essential tasks during mammalian hibernation to ensure the animal's survival.

REFERENCES

Adibhatia, R.M., and Hatcher, J.F. (2010) Lipid oxidation and peroxidation in CNS health and disease from molecular mechanisms to therapeutic opportunities. *Antioxid Redox Signal* **12(1)**:125-169.

Allen, C.L., and Bayraktutan, U. (2009) Oxidative stress and its role in the pathogenesis of ischaemic stroke. *International Journal of Stroke* **4**: 461-470.

Ammirante, M., Rosati, A., Festa, M., Petrella, A., Marzullo, L., Pascale, M., Bellisario, M.A., Leone, A., and Turco, M.C. (2008) The activity of hsp90 alpha promoter is regulated by NF-kappa B transcription factors. *Oncogene* **27(8)**:1175-1178.

Andrews, M.T. (2007) Advances in molecular biology of hibernation in mammals. B*ioEssays* **29:** 431-440.

Andrews, M.T., Russeth, K.P., Drewwa, L.R., and Henry, P.G. (2009) Adaptive mechanisms regulate preferred utilization of ketones in the heart and brain of a hibernating mammal during the arousal from torpor. *Am J Physiol* **296:** R383-R393.

Andrews, M.T., Squire, T.L., Bowen, C.M., and Rollins M.B. (1998) Low-temperature carbon utilization is regulated by novel gene activity in the hear of a hibernating animal. Proc. *Natl Acad Sci USA* **95**: 8392-8397.

Atreya, I., Atreya, R., and Neurath, M.F. (2008) NF-kappaB in inflammatory bowel disease. *J Intern Med* **283(6)**: 591-596.

Azad, N., Rojanasakul, Y., and Vallyathan, V. (2008) Inflammation and lung cancer: roles of reactive oxygen nitrogen species. *Journal of Toxicology and Environmental Health, part B* **11**:1-15.

Bag, A., and Bag, N. (2008) Target sequence poloymorphism of human manganese superoxide dismutase gen and its association with cancer risk: a review. *Cancer Epidemiol Biomarkers Prev* **17(12)**: 3298-3300.

Baker, J.A., and van Breukelen, R. (2009) Bile constituents in hibernation golden-mantled ground squirrels (*Spermophilus lateralis*) *Comparative Hepatology* **8**:2.

Bakker, N., and Guttridge, D.C. (2010) NF-κB signaling: a tale of two pathways in skeletal myogenesis. *Physiol Rev* **90**:495-511

Bakker, N., Wang, J., Ladner, K., Wang, H., Dahlman, J.M., Carathers, M., Acharyya, S., Rudnicki, M.A., Hollenbach, A.D., and Guttridge, D.C. (2008) IKK/NF-κB regulates skeletal myogenesis via a signaling switch to inhibit differentiation and promote mitochondrial biogenesis. *The Journal of Cell Biology* **180(4):** 787-802.

Banerjee, M.S., Chakraborty, P.K., Dey, R.A., and Raha, S. (2009) Heat stress regulates chaperone hear shock protein 70 and antioxidant manganese superoxide dismutase through reactive oxygen species (ROS) p38 MAPK and Akt. *Cell Stress Chaperones* **14(6)**: 579-589.

Bar-Shai, M., Carmeli, E., Ljubuncic, P., and Reznick, A. Z. (2008) Exercise of immobilization in aging animals: the involvement of oxidative stress and NF-κB activation. *Free Radical Biology & Medicine* **44**:202-214.

Bashan, N., Kovsan, J., Kachko, I., Ovadia, H., and Rudich, A. (2009) Positive and negative regulation of insulin signaling by reactive oxygen and nitrogen species. *Physiol Rev* **89**: 27-71.

Bėraud, C., Henzel, W.J., and Baeuerle, P.A. (1999) Involvement of regulatory and catalytic subunits of phosphoinositide 3-kinase in NF-κB activation. *Proc Natl Acad Sci* **96**:429-434.

Biswas, D.K., Cruz, A.P., Gansberger, E., and Pardee, A.B. (2000) Epidermal growth factor-induced nuclear factor kappa B activation: A major pathway of cell-cycle progression in estrogen-receptor negative breast cancer cells. *Proc Natl Acad Sci USA* **97(15):** 8542-8547.

Blagojević, D.P. (2007) Antioxidant systems in supporting environmental and programmed adoptions to low temperatures. *Cryo Letters* **28(3)**:137-150.

Boateng, S.Y., and Goldspink, P.H. (2008) Assembly and maintenance of the sarcomere night and day. *Cardiovascular Research* **77**: 667-675.

Breuhahn, K., and Schirmacher, P. (2008) Reactivation of the insulin-like growth factor-II signaling pathway in human hepatocellular carcinoma. *World J Gastroenterol* **14(11)**: 1690-1698.

Buck, C.L., and Barnes, B.M. (2000) Effects of ambient temperature on metabolic rate, respiratory quotient, and torpor in an arctic hibernator. *Am J Physiol* **279**: R255-R262.

Buck, M.J., Squire, T.L., and Andrews, M.T. (2002) Coordinate expression of the PDK4 gene: a means of regulating fuel selection in a hibernating mammal. *Physiol Genomics* **8(1)**: 5-13.

Bullard, R.W., and Funkhouser, G.E. (1962) Estimated regional blood flow by rubidium 86 distribution during arousal from hibernation. *Am J Physiol* **203(2)**:266-270.

Buzadzic, B., Spasic, M., Saicic, Z.S., Radojicic , R., Petrovic, V.M., and Halliwell,B., (1990) Antioxidant defences in the ground squirrel *Citellus citellus*. *Free Radic Bio Med* **9**:407-413.

Cai, D., Frantz, J.D., Tawa, N.E., Melendez, P.A., Oh, B.C., Lidov, H.G., Hasselgren, P.O., Frontera, W.R., Lee, J., Glass, D.J., and Shoelson, S.E. (2004) IKKbeta/NF-kappaB activation causes severe muscle wasting in mice. *Cell* **119(2)**: 285-298.

Carey, H.V., Andrews, M.T., and Martin, S.L. (2003A) Mammalian hibernation: cellular and molecular responses to depressed metabolism and low temperature. *Physiol Rev* **83(4)**: 1153-1181.

Carey H.V., Frank, C.L., and Seifert, J.P. (2000) Hibernation induces oxidative stress and activation of NK-kappaB in ground squirrel intestine. *J Comp Physiol B.* **170(7)**: 551-559.

Carey, H.V. Mangino, M.J., and Southland, J.H. (2001) Changes in gut function during hibernation: implications for bowel transplantation and surgery. *Gut* **49**: 459-461.

Carey, H.V., Rhoads, C.A., and Aw, T.Y. (2003B) Hibernation induces glutathione redox imbalance in ground squirrel intestine. *J Comp Physiol B* **173(4)**: 269-276.

Chakraborty, J.B., and Mann, D.A. (2010) NF-κB signaling: embracing complexity to achieve translation. *Journal of Hepatology* **52**: 285-291.

Chen, H., Li, X., and Epstein, P.N. (2005) MnSOD and catalase transgenes demonstrate that protection of islets from oxidative stress does not alter cytokine toxicity. *Diabetes* **54**: 1437-1446.

Cogswell, P.C., Scheinman, R.I., and Baldwin, A.S. Jr. (1993) Promoter of human NF-kappa B p50/p105 gene. Regulation of NF-kappa B subunits and by c-REL. *Journal of Immunology* **150(7)**: 2794-2804.

Collister, K.A., and Albensi, B.C. (2005) Potential therapeutic targets in the NF-kappaB pathway for Alzheimer's disease. *Drug News Perspect.* **18(10)**:623-629.

Crichton, R.R., Wilmet, S., Legssyer, R., and Ward, R.J. (2002) Molecular and cellular mechanisms of iron homeostasis and toxicity in mammalian cells. *Journal of Inorganic Biochemistry* **91**: 9-18.

Daan, S., Barnes, B.M., and Strijkstra, A.M. (1991) Warming up for sleep? ground squirrels sleep during arousals from hibernation. *Neurosci Lett* **128(2)**: 265-268.

D'Abusco, A.S., Politi L., Giordano, C., and Scandurra, R..(2010) A peptidyl-gluscosamine derivative affects IKKα kinase activity in human chondrocytes. *Arthritis Research &Therapy* **12**:18-19.

Danese, S., and Mantovani, A. (2010) Inflammatory bowel disease and intestinal cancer: a paradigm of the Yin-Yang interplay between inflammation and cancer. *Oncogene* **29**:3313-3323.

Dark, J. (2005) Annual lipid cycles in hibernators: integration of physiology and behavior. *Annu Rev Nutr* **25**: 469-497

Dark, J., and Miller, D.R. (1998) Metabolic fuel privation in hibernating and awake ground squirrels. *Physiology & Behavior* **63(1)**:59-65.

Deavers, D.R., and Musacchia, X.J. (1980) Water metabolism and renal function during hibernation and hypothermia. *Fed Proc* **39(12)**:2969-2973.

Dejardin, E. (2006) The alternative NF-κB pathway from biochemistry to biology: pitfalls and promises for future drug development. *Biochemical Pharmacology* **72**:1161-1179.

Delhalle, S., Deregowski, V., Benoit, V., Merville, M.P., and Bours, V. (2002) NF-kappaB-dependent MnSOD expression protects adenocarcinoma cells from TNF-alpha-induced apoptosis. *Oncogene* **21(24)**:3917-3924.

Djavaheri-Mergny, M., Javelaud, D., Wietzerbin, J., and Basancon, F. (2004) NF-kappaB activation prevents apoptotic oxidative stress via an increase of both thioredoxin and MnSOD levels in TNFalpha-treated Ewing sarcoma cells. *FEBS Lett* **578(1-2)**:111-115.

Drew, K.L., Tøien, Ø., Rivera, P.M., Smith, M.A., Perry, G., and Rice, M.E. (2002) Role of the antioxidant ascorbate in hibernation and warming from hibernation. *Comp Biochem Physiol C Toxicol Pharmacol* **133(4)**:483-492.

Dröge, W. (2002) Free radicals in the physiological control of cell function. *Physiol Rev* **82**: 47-95.

Eddy, S.F., McNally, J.D., and Storey, K.B. (2005) Up-regulation of a thioredoxin peroxidase-like protein, proliferation-associated gene, in hibernating bats. *Archives of Biochemistry and Biophysics* **435**:103-111.

Eldor, R., Yeffet, A., Baum, K., Doviner, V., Amar, D., Ben-Neriah, Y., Christofori, G., Peled, A., Carel, J.C., Boitard, C., Klein, T., Serup, P., Eizirik, D.L., and Melloul, D. (2006) Conditional and specific NF-kappaB blockade prtect pancreatic beta cells form diabetogenic agents. *Proc Natl Acad Sci USA* **103(13)**: 5072-5077.

Fan, C., Li, Q., Ross, D., and Engelhardt, J.F. (2002) Tryosine phosphorylation of IκBα activates NFκB through redox-regulated and c-Src-dependant mechanism following hypoxia/reoxygenation. *Journal Biological Chemisry* (Downloaded July 15, 2010 from http://www.jbc.org).

Fan, C., Zwacka, R.M., and Engelhardt J.F. (1999) Therapeutic approaches for ischemia/reperfusion injury in the liver. *J Mol Med.* **77(8)**:577-592.

Ferguson, L.R. (2010) Chronic inflammation and mutagenesis. *Mutat Res.* **Mar 17**(Epub ahead of printing: Downloaded March 2010 from http://www.ncbi.nlm.nih.gov/pubmed/20223251).

Fialkow, L., Wang, Y., and Downey, G.P. (2007) Reactive oxygen and nitrogen species as signaling molecules regulating neutrophil function. *Free Radic Biol Med* **42(2)**:153-164.

Fleck, C., and Carey, H.V. (2005) Modulation of apoptotic pathways in intestinal mucosa during hibernation. *Am J JPhysiol Regul Integr Comp Physiol* **289(2)**:R586-R595.

Forder, J.P., and Tymianski, M. (2009) Postsynaptic mechanisms of excitotoxicity: involvement of postsynaptic density proteins, radicals and oxidant molecule. *Neuroscience* **158(1)**:293-300.

Franck, C.L., Karpivich, S., and Barnes, B.M. (2008) Dietary Fatty acid composition and the hibernation patterns in free-ranging arctic ground squirrels. *Physiological and Biochemical Zoology* **81(4)**:486-495.

French, A.R. (1985) Allometries of the durations of torpid and euthermic intervals during mammalian hibernation: a test of the theory of metabolic control of the timing of changes in body temperature. *J Comp Physiol B* **158(1):** 13-19.

Frerichs, K,U., Smith ,C.B., Brenner, M., DeCracia, D.J., Krause, G.S., Marrone, L., Denver, T.E., and Hallenbeck, J.M. (1998) Suppression of protein synthesis in brain during hibernation involves inhibition of protein initiation and elongation. *Proc Natl Acad Sci USA* **95(24)**: 14511-14516.

Friedman, S.L. (2008) Hepatic stellate cells: protean, multifunctional, and enigmatic cells of the liver. *Physiol Rev* **88**:125-172.

Galster, W., and Morrison, P.R. (1975) Gluconeogenesis in arctic ground squirrels between periods of hibernation. *Am J Physio* **228(1)**: 325-330.

Geiser, F. (1988) Reduction of metabolism during hibernation and daily torpor in mammals and birds: temperature effect or physiological inhibition? *J Comp Physiol B* **158**:25-37.

Geiser, F., and Turbill, C. (2009) Hibernation and daily torpor minimize extinctions. *Naturwissenschaften* **96(10)**:1235-1240.

Gerson, A.R., Brown, J.C.L., Thomas, R., Bernards, M.A., and Staples, J.F. (2008) Effects of dietary polyunsaturated fatty acids on mitodhondrial metabolism in mammalian hibernation. *Journal of Experimental Biology* **211**: 2689-2699.

Gluck, E.F., Stephens, N., and Swoap, S.J. (2006) Peripheral ghrelin deepens torpor bouts in mice through the arcuate nucleus neuropeptide Y signaling pathway. *Am J Physiol Regul Integr Comp Physiol* **291(5)**: R1303-R1309.

Greenberg, H., Ye, X., Wilson, D., Htoo, A.K., Henderson, T., and Liu, S.F. (2006) Chronic intermittent hypoxia activates nuclear factor-kappaB in cardiovascular tissues in vivo. *Biochem Biophys Res Commun* **343(2)**: 591-596.

Grimm, T., Schneider, S., Naschberger, E., Huber, J., Guenzi, E., Kieser, A., Reitmeir, P., Schulz, T.F., Morris, C.A., and Stürzl, M. (2005) EBV latent membrane protein-1 protects B cells from apoptosis by inhibition of BAX. *Blood* **105(8)**:3263-3269.

Grundy, J.E., and Storey, K.B. (1998) Antioxidant defenses and lipid peroxidaton damage in estivating toads, Scaphiopus couchii. *J Comp Physio B* **168(2)**:132-142.

Guo, Y., Xiao, P., Lei, S., Deng, F., Xiao, G.G., Liu, Y., Chen, X., Li, L., Wu, S., Chen, Y., Jiang, H., Tan, L., Xie, J., Zhu, X., Liang, S., and Deng, H. (2008) How is mRNA expression predictive of protein expression? A correlation study on human circulating monocytes. *Acta Biochim Biopys Sin* **40(5)**:426-436.

Häcker, H., and Karin, M. (2006) Regulation of function of IKK and IKK related kinases. *Sci STKE* **357:** re13.

Harlow, H.J., and Frank, C.L. (2001) The role of dietary fatty acids in the evolution of spontaneous and facultative hibernation patterns in prairie dogs. *J Comp Physiol B* **171(1)**: 77-84.

Hasselgren, P.O. (2007A) Transcription Factors and nuclear cofactors in muscle wasting. In *Yearbook of intensive care and emergency medicine.* **Volume 2007**: 229-237.

Hasselgren P.O. (2007B) Ubiquitination, phosphorylation, and acetylation—triple threat in muscle wasting. *J Cell Physiol* **213(3)**: 679-689.

He, M., Siow, R.C., Sugden D., Gao, L., Cheng, X., and Mann, G.E. (2010) Induction of HO-1 and redox signaling in ehdothelial cells by advances glycation and end products: a role for Nrf2 in vascular protection in diabetes. *Nutr Metac*

Cardiovasc Dis. **Mar 12** (Epub ahead of printing: downloaded March 2010 from http://www.ncbi.nlm.nih.gov/pubmed/20227863).

He, Song-Qing, Zhang, Yan-Hong, Venugopal S.K., Dicus, C.W., Perez, R.V., Ramsamooj, R., Nantz, M.H., Zern, M.A., and Wu, J. (2006) Delivery of antioxidative enzyme genes protects against ischemia/reperfusion-induced liver injury in mice. *Liver Transplantation* **12**: 1869-1879.

Herrmann, O., Baumann,B., de Lorenzi, R., Muhammad, S., Zhang, W., Klessiek, J., Malfertheiner, M., Köhrmann, M., Potrovita, I., Maegele, I., Byer, C., Burke, J.R., Hasan, M.T., Bujard, H., Wirth, T., Pasparakis, M., and Schwaninger, M. (2005) IKK mediates ischemia-induced neuronal death. *Nat Med* **11(12)**: 1322-1329.

Heldmaier, G., Ortmann, S., and Elvert, R. (2004) Natural hypometabolism during hibernation and daily torpor in mammals. *Repir Physiol Neurobiol* **141(3)**:317-329.

Herscovitch, M., Comb, W., Ennis, T., Coleman, K., Yong, S., Armstead, B., Kalaitzidis, D., Chandani, S., and Gilmore T.D. (2008) Intermolecular disulfide bond formation in the NEMO dimmer requires Cys54 and Cys 347. *Biochem Biophys Res Commun* **367(1)**: 103-108.

Hittel, D., and Storey, K.B. (2001) Differential expression of adipose- and heart-type fatty acid binding proteins in hibernating ground squirrels. *Biochim Biophys Acta* **1522(3)**: 238-243.

Hoffmann, A., Levchenko, A., Scott, M.L., and Baltimore, D. (2002) The IkappaB-NF-kappaB signaling module: temporal control selective gene activation. *Science* **298(5596)**: 1241-1245.

Hooper, C. (2010) *Overview of NFκB signaling*. Retrieved July 18, 2010, from http://www.abcam.com/index.html?pageconfig=resource&rid=11255&pid=10629

Huber, N., Sakai, N., Eismann, T., Shin, T., Kuboki, S., Blanchard, J., Schuster, R., Edwards, M.J., Wong, H.R., and Lentsch, A.B. (2009) Age-related decrease in proteasome expression contributes to defective NF-κB activation during hepatic ischemia/reperfusion. *Hepatology* **49(5)**: 1718-1728.

Hudson, H.J., and Franklin, C.E. (2002) Maintaining muscle mass during extended disuse: aestivating frogs as a model species. *Journal of Experimental Biology* **205**: 2297-2303.

Humphries, M.M., Thomas, D.W., and Kramer, D.L. (2003) The role of energy availability in mammalian hibernation: a cost-benefit approach. *Physiological and Biochemical Zoology* **76(2)**: 165-179.

Hunter, R.B., and Kandarian, S.C. (2004) Disruption of either the Nfkb1or the Bcl3 gene inhibits skeletal muscle atrophy. *J Clin Invest* **114**: 1504-1511.

Imbert, V., Rupec, R.A., Livolsi, A., Pahl, H.L., Traenckner, E.B., Mueller-Dieckmann, C., Farahifar, D., Rossi, B., Auberger, P., Baeuerle, P.A., and Peyron, J.F. (1996) Tyrosine phosphorylation of I kappa B-alpha activates NF-kappaB without proteolytic degradation of I kappa B-alpha. *Cell* **86(5)**: 787-798.

Janssen-Heininger, Y.M., Poynter, M.E., Aesif, S.W., Pantano, C., Ather, J.L., Reynaert, N.L., Ckless, K., Anathy, V., van der Velden, J., Irvin, C.G., and van der Vliet, A. (2009) Nuclear factor kappaB, airway epithelium, and asthma: avenues for redox control. *Proc Am Thorac Soc* **6(3):** 249-255.

Ji, L., L. (2008) Modulation of skeletal muscle antioxidant defense by exercise: role of redox signaling. *Free Radical Biology and Medicine* **44**: 142-152.

Ji, L, L.. Gomez-Cabrera, M., and Vina, J. (2007) Role of nuclear factor κB and mitogen-activated protein kinase signaling in exercise-induced antioxidant enzyme adaptation. *Appl Physiol Nutr Mutab* **32**: 930-935.

Jozkowicz A., Was, H., and Dulak, J. (2007) Heme oxygenase-1 in tumors: is it a false friend. *Anatioxid Redox Signal* **9(12)**: 2099-2117.

Jung, J.E., Kim, G.S., Narasimhan, P., Song, Y.S., and Chan, P.H. (2009) Regulation of Mn-superoxide dismutase activity and neuroprotection by STAT 3 in mice after cerebral ischemia. *J Neurosci* **29(21)**: 7003-7014.

Kalter, V.G., and Folk Jr., G. E. (1979) Hurmoral induction of mammalian hibernation. *Comp Biochem Physiol* **63A:**7-13.

Kaneto, H., Katakami, N., Matsuhisa, M., and Matsuoka, T.A. (2010) Role of reactive oxygen species in the progression of type 2 diabetes and atheroselclerosis. *Mediators Inflamm.* **2010**: 453892.

Karin, M., and Ben-Neriah, Y. (2000) Phosphorylation meets ubiquitination: the control of NF-κB activity. *Annual Review of Immunology* **18**: 621-663.

Kefaloyianni, E., Gaitanaki, C., and Beis, I. (2006) ERk1/2 and p38-MAPK signaling pathways, through MSK1, are involved in NF-κB transactivation during oxidative stress in skeletal myoblasts. *Cellular Signalling* **18**: 2238-2251.

Kharrazi, H., Vaisi-Raygani, A., Rahimi, Z., Tavilani, H., Aminian, M., and Pourmotabbed. (2008) Association between enzymatic and non-enzymatic

antioxiadant defense mechanism with apolipoprotein E genotypes in Alzheimer disease. *Clinical Biochemistry* **41**: 932-936.

Kiningham, K.K., Cardoze, Z.A., Cook, C., Cole, M.P., Stewart, J.C., Tassone, M., Coleman, T.M., and Spitz, D.R. (2008) All trans-retinoic acid induces manganese superoxide dismutase in human neruoblastoma through NF-kappa B. *Free Radical Biol Med* **44(8)**: 1610-1616.

Kitamura, T., Sekimata, M., Kikuchi, S., and Homma, Y. (2005) Involvement of poly(ADP-ribose) polymerase 1 in ERBB2 expression in rheumatoid synovial cells. *Am J Physiol Cell Physiol* **289(1)**: C82-C88.

Kondo, H., Miura, M., and Itokawa, Y. (1991) Oxidative stress in skeletal muscle atrophied by immobilization. *Acta Physiol Scand* **142**: 527-528.

Knovich, M.A., Storey, J.A., Coffman, L.G., Toriti, S.V., and Torti, F.M. (2009) Ferritin for the clinician. *Blood Rev* **23(3)**:95-104.

Kondo, H., Nakagaki, I., Sasaki, S., Hori, S., and Itokawa, Y. (1993) Mechanism of oxidative stress in skeletal muscle atrophied by immobilization. *Am J Physiol* **265**: E839-E844.

Kong, Q., and Lin, C.G. (2010) Oxidative damage to RNA: mechanisms, consequences, and diseases. *Cell Mol Life Sci* **67**: 1817-1829.

Krivoruchko, A., and Storey, K.B. (2010) Forever Young: mechanisms of natural anoxia tolerance and potential links to longevity. *Oxidative Medicine and Cellualr Longevity* **3-3**: 1-13.

Kuboki, S., Okaya, T., Schuster, R., Blanchard, J., Denenberg, A., Wong, H.R., and Lentsch, A.B. (2007) Hepatocyte NF-κB activation is hepatoprotective during ischemia-reperfusion injury and is augmented by ischemic hypothermia. *Am J Physiol Gastrointest Liver Physiol.* **292**: G201-G207.

Kuboki, S., Sakai, N., Clarke, C., Schuster,R., Blanchard, J., Edwards, M.J., and Lentsch, A.B. (2009) The peptidyl-prolyl isomerase, Pin1, facilitates NF-κB binding in hepatocytes and protects against hepatic ischemia/reperfusion injury. *Journal of Hepatology* **51**: 296-306.

Kumar, A. Takada, Y., Boriek, A.M., and Aggarwal, B.B. (2004) Nuclear factor-κB: its role in health and disease. *J Mol Med* **82**:434-448.

Lawrence, T., and Fong, C. (2010) The resolution of inflammation: anti-inflammatory roles for NF-κB. *International Journal of Biochemistry & Cell Biology* **42**:519-523.

Lee, C.H., Jeon, Y.T., Kim, S.H., and Song, Y.S. (2007) NF-kappaB as a potential molecular target for cancer therapy. *Biofactors* **29(1)**: 19-35.

Li, H., Malhotra, S., and Kumar, A. (2008) Nuclear factor-kappa B signaling in skeletal muscle atrophy. *J Mol Med* **86(10)**: 1113-1126.

Li, N., and Karin, M. (1999) Is NF-$_{\kappa}$B the sensor of oxidative stress? *FASEB J.* **13**: 1137-1143.

Li, T., and Chiang, J.Y.I. (2009) Regulation of bile acid cholesterol metabolism by PPARs. *PPAR Research* **2009** Article ID 501739, 15 pages. (Down loaded March 2010 from http://www.ncbi.nlm.nih.gov/pmc/articles/PMC2712638/)

Lin, C.C., Chiang, L.L., Lin, C.H., Shih, C.H., Liao, Y.T., Hsu, M.J. and Chen, B.C. (2007) Transforming growth factor-beta1 stimulates heme oxygenase-1 expression via the PI3K/Akt and NF-kappaB pathways in human lung epithelial cells. *Eur J Pharmacol* **560(2-3)**: 101-109.

Lindel, S.L., Klahn, S.L., Piazza, T.M., Mangino, M.J., Torrealba, J.R., Southard, J.H., and Carey, H.V. (2005) Natural resistance to liver cold ischemia-reperfusion injury associated with the hibernation phenotype. *Am J Gastrointest Liver Physiol* **288**:G473-G480.

Liu, A.Y., Lee, Y.K., Manalo, D., and Huang, L.E. (1996) Attenuated heat shock transcriptional response in aging: molecular mechanisms and implication in the biology of aging. *EXS* **77**: 393-408.

Llacuna, L., Mari, M., Lluis, J.M., Garcia-Ruiz, C., Fermández-Checa, J.C., and Morales, A. (2009) Reactive oxygen species mediate liver injury through parenchymal nuclear factor-kappaB inactivation in prolonged ischemia/reperfusion. *Am J Pathol* **174(5)**: 1776-1785.

Lluis, J.M., Buricchi, F., Chiarugi, P., Morales, A., and Fernández-Checa, J.C. (2007) Dual role of mitochondrial reactive oxygen species in hypoxia signaling: activation of Nuclear factor-κB via c-SRC- and oxidant-dependant cell death. *Cancer Res* **67(15)**: 7368-7377.

Loukili, N., Rosenblatt-Velin N., Rolli, J., Levrand, S., Feihl, F., Waeber, B., Pahcer, P., and Liaudet, L. (2010) Oxidnats positively or negatively regulate nuclear factor κB a context -dependent manner. *Journal of Biological Chemistry* **285(21):**15746-15752.

Luedde, T., Assmus, U., Wüstefeld, T., zu Vilsendorf, A.M., Roskams, T., Schmidt-Supprian, M., Rajewsky, K., Brenner, D.A., Manns, M.P., Pasparakis, M., and Trautwein, C. (2005) Deletion of IKK2 in hepatocytes does not sensitize these cells to TNF-induced apoptosis but protects from ischemia/reperfusion injury. *J Clin Invest* **115**:849-859.

Luedde, T., Beraza, N., Kotsikoris, V., van Loo G., Nenci, A., De Vos, R., Roskams, T., Trautwein, C., and Pasparakis,M. (2007) Deletion of NEMO/IKKgamma in liver paranchymal cells causes steatohepatitis and hepatocellular carcinoma. *Cancer Cell* **11(2)**: 119-132.

Luther, P.K. (2009) The vertebrate muscle Z-disc: sarcomere anchor for structure and signalling. *J Muscle Res Cell Motil* **30**:171-185.

Lyman, C.P., Willis, J.S., Malan, A., and Wang, L.C.H. (1982) Mechanisms of Arousal *In* Hibernation and Torpor in Mammals and Birds. Associated Press. New York, pp. 104-123:

Ma, Q. (2010) Transcriptional responses to oxidative stress pathological and toxicological implications. *Pharmacology &Therapeutics* **125**: 376-393.

Ma, Y.L., Zhu, X., Rivera, P.M., Tø, Ø., Barnes, B.M., LaManna, J.C., Smith, M.A., and Drew, K.L. (2005) Absence of cellular stress in brain after hypoxia induced by arousal from hibernation in arctic ground squirrels. *J Physiol Regul Integr Comp Physiol* **289**: R1297-R1306.

MacDonald, J.A., and Storey, K.B. (2005) Mitrogen-activated protein kinases and selected downstream targets display organ-specific responses in the hibernating ground squirrel. *International Journal of Biochemistry & Cell Biology* **37**: 679-691.

Malatesta, M., Biggiogera, M., Baldelli, B., Barabino, S. M., Martin, T.E., and Zancanaro, C. (2008) Hibernation as a far-reaching program for the modulation of RNA transcription. *Microsc Res Tech* **71(8)**:564-572.

Mamady, H., and Storey, K.B. (2008) Coping with the stress: expression of ATF4, ATF6, and downstream targets in organs of hibernating ground squirrel. *Arch Biochem Biophys* **477(1)**:77-85.

Manna, S.K., Zhang, H.J., Yan, T, Oberley, L.W., and Aggarwal, B.B. (1998) Overexpression of manganese superoxide dismutase suppresses tumor necrosis

factor-induced apoptosis and activation of nuclear transcription Factor κB and activated protein-1. *Journal of Biological Chemistry* **273(21)**:13245-13254.

Martinon, F. (2010) Signaling of ROS drives inflammasome activation. *Eur J Immunol* **40**: 595-653.

McArthur, M.D., and Milsom, W.K. (1991) Ventilation and respiratory sensitivity of euthermic Columbia and Golden-mantled Ground Squirrels (*Sjermopphilus columbianus and Spermophilus leteralls*) during the summer and winter. *Physiological Zoology* **64(4)**: 921-939.

McCaddon, A., and Hudson, P.R. (2010) L-methylfolate, methylcobalamin, and N-acetylcysteine in the treatment of Alzheirmer's disease-related cognitive decline. *CNS Spect* **15(1suppl 1)**:7.

Medina, E., Anders, D., and Chhatwal, G.S. (2002) Induction of NF-kappaB nuclear translocation in human respiratory epithelial cells by group A streptococci. *Microb Pathog* **33(6)**:307-313

Melvin, R.G., and Andrews, M,T. (2009) Torpor induction in mammals: recent discoveries fueling new ideas. *Trends in Endocrinology and Metabolism* **20(10)**:490-498.

Michalopoulos, G.K. (1990) Liver regeneration: molecular mechanisms of growth control. *FASEB J* **4**:176-187.

Mori, N., and Prager, D. (1996) Transactivation of the Interleukin-1α promoter by human T-Cell leukemia virus type I and type II tax proteins. *Blood* **87(8)**:3410-3417.

Morin, P., Jr., Dubuc, A., and Storey, K.B. (2008A) Differential expression of microRNA species in organs of hibernating ground squirrels: a role in translational suppression during torpor. *Biochim Biophys Acta* **1779(10)**:628-633.

Morin, P. Jr., Ni, Z., McMullen, D.C., and Storey, K.B. (2008B) Expression of Nrf2 and its downstream gene targets in hibernating 13-lined ground squirrels, *Spermophilus tridecemlineatus. Mol Cell Biochem* **312**:121-129

Morin, P., Jr., and Storey, K.B. (2009) Mammalian hibernation: differential gene expression and novel application of epigenetic controls. *Int J Dev Biol* **53(2-3)**: 433-442.

Morin, P. Jr., and Storey, K.B. (2007) Antoxidant defense in hibernation: cloning and expression of peroxiredoxins from hibernating ground squirrels, *Spermophilus tridecemlineatus. Archives of Biochemistry and Biophysics* **461**:59-65.

Morin, P. Jr., and Storey, K.B. (2005) Cloning and expression of hypoxia-inducible factor 1alpha from the hibernating ground squirrel, *Spermophilus tridecemlineatus. Biochim Biophys Acta* **1729(1)**:32-40.

Muleme, H.M., Walpole, A.C., and Staples, J.F. (2006) Mitochondrial metabolism in hibernation: metabolic suppression, temperature effects, and substrate preferences. *Physio Biochem Zool* **79**: 474-483.

Muller, F. L., Liu, Y., and Van Remmen, H. (2004) Complex III releases superoxide to both sides of the inner mitochondrial membrane. *J Biol Chem* **279(47)**: 49064-49073.

Nathan, C., and Ding, A. (2010) Nonresolving inflammation. *Cell* **140**:871-882.

Nelson, R.J. (2004) Leptin:the "skinny" on torpor. *Am J. Physiol Regul Integr Comp Physiol* **287**:R6-R7.

Nelson, C.J., Otis, J.P., Martin, S.L., and Carey, H.V. (2009) Analysis of the hibernation cycle using LC-MS-based metabolomics in ground squirrel liver. *Physiol Genomics* **37**:43-51.

Neo, J.H., Ager, E.I., Angus, P.W., Zhu, J., Herath, C.B., and Christophi, C. (2010) Changes in the rennin angiotensin system during the development of colorectal cancer liver metastases. *Cancer* **10**: 134-145.

Ni, Z., and Storey, K.B. (2010) Heme oxygenase expression and Nrf2 signaling during hibernation in ground squirrels. *Can J Pharmacol* **88**: 379-387.

Ohlmann, A., Giffhorm-Katz, S., Becker, I., Katz, N., and Immenschuh, S. (2003) Regulation of heme oxygenase-1gene expression by anoxia and reoxygenation in primary rat hepatocyte cultures. *Exp Biol Med (Maywood)* **228(5)**:584-589.

Ohta, H., Okamoto, I., Hanaya, T., Arai, S., Ohta, T., and Fukuda, S.(2006) Enhanced antioxidant defense due to extracellular catalase activity in Syrian hamster during arousal form hibernation. *Comp Biochem Physiol C* **143**: 484-491.

Okamoto, I., Kayana, T., Hanaya, T., Arai, S., Ikeda, M., and Kurimoto, M.(2006) Up-regulation of an extracellular superoxide dismutase-like activity in hibernating hamsters subjected to oxidative stress in mid- to late arousal form torpor. *Comp Biochem Physiol C* **144:**484-491.

Okamoto, T. (2006) NF-kappaB and rheumatic diseases. *Endocr Metab Immune Disord Drug Targets* **6(4)**:359-372.

Pahl, H,L. (1999) Activators and target genes of the Rel/NF-kappaB transcription factors. *Ocogene* **18(49)**:6853-6866.

Papa, S., Bubici, C., Zazzeroni, F., and Franzoso, G. (2009) Mechanisms of liver disease cross-talk between the NF-kappaB and JNK pathways. *Biol Chem.* **390(10)**:965-976.

Pardo, M., Budick-Harmelin, N., Tirosh, B., and Tirosh, O. (2008) Antioxidant defense in heptatic ischemia-reperfusions injury is regulated by damage-associated molecular pattern signal molecules. *Free Radic Bo Med* **45(8)**:1073-1083.

Pasparakis, M. (2009) Regulation of tissue homeostasis by NF-κB signaling: implications for inflammatory diseases. *Nat Rev Immunol* **9(11)**:778-788

Perry, J.J.P., Shin, D.S., Getzoff, E.D., and Tainer, J.A. (2010) The structural biochemistry of superoxide dismutases. *Biochimica et Biophisica Acta* **1804**:245-262.

Petrović, V.M., Saicić, Z., Milić, B., Spasić, M., and Radojicić, R. (1983) Distribution of superoxide dismutase in the ground squirrel (*Citellus citellus*): effect of hibernation and arousal. *Comp Biochem Physio B* **(75(4)**:699-700.

Pette, D., Spamer, M. (1986) Metabolic properties of muscle fibers. F*ed Proc* **45(13)**:2910-2914.

Ralph, S.J., Rodriguez-Enriquez, S., Neuzil, J., Saavedra, E., and Moreno-Sánchez, R. (2010) The causes of cancer revisited: "mitrochondrial malignancy" a ROS-induced ocogenic transformation - why mitochondria are targets for cancer therapy. *Mol Aspects Med* **31(2)**: 145-170.

Rojo, A., Salinas, M., Martin, D., Perona, R., and Cuadrado, A. (2004) Regulation of Cu/Zn-superoxide dismutase expression via the phosphatidylinositaol 3 kinase/Akt pathway and nuclear factor-kappaB. *J Neurosci* **24(33)**: 7324-7334.

Ryter, S.W., and Choi, A.M. (2002) Heme oxygenase-1: molecular mechanisms of gene expression in oxygen-related stress. *Antioxid Redox Signal* **4(4)**:625-632.

Ryter, S.W., and Choi, A.M. (2005) Heme oxygenase-1: redox regulation of a stress protein in lung and cell culture models. *Antioxid Redox Signal* **7(1-2)**:80-91.

Safronova, O., and Morita, I. (2010) Transcriptome remodeling in hypoxic inflammation. *J Dent Res* **89(5)**:430-444.

Scanlan, T.S., Suchland, K.L., Hart, M.E., Chiellini, G., Huang, Y., Kruzich P.J., Frascarelli, S., Crossley, D.A., Bunzow, J.R., Ronca-Testoni, S., Lin, E.T.,

Hatton, D., Zucchi, R., and Grandy, D.K. (2004) 3-Idothyronamine is an endogenous and rapid-acting derivative of thyroid hormone. N*at Med* **10(6)**: 638-642.

Schapira, A.H., and Tolosa, E. (2010) Molecular and clinical prodrome of Parkinson disease: implications for treatment. *Nat Rev Neurol* **6(6)**: 309-317.

Schipke, D. (1995) Myocardial hibernation. *Basic Res Cardiol* **90(1)**: 26-28.

Schipper, H.M., Song, W., Zukor, H., Hascalovici, J.R.,and Zeligman, D. (2009) Heme oxygenase-1 and neurodegeneration: expanding frontiers of engagement. *J Neurochem* **110(2)**: 469-485.

Schmidt-Supprian, M., Bloch, W., Cortois, G., Addiks, K., Israël, A., Rajewsky, K., and Pasparakis, M. (2000) NEMO/IKKγ-deficient mice model Incontinentia Pigmenti. *Molecular Cell* **5**: 981-992.

Schreck , R., Reiber, P., and Baeuerle, P.A. (1991) Reactive oxygen intermediates a apparently widely used messengers in the activation of the NF-kappaB transcription factor and HIV-1. *EMBO J* **10(8)**:2247-2258.

Scott, M. L., Fujita, T., Liou, H., Nolan, G.P., and Baltimore, D. (1993) The p65 subunit of NF-κB regulates IκB by two distinct mechanisms. *Genes and Development* **7**:1266-1276.

Seldon, M.P., Silva, G., Pejanovic, N., Larsen, R., Gregoire, I.P., Filipe, J., Anrather, J., and Soares, M.P. (2007) Heme oxygenase-1 inhibits the expression of adhesion

molecules associated with endothelial cell activation via inhibition of NF-$_{\kappa}$B RelA phosphorylation at Serine 276. *Journal of Immunology* **179**:7840-7851.

Sen C.K., Atalay, M., Ågren, J., Laaksonen, D.E., Roy, S., and Hänninen, O. (1997) Fish oil and vitamin E supplementation in oxidative stress at rest and after physical exercise. *J Appl Physiol* **83(1)**:189-195.

Sen, R., and Baltimore, D. (1986) Multiple Nuclear factors interact with the immunoglobulin enhancer sequences. *Cell* **46**: 705-716.

Shalom-Barak T., Quach, J., and Lotz, M. (1998) Interleukin-17-induced gene expression inarticular chondrocytes is associated with activation of mitogen-activated protein kinases and NF-kappaB. *J Biol Chem* **273(42)**:27467-27473.

Shifera, A.S. (2010A) Proteins that bind o IKKgamma (NEMO) and down-regulate the activation of NF-kappaB. *Biochem Biophys Res Commun.* **396(3)**:585-589.

Shifera, A.S. (2010B) Protein-protein interactions involving IKKgamma(NEMO) that promote the activation of NF-kappaB *J Cell Physio* **223(3)**:558-561.

Shin, T., Kuboki, S., and Lentsch, A.B. (2008) Roles of nuclear factor-κB in postischemic liver. *Hepatology Research* **38**:429-440.

Snyder, G.K., and Nestler, J.R. (1990) Relationships between body temperature, thermal conductance, Q10 and energy metabolism during daily torpor and hibernation in rodents. *J Comp Physiol B* **159(6)**: 667-675.

Soós, J., Engelhardt, J. I., Siklós, L., Havas, L., and Majtényi,K. (2004) The expression of PARP, NF-kappa B and parvalbumin is increased in Parkinson disease. N*euroreprot* **15(11):**1715-1718.

Squire, T.L., Lowe, M. E., Bauer, V.W., Andrews, M.T. (2003) Pancreatic triacylglycerol lipase in a hibernating mammal. II. Cold adapted function and differential express. *Physiol Genomics* **16(1)**: 131-140.

Srere, H.K., Wang, L.C.H., and Martin S.L. (1992) Central for differential gene expression in mammalian hibernation. *Proc Natl Acad Sci USA* **89**: 7119-7123.

Storey, K.B. (1987) Regulation of liver metabolism by enzyme phosphorylation during mammalian hibernation. *Journal of Biological Chemistry* **162(4)**: 1670-1673.

Storey, K.B. (2003) Mammalian hibernation. Transcriptional and translational controls. *Adv Exp Med Biol* **543**:21-38.

Storey, K.B. (2010) Out cold: biochemical regulation of mammalian hibernation- a mini-review. *Gerontology* **56(2)**:220-230.

Suh, S.H., Paik, I.Y., and Jacobs, K. (2007) Regulation of blood glucose homeostasis during prolongs exercise. *Mol Cells* **23(3)**: 272-279.

Swoap, S.J. (2008) Why one enters torpor: focus on the "NPF Y1 receptor abtaginist prevents NPY-induced torpor-like hypothermia in cold-acclimated Siberian hamsters". *Am J Physiol Regul Integr Comp Physiol* **294(1)**:R235-R235.

Tacchini, L., Cairo, G., De Ponti, C., Massip, M., Ressellò-Castafau, J., and Peralta, C. (2006) Up regulation of IL-6 by ischemic preconditioning in normal fatty rat livers: association with reduction of oxidative stress. *Free Radic Res* **40(11)**:1206-1217.

Tak, P.P., and Firestein, G.S. (2001) NF-κB: a key role in inflammatory diseases. *Journal of Clinical Investigation* **107(1)**: 7-11.

Tanaka, M., Fuentes, M, E., Yamaguchi, K., Durnin, M.H., Dalrymple S.A., Hardy, K.L, and Goeddel D.V. (1999) Embryonic lethality, liver degeneration, and impaired NF-κB activation in IKK-ß-deficient mice. *Immunity* **10**:421-429.

Taub, R. (1996) Transcriptional control of liver regeneration. *FASEB J* **10**:413-427.

Tempel, G.E., Musacchia X.J., and Jones, S.B. (1977) Mechanisms responsible for decreased glomerular filtration in hibernation and hypothermia. *J Appl Physiol Respirat Environ Exercise Physiol* **42(3)**: 420-425.

Ten, R.M., Paya, C.V., Israël, N., Le Bail, O., Mattei, M.G., Virelizier, J.L., Kourilsky, P., and Israël A. (1992) The characterization of the promoter of the gene encoding the p50 subunit of NF-kappa B indicates that it participates in it own regulation. *EMBO J* **11(1)**:195-203.

Tessier, S.N., and Storey, K.B. (2010) Expression of myocyte enhancer factor-2 and downstream genes in ground squirrel skeletal muscle during hibernation. *Mol Cell Biochem* **Jul 9** (Epub ahead of printing).

Tøien, Ø., Drew, K.L., Chao, M.L., and Rice, M.E. (2001) Ascorbate dynamics and oxygen consumption during arousal from hibernation in arctic ground squirrels. *Am J Physiol Regulatory Integrative Comp Physiol* **281**:R572-R583.

Tomeczak, M.F., Erdman, S. E., Davidson, A., Wang, Y.Y., Nambiar, P.R., Rogers, A.B. Rickman, B., Luchetti, D., Jox, J.G., and Horwitz, B.H. (2006) Inhibition of *Helicobacter hepaticus*-induced colitis by IL-10 requires the p50.p105 subunit of NF-$_{\kappa}$B. *Journal of Immunology* **177**:7332-7339.

Ueberla, K.,Lu, Y.C., Chung, E., and Haseltin, W.A. (1993) The NF-κB p65 promotor. *J AIDS Res* **6**: 227230.

Valen, G., Yan, Z.Q., Hansson, G.K. (2001) Nuclear factor kappa-B and the heart. *J AM Coll Cardiol* **38(2)**:307-314.

Valko, M., Leibrritz,, D., Moncol, J., Cronin, M.T.D., Mazur, M., and Telser, J. (2007) Free radicals and antioxidants in normal physiological functions and human disease. *International Jurnal of Biochemistry & Cell Biology* **39**:44-84.

Valko,M., Rhodes, C.J., Moncol, J., Izakovic, M., and Mazur, M. (2006) Free radicals, metals and antioxidants in oxidative stress-induced cancer. *Chemico-Biological Interactions* **160**: 1-40.

Von der Ohe, C.G., Garner, C.C., Darian-Smith, C., and Heller, H.C. (2007) Synaptic protein dynamics in hibernation. *Journal of Neuroscience* **27(1)**:84-92.

Wagener, F.D.T.G., Volk, H., Willis, D., Abraham, N.G., Soares, M.P., Adema, G.J., and Figdor, C.G. (2003) Different faces of the heme-heme oxygenase system in inflammation. *Pharmaco Rev* **55**:551-571.

Wang, C.Y., Chau, L.Y., (2010) Heme oxygenase-1 in cardiovascular diseases: molecular mechanisms and clinical perspectives. *Chang Gung Med J* **33**:13-24.

Wang, L.C.H., and Lee, T.F. (1996) Torpor and hibernation in mammals: metabolic, physiological and biochemical adaptations. *In* Handbook of Physiology:

Environmental Physiology (Fregley, M.J., and Blatteis, C.M. eds.) Oxford University Press, New York, pp.507-532.

Wang, Y., Yamamoto, S., Miyakawa, A., Sakurai, T., Ibaraki, K., and Terakawa, S. (2010) Intravital oxygen radical imaging in normal and ischemic rat cortex. *Neurosurgery* **67(1)**:118-127.

Warner, B.B., Stuart, L., Gebb, S., and Wispé, J.R. (1996) Redox regulation of manganese superoxide dismutase. *Am J Physiol* **217**:L150-L158.

Wei, Z.B., Miao, X.Y., Yang, M.Q., and Luo, X.G. (2008) Advances in the expression and regulation of MnSOD gene. *Yi Chuan* **30(7)**:831-837.

Wells, LA. (1971) Circulatory patterns of hibernators. *Am J Physiol* **221(5)**:1517-1520.

Wullaert, A., van Loo G., Heyninck, K., and Beyaert, R. (2007) Hepatic tumor necrosis factor signaling and nuclear factor-κB: effects on liver homeostasis and beyond. *Endocrine Reviews* **28**:365-386.

Xu, Y., Porntadavity, S., St. Clair, D.K. (2002) Transcriptional regulation of human manganese superoxide dismutase gene: the role of specificity protein 1 (Sp1) and activating protein -2 (AP-2). *Biochem J* **362**: 401-412.

Xue, H., Guo, H., Li, Y.C., and Hao, Z.M. (2007) Heme oxygenase-1 induction by hemin protects liver cells from ischemia/reperfusion injury in cirrhotic rats. *World J Gastroenterol* **13(40)**:5384-5390.

Yamamoto Y., Verma, U.N., Prajapati, S., Kwak, Y,T., and Gaynor, R.B. (2003) Histone H3 phosphorylation by IKK-alpha is critical for cytokine-induced gene expression. *Nature* **423(6940)**:655-659.

Yamazaki, H., Hiramatsu, N., Hayakawa, K., Tafawa, Y., Okamura, M., Ogata, R., Huang, T., Nakajima, S., Yao, J., Paton, A.W., Paton, J.C., and Kitamura, M. (2009) Activation of the Akt-NF-kappaB pathway by subtilase cytotoxin through the ATF6 branch of the unfolded protein response. *J Immunol* **183(2)**:1480-1487.

Yan, J., Barnes, B.M., Kohl, F., and Marr, T.G. (2008) Modulation of gene expression in hibernating arctic ground squirrels. *Physiol Genomics* **32(2)**: 170-181.

Yuan, G.J., Ma, J.C., Gong, Z.J., Sun, X.M., Zheng, S,H., and Li, X. (2005) Modulation of liver oxidant-antioxidant system by ischemic preconditioning during ischemia /reperfusion injury in rats. *World J Gastroerol* **11(12)**:1825-1828.

Zancanaro C., Malatesta, M., Mannello, F., Vogel, P., and Fakan, S. (1999) The kidney during hibernation and arousal from hibernation. A natural model of organ preservation durng cold ischaemia and reperfusion. *Nephrol Dial Tranplant* **14**:1982-1990.

Zatzman, M.L. (1984) Renal and cardiovascular effects of hibernation and hypothermia. *Cryobiology* **21**:593-614.

Zhegunov, G.F., Mikkulinsky, Y.E., and Kudokotsseva, E.V. (1988) Hyperactivation of protein-synthesis in tissues of hibernating animals on arousal. *Cryo-Letters* **9(4)**:236-245.

Zhu, X., Smith, M.A., Perry, G., Wang, Y., Ross, A.P., Zhao H. W., LaManna, J.C., and Drew, K.L. (2005) MAPKs are differently modulated in arctic ground squirrels during hibernation. *Journal of Neuroscience Research* **80**:862-868.

Appendix I

Table 1: Examples of constantly expressed proteins in 13-lined ground squirrel skeletal muscle and liver

Tissue	Protein
Skeletal Muscle	Actin, Alpha-tubulin, Myosin, GRP78, GADD34, BAD, histone H3, RNA polymerase II, ATF-2, HSP27 , eIF2α, eEF2, Rb, E2F1, SUV39H1, HO1, Nrf257kDa, Nrf2 100kDa, MafG, TrxR2, HSP73, eIF4E, 4E-BP1, eIF4B
Liver	HSP72, HSP73, HSP90a/b, 4E-BP1, eIF4B, Actin, Alpha-tubulin, Beta-tubulin, ATF4, Bcl-XL, HIF-1α, EGFR, Cu/Zn SOD, MnSOD

Table 2: Examples of constantly expressed mRNAs in 13-lined ground squirrel skeletal muscle and liver

Tissue	mRNA
Skeletal Muscle	*Alpha-tubulin, grp78, atf4, foxo1a ,hif1, cox-4, a-fabp, Cu/Zn SOD, grp75*
Liver	*Alpha-tubulin, grp78, bcl-xl, hif1, ho-2, grp75, grp94, grp170*

Appendix 2

Table 1: Summary table for NF-κB signaling pathway expression (protein & mRNA) and nuclear distribution results during hibernation in skeletal muscle of *S. tridecemlineatus* over the torpor-arousal cycle.

Time Point		ACR	ENT	EHIB	LHIB	EAR	LAR
Protein Level	P50	↔	↔	↑	↔	↑	↑
	P65	↔	↑	↑	↔	↑	↑
	P-IKK	↔	↔	↔	↔	↑	↔
	IKKα	↔	↔	↔	↔	↔	↔
	IKKβ	↔	↔	↔	↔	↑	↔
	IκBα	↔	↔	↔	↔	↑	↔
	P-IκBα	↔	↑	↔	↔	↔	↔
	HO-1	↔	↔	↔	↔	↑	↔
	MnSOD	↔	↔	↑	↑	↔	↔
Nuclear Distribution	P50	↔	NA	NA	↔	NA	NA
	P65	↔	NA	NA	↑	NA	NA
mRNA Level	P50	↔	↓	↓	↓	↔	↓
	P65	↔	↔	↑	↔	↔	↔
	HO-1	↔	↓	↔	↓	↓	↔
	MnSOD	↔	↔	↓	↓	↓	↓

NA= Not Applicable

Table 2: Summary table for NF-κB signaling pathway expression (protein & mRNA) and nuclear distribution results during hibernation in liver of *S. tridecemlineatus* over the torpor-arousal cycle.

Time Point		ACR	ENT	EHIB	LHIB	EAR	LAR
Protein Level	P50	↔	↔	↔	↑	↔	↔
	P65	↔	↔	↔	↑	↔	↔
	P-IKK	↔	↑	↔	↑	↑	↑
	IKKα	↔	↑	↓	↑	↑	↑
	IKKβ	↔	↓	↓	↓	↓	↓
	IκBα	↔	↓	↓	↓	↔	↔
	P-IκBα	↔	↓	↔	↑	↔	↑
	HO-1	↔	↔	↔	↑	↔	↔
	MnSOD	↔	↑	↓	↔	↓	↔
Nuclear Distribution	P50	↔	NA	NA	↑	NA	NA
	P65	↔	NA	NA	↑	NA	NA
mRNA Level	P50	↔	↑	↔	↔	↔	↔
	P65	↔	↑	↑	↑	↑	↑
	HO-1	↔	↑	↑	↑	↑	↑
	MnSOD	↔	↑	↑	↔	↔	↔

NA= Not Applicable